

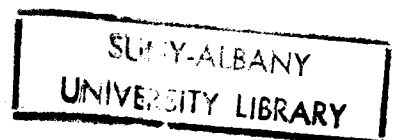
Geology
of the
Mafic/Ultramafic Transition,
Table Mountain, Western Newfoundland

A thesis presented to the Faculty
of the State University of New York
at Albany

in partial fulfillment of the requirements
for the degree of
Master of Science

School of Arts and Science
Department of Geology

Suzanne O'Connell
1979



Geology
of the
Mafic/Ultramafic Transition,
Table Mountain, Western Newfoundland

Abstract of
a thesis presented to the Faculty
of the State University of New York
at Albany
in partial fulfillment of the requirements
for the degree of
Master of Science
School of Arts and Science
Department of Geology

Suzanne O'Connell
1979

913154

ABSTRACT

A thin (<200 m.) mafic suite and well developed mafic/ultramafic transition zone are exposed above a flat lying peridotite contact on northwestern Table Mountain. The igneous layering and sedimentary features indicate mineral deposition under conditions which promoted adcumulate growth, were capable of minor transport, and were subjected to at least minor tectonic activity during consolidation. Feldspathic, mafic, and ultramafic dikes and veins cross-cut the layering. Microscopic features indicate deformation at elevated temperature and/or low strain rates. Deformation is best developed within the transition zone, but cataclastic zones are most common in the hornblende gabbros. Orientations of layering, foliation, and lineation indicate a variable mafic/ultramafic transition and macroscopic folding. Geometric analysis indicates three distinct fold axis orientations: an east - west horizontal fold axis, a northeast trending moderately plunging axis, and a vertical though poorly defined axis. Such features demonstrate that an apparently simple contact relationship may be extremely complex. This has important implications for ocean floor accretion. The relatively simple ocean floor seismic stratigraphy masks very complex petrological and structural processes. Such processes may involve deposition in an actively convecting magma chamber with a differentially subsiding wedge (Dewey and Kidd, 1977), in which folding occurs in response to the steepening angle between the cumulate

banding and the base of the magma chamber. The instability is enhanced by the different accumulation rates and densities of the minerals involved. The lineation may originally be a sedimentary feature indicative of transport direction from the convection cell, and perpendicular to the compressive stress which produced the folding. The different orientations of lineations and fold axes could be produced by rotation of the ocean crustal blocks during lateral transport along the ocean floor and/or obduction. Further detailed study of ophiolite complexes will continue to shed light upon the nature and development of oceanic crust.

ACKNOWLEDGMENTS

The list of people to acknowledge and thank for assistance during the trying times of this thesis is long and grows longer as the months have passed. Will that rock ever make it up the hill? Typing this says that it may.

I would like to thank my advisor, John F. Dewey, and W.S.F. Kidd for introducing this problem and providing assistance and support during the duration of this thesis. W.S.F. Kidd read the first handwritten draft, suggesting many critical changes. John F. Dewey provided many useful suggestions to the first typed draft. Akiho Miyashiro and Don Videger made useful suggestions to the petrography section. Win Means and Bill Gregg provided critical and helpful comments to the microstructure chapter. George Putman aided in much of the petrographic identification. Jeff Karson provided a valuable introduction to the field during my summer as a field assistant in the Lewis Hills, and helped with many of the frustrations of writing this thesis. My committee, John F. Dewey, P. Jeff Fox, and W.S.F. Kidd, provided an interesting and survivable thesis defence. My fellow graduate students, particularly Karlene Davis, Bill Gregg, and Janet Stroup, gave continuing moral support and encouragement.

During the field season several people in Newfoundland were outstanding in their friendliness and opening their homes to me, Ella Manuel, Bridie Toner, and Euna Warham. My sister Adrienne and Dave Rowley provided companionship during the

field season.

Jim Pawlowski (the keyboard phantom), transformed the written draft into a typed draft and that into the final copy.

This research was supported by NSF grant #EAR-76-14459.



Get out of my way said the lightning to
the tree or take what's coming to you.

. . . Sufi

CONTENTS

| | <u>Page</u> |
|---|-------------|
| CHAPTER I. INTRODUCTION. | 1 |
| A. Purpose | 1 |
| B. Location Exposure and Setting | 3 |
| C. Previous Field Work | 4 |
| CHAPTER II. REGIONAL GEOLOGY OF WESTERN NEWFOUNDLAND. | 6 |
| CHAPTER III. PETROGRAPHY | 16 |
| A. Introduction | 16 |
| B. Rock Descriptions | 16 |
| C. Primary Mineral Assemblage | 28 |
| D. Secondary Mineral Assemblage | 34 |
| E. Summary | 39 |
| CHAPTER IV. PETROGRAPHY OF OCEAN FLOOR GABBROS. | 41 |
| CHAPTER V. STRUCTURAL GEOLOGY. | 50 |
| A. Mesoscopic Relationships | 50 |
| B. Macroscopic and Geometric Relationships | 69 |
| CHAPTER VI. MICROSTRUCTURE. | 78 |
| A. General Introduction | 78 |
| B. Plagioclase | 78 |
| C. Diopside | 100 |
| D. Summary | 107 |
| CHAPTER VII. CATACLASTIC ROCKS | 109 |
| A. Introduction | 109 |
| B. Non-Foliated Cataclastic Rocks | 111 |
| C. Foliated Cataclastic Rocks | 113 |
| D. Summary | 128 |
| CHAPTER VIII. SUMMARY AND CONCLUSIONS | 131 |
| BIBLIOGRAPHY. | 135 |

TABLES

| <u>Table Number</u> | | <u>Page</u> |
|---------------------|--|-------------|
| I. | Modal Compositions from the Table Mountain-Mafic Suite | 17 |
| II. | Albite and Pericline Twinning in Plagioclase | 86 |
| III. | Angle of Compressive Stress Direction to Layering, Determined from Twin Orientations | 94A |
| IV. | Classification of Cataclastic Rocks | 110 |

ILLUSTRATIONS

| <u>Figure Number</u> | <u>Page</u> |
|---|-------------|
| 1. Dewey and Kidd (1977) Plate Accretion Model | 2 |
| 2. Tectonic Setting of Bay of Islands Ophiolite Complex | 7 |
| 3. Stratigraphic Relationships of Facies in Western Newfoundland Showing Deposition and Transport | 13 |
| 4. Location Map for Modal Analysis Samples Listed in Table I | 18 |
| 5. Ophitic Hornblende Gabbro Containing Rounded an Lobate Plagioclase and Pyroxene Grains | 21 |
| 6. Olivine Gabbro with Texture Indicating Simultaneous Crystallization of Grains | 21 |
| 7. Anorthosite Layer Parallel to Gabbroic Layering | 24 |
| 8. Anorthosite Wedging Between Troctolite Layers | 24 |
| 9. Troctolite Engulfing Anorthosite | 25 |
| 10. Anorthosite Dikes Cutting Both Mafic and Ultramafic Layering | 25 |
| 11. Pyroxene Fragments in Adjacent Pyroxene Grains | 27 |
| 12. Fine Grained Phenocryst Baring Dike | 27 |
| 13. Twinned Plagioclase Lath in Clinopyroxene Grain | 29 |
| 14. Rounded Clinopyroxene Grain in Twinned Plagioclase | 29 |
| 15. A. Large Plagioclase Grain in Mylonite Showing Alteration which is Developed in a Conjugate Pattern Preferentially in the Areas Experiencing the Most Compression | 31 |
| B. Large Plagioclase Grain Showing Preferential Alteration at the Top of the Grain which would have Experienced the Most Stress | 31 |

| <u>Figure Number</u> | <u>Page</u> |
|--|-------------|
| 16. Mosaic Texture Suggesting Recrystallization Around Edges of Large Clinopyroxene Grain | 31 |
| 17. Fiberous Chlorite Pseudomorphs after Clino- pyroxene | 37 |
| 18. En-Echelon Blue-Green Hornblende Laths Filling Fracture in Hornblende Gabbro | 37 |
| 19. Irregularities in Mafic Layering Suggesting Small Channels | 52 |
| 20. Cross-Lamination in Gabbro Channel Structure | 52 |
| 21. Cross-Lamination in Leuco Gabbro with Steep Angle of Repose | 54 |
| 22. Weak Size Grading in Anorthosite Layer with the Appearance of a "Pseudo-Fold" | 54 |
| 23. Symmetric Intrafolial Fold | 56 |
| 24. Asymmetric, S-Style Intrafolial Fold | 56 |
| 25. Large Fold in Two-Dimensions Showing Limbs with Appearance of Layering | 58 |
| 26. Multiple Folds in Transition Area | 58 |
| 27. Pseudo-Fold Caused by the Intersection of an Anorthosite Dike and Anorthosite Layer or Two Anorthosite Dikes | 60 |
| 28. Pre-Lithification Slumping in Anorthosite/ Gabbro Block | 60 |
| 29. Intersecting Dunite Dikes in Layered Ultra- mafic Rock | 62 |
| 30. Dunite Dike in Layered Mafic Rock | 62 |
| 31. Multiple Large Pyroxene Grains in Layered Gabbro | 64 |
| 32. Single Large Pyroxene Grain | 64 |
| 33. Detail from Fig. 32 | 66 |
| 34. Deformation of Layered Gabbro Terminating Against Homogeneous Gabbro | 66 |

| <u>Figure Number</u> | <u>Page</u> |
|---|-------------|
| 35. Deformation of Feldspar Lineation | 68 |
| 36. The Six Subareas of the Table Mountain Mafic Suite | 69 |
| 37. A. Poles to Layering, Subarea IV | 70 |
| B. Lineations, Subarea IV | 70 |
| 38. A. Poles to Layering, Subarea V | 70 |
| B. Lineations, Subarea V | 70 |
| 39. A. Poles to Layering, Subarea I | 72 |
| B. Lineations, Subarea I | 72 |
| 40. A. Poles to Layering, Subarea II | 72 |
| B. Lineations, Subarea II | 72 |
| 41. A. Poles to Layering, Subarea III | 74 |
| B. Lineations, Subarea III | 74 |
| 42. A. Poles to Layering, Subarea VI | 74 |
| B. Lineations, Subarea VI | 74 |
| 43. A. Composite Poles to Layering | 77 |
| B. Composite Lineations | 77 |
| 44. Relative Development of Cataclasis, Deformation Lamellae, and Twinning at Different P and T for Experimentally Deformed Anorthite | 80 |
| 45. Bending in Plagioclase Twin | 89 |
| 46. Tapered and Bent Plagioclase Twins Possibly Due to Kinking | 89 |
| 47. Schematic Representation of Twin Planes and Directions and Their Bisector (C') Which May Represent a Compressive σ Direction | 92 |
| 48. Recrystallization in Plagioclase Grains Showing Mosaic Texture in Smaller Grains | 99 |
| 49. Microfractures Forming in a Single Large Plagioclase Grain Surrounded by Cataclastic Material | 99 |
| 50. Kinking in Diopside at High Angles to the Cleavage | 103 |

| <u>Figure Number</u> | <u>Page</u> |
|--|-------------|
| 51. Fracturing in Diopside Perpendicular to Cleavage | 103 |
| 52. Rotation of Pyroxene Fragments | 105 |
| 53. Plagioclase Tactinolite Filling Large Fracture in Diopside Grain | 105 |
| 54. Detail From Fig. 53 | 106 |
| 55. Incipient Recrystallization in Diopside Grain | 106 |
| 56. Irregular and Interfingering Boundaries of Cataclastic Material in Host Rock | 112 |
| 57. Tension Gashes Forming Perpendicular to a High Strain Zone | 112 |
| 58. Mylonite in Contact with Gabbro | 114 |
| 59. Large Euhedral Plagioclase Grain in Mylonite | 114 |
| 60. Deformation of Large Pyroxene Grain (Crossed-Polarizers) | 117 |
| 61. Deformation of Large Pyroxene Grain (Uncrossed-Polarizers) | 117 |
| 62. Pyroxene Sheared Parallel to Cleavage Trace and Mylonite Foliation | 118 |
| 63. Reconstruction of Fig. 62 Pyroxene | 118 |
| 64. Pyroxene with Sheared Appearance Probably Due to Kinking and Loss of Kinked Fragments (Crossed-Polarizers) | 119 |
| 65. Figure 64 (Uncrossed-Polarizers) | 119 |
| 66. Boudinaged Pyroxene Fragment Separated from Larger Pyroxene by a Thin Layer of Plagioclase | 120 |
| 67. Detail of Boudin from Figure 66 | 120 |
| 68. Two Generations of Boudins in Pyroxene | 122 |
| 69. Detail of Boudin from Figure 68 | 122 |
| 70. Folding of Mylonite Foliation | 123 |

| <u>Figure Number</u> | <u>Page</u> |
|---|-------------|
| 71. Fractures Oblique to Mylonite Foliation | 124 |
| 72. Strain Analysis Using Formular: Strain = $(l' - L)/L$ | 124 |
| 73. Section Through a Rock Made Up of an Aggregate of Undeformed Spheres | 127 |
| 74. Plot of d against δ for the Material of Fig. 73 | 127 |
| 75. Section Through a Deformed Aggregate of Partially Deformed Spheres Which Have Undergone Partial Pressure Solution Along Their Mutual Contacts | 127 |
| 76. Plot of d against δ for the Material of Fig. 75 | 127 |
| 77. Random Distribution of 21 Points in Attempt to Apply Ramsay's (1967) Center Point Method for Strain Analysis to a Table Mountain Mylonite | 129 |
| 78. Block Diagram Interpreting the Table Mountain Mafic/Ultramafic Relationships | 133 |

CHAPTER I
INTRODUCTION

Purpose

Model building from geophysical evidence, ocean floor dredging and drilling, and ophiolite mapping has suggested a generalized structure for "normal" ocean crust and upper mantle, consisting of residual harzburgite, cumulate ultramafics, cumulate mafics, plated gabbro, sheeted dikes and pillow basalt. This layered sequence is produced at oceanic spreading ridges, elevated sites of high heat flow and shallow seismic activity. Magnetic anomaly patterns suggest that the accretion process is roughly symmetrical about the ridge axis. Several investigators have developed models to aid in the explanation of the observed structure. Models using petrologic, geochemical, structural, geophysical, geometric, and thermal constraints from oceanic and ophiolite data, have been developed by Moores and Vine (1971), Greenbaum (1972), Dewey, Fox, and Kidd (1973), Church and Riccio (1974), Moore et. al. (1974), Cann (1974), Sleep (1975), Bottinga and Allegre (1976), and Dewey and Kidd (1977).

The Dewey and Kidd (1977) model (Fig. 1) suggests a wedge shape, concave upward, flat-floored magma chamber. This model is capable of explaining: 1) thickness variations between the different lithologic units, by varying the depth/width ratio of the magma chamber, 2) on-strike compositional changes in the cumulates, by depositing the cumulate material on a flat floored magma chamber which undergoes differential subsidence

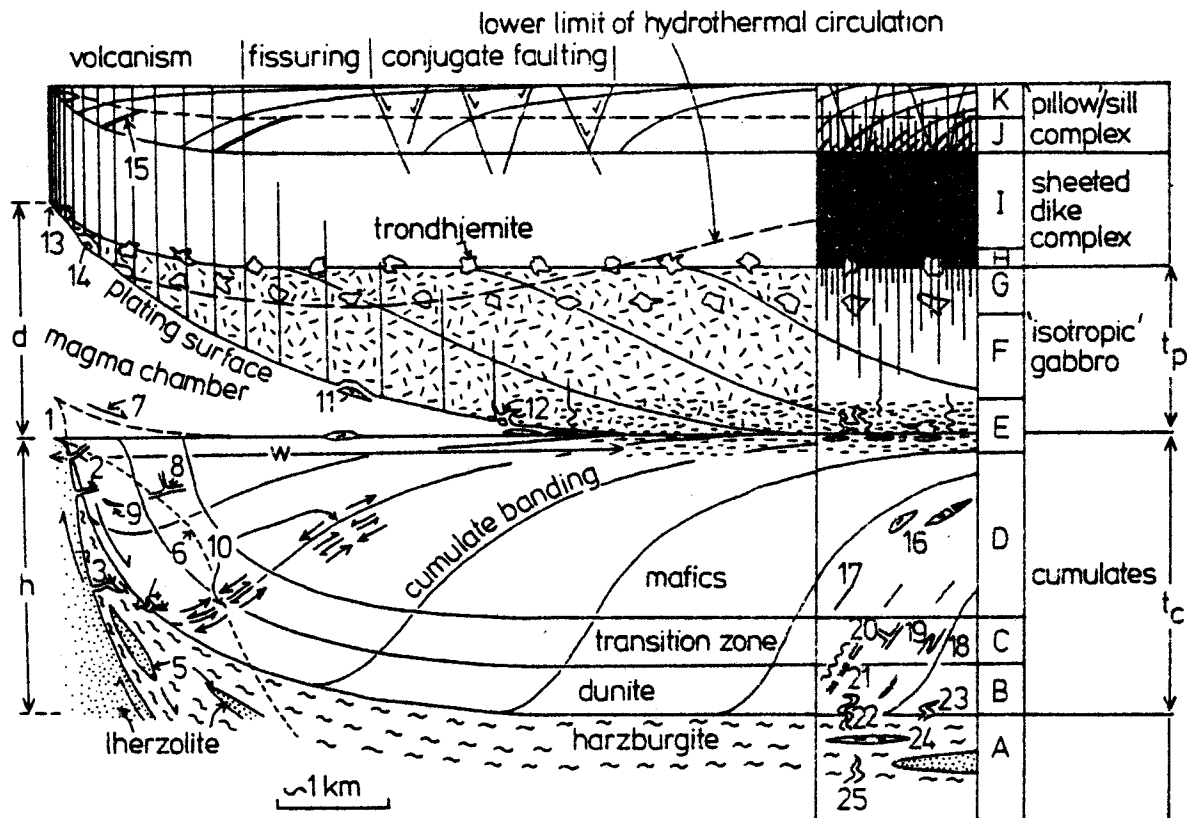


Fig. 1 (from Dewey and Kidd, 1977)

Proposed steady-state model for development of oceanic crust and upper mantle at accreting plate margin. No account is taken of topography, and surface of pillow complex is taken as level datum surface assuming perfect isostatic condensation.

in response to varying sedimentation rates and densities, 3) the termination of sheeted dikes at differing depths underplated by gabbro by a convective cooling lid accelerating from the ridge axis across a zone of decreasing dike injection, and 4) the presence of residual harzburgite which gets plated on to the ultramafic cumulates after yielding a basaltic melt to the magma chamber.

This mapping project was conceived to be a detailed investigation of the Table Mountain Mafic Suite to find out if the observed structure and petrology would be consistent with a differentially subsiding cumulate model.

Location, Exposure, and Setting

Table Mountain is the northernmost of the massifs of the Bay of Islands ophiolite complex on the western coast of Newfoundland. It lies south of Bonne Bay between the towns of Woody Point and Trout River, and within the boundaries of the Gros Morn National Park.

Table Mountain has almost 2,000 feet of vertical relief and is bounded on all sides by faults. Boulders rim the base of the cliff, and near Trout River Pond on the southern side of the massif, large landslides have a concave profile. Intermittent streams have incised the sides of the massif and the valleys vary in morphology from thin V-shapes to small cirque valleys.

The upper surface of Table Mountain is relatively flat. This is attributed to glaciation (Smith, 1958), although glacial polish and striations are rare. Outcrop exposure is

fairly good around the edge of the upper surface. Most of the interior, however, has either a felsenmeer texture, probably the result of frost action, or is covered by bog.

Vegetation is scarce on the ultramafic rocks, and is largely confined to the bog areas. The lack of vegetation has been attributed to both the toxic effects of chrome and magnesium silicates, and the lack of proper nutrients such as calcium. Vegetation is common in the mafic areas, but growth is stunted and has the typical krumholtz morphology attributed to severe winds, harsh winters, and inadequate nutrients.

Previous Work

The Bay of Islands ophiolite complex has been included in reconnaissance surveys of Western Newfoundland geology beginning with Logan's Geology of Canada (1863) and Howley's map (1906). More detailed surveys of the area were conducted in the 1930's and 40's by the Smithsonian Institute, and Yale and Princeton Universities. Many of these investigations had a sedimentological orientation, e.g., Schuchert and Dunbar, 1934; Troelsen, 1947; and Weitz, 1953.

The mafic and ultramafic rocks of the Bay of Islands received individual attention in the 1930's when they were mapped and described by Ingerson (1935, 1937), Buddington and Hess (1937), and Cooper (1936). Ingerson (1935, 1937) considered the massifs to be four separate layered Devonian lacoliths. Buddington and Hess (1937), investigating North Arm and Table Mountain, considered them one lopolith separated by westward thrusting, Cooper (1936) examining the southern

two massifs, concurred with Buddington and Hess, and mapped Blow Me Down and the Lewis Hills as dissected remnants of a continuous lopolith overlying schists from the Humber Arm Sediments and underlain by sediments and volcanics.

Smith (1958), on a 1:126,720 scale, mapped the northern massifs as part of a huge sill. His map was only slightly changed by Williams (1973), the most recently completed reconnaissance map. All four of the massifs are currently being mapped in greater detail (1:15,000) as part of a project under J. Dewey at the State University of New York at Albany to understand ocean crust accretion and ophiolite emplacement.

The Bay of Islands ophiolites have also been sampled for geophysical, structural, and geochemical studies particularly for comparison with and an understanding of ocean floor processes (e.g., Mercier, 1978; Salisbury and Christensen, 1978).

CHAPTER II

REGIONAL GEOLOGY OF WESTERN NEWFOUNDLAND

The Western Platform of Newfoundland consists of four distinct geologic units; a Precambrian crystalline basement, an autochthonous shallow water miogeoclinal sequence, an allochthon consisting of two stratigraphically correlatable sequences, and a neo-autochthonous shallow water sequence. (Fig. 2).

The Precambrian crystalline basement, consisting mainly of gneiss and granite, is exposed in the Indian Head and Long Ranges. Northeast trending tholeiitic mafic dikes cut the basement (Strong and William, 1972). Isotope determinations indicate ages of 950 m.y. for the granite (Neale, 1972) and 605 ± 10 m.y. for the dikes (Stukas and Reynolds, 1974).

The autochthonous groups consist of shallow water sediments unconformably overlying the basement. Good exposures have been described from Belle Isle (Williams and Stevens, 1969) and the Port au Port area (Whittington and Kindle, 1963; Stevens, 1970) and they are interpreted as sediments deposited on a rifted continental margin.

North and northwesterly derived, clastic sedimentation commenced in the Eo Cambrian. The oldest exposed group, the Bateau Formation, is cut by mafic dikes, which feed the overlying basalt flows of the Lighthouse Cove Formation. Clastic sedimentation continues with only minor disconformities until the mid-Cambrian when carbonate deposition predominated in the St. George and Table Head Formations. The carbonates are over-

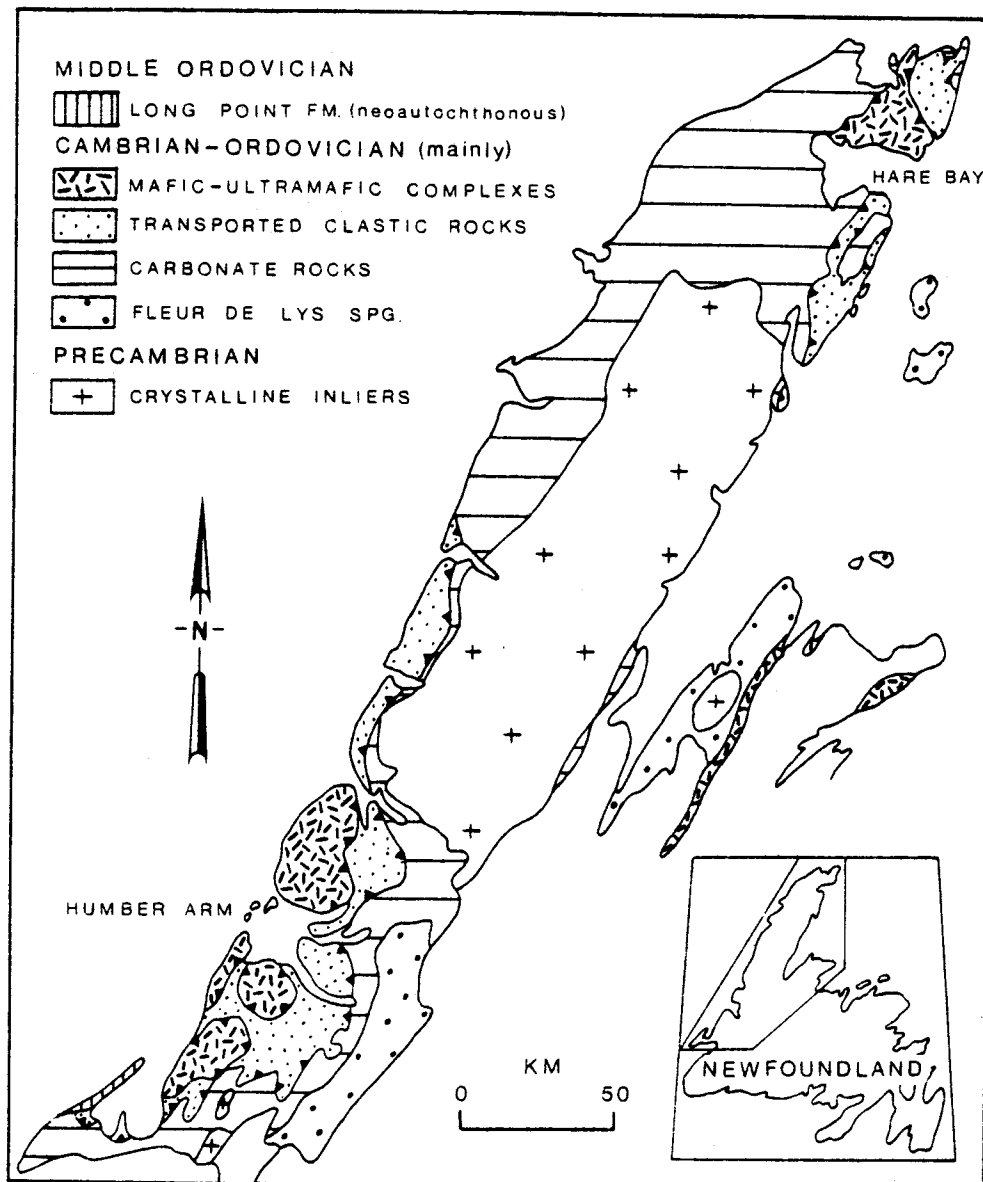


Fig. 2 (from Williams, 1975)

Generalized geology of the Western Platform of Newfoundland.

lain by the easterly-derived greywacke, shale and carbonate sequence of the Goose Tickle Formation.

The allochthon consists of two separate transported sequences, the Humber Arm allochthon in the south, and the Hare Bay allochthon in the north. The structural succession and nomenclature of these two sequences has recently been reviewed (Williams, 1975). The stratigraphy is correlatable between the sequences and melanges separate individual slices. The Humber Arm supergroup is composed of four or five separate slices; the Humber Arm slice, the Skinner Cove slice, the Old Man Cove slice, the Little Port slice, and the Bay of Islands slice. Lithologies of the Humber Arm slice show considerable lateral variation and have been separated into two subgroups. The Cow Head group, an outstanding sedimentary breccia composed of limestone blocks in a shaley matrix, occurs north of Bonne Bay, and ranges from Mid-Cambrian to Mid-Ordovician in age. The Curling group, south of Bonne Bay, contains three distinct lithologies, a westerly-derived quartzofeldspathic "flysch" overlain by a shale carbonate unit, successively overlain by an easterly-derived quartzofeldspathic flysch containing ophiolite detritus. Fossil ages indicate Mid-Cambrian to Late Arenigian deposition (Stevens, 1976).

The Skinner Cove Slice, overlying the Humber Arm Slice, consists of fresh alkalic mafic pillow lavas, red agglomerate, latite flows, and shale (with Ordovician faunas, Berger and Fahraeus, in Williams, 1975). Strong (1974), noting the continuous alkaline differentiation to trachytes suggested an

off axis spreading ridge origin. Alkalic basalts have also been described from an ophiolite sequence in Southern Turkey (Gracinsky, 1973).

To the east of and in steep faulted contact with the Skinner Cover Slice, is a unit of polydeformed greenschist cut by undeformed mafic dikes, the Old Man Cove Slice. This unit and the overlying Little Port Slice has recently been interpreted as having formed at a mid-ocean ridge and subsequently deformed in a transform domain of an oceanic fracture zone (Karson and Dewey, 1978).

The Little Port Slice is a complex unit of foliated gabbro and amphibolite, cut by quartz diorite and then intruded by porphyritic and nonporphyritic diabase dikes. Locally ultramafic rocks are common. These appear undeformed, but in thin section, show evidence of extremely high strain rates (Stevens, 1976, quoting A. Nicolas). Zircons in the quartz diorite yield ages of 508 ± 5 m.y. (Mattinson, 1975). Previous interpretations for this slice included deformed continental crust (Comeau, 1972; Williams and Malpas, 1972), a fragment of the Fleur de Lys (Dewey, 1974), and an oceanic accretion melange formed at the leading edge of an obducting oceanic plate (Malpas et. al., 1973).

The structurally highest slice of the Humber Arm Allochthon is the Bay of Islands Slice. This contains sediment, pillow basalts, sheeted dikes, gabbros, and ultramafics, and is therefore a complete ophiolite sequence. A thin metamorphic aureole occurs at its base and is cut by the melange unit which separates

it from the lower slice. The aureole may indicate detachment of hot ocean floor (Dewey and Bird, 1971; Williams and Smyth, 1973). Amphiboles from the aureole give isotopic ages of 460 ± 5 m.y. (Dallmeyer and Williams, 1975).

The Hare Bay Allochthon contains six separate slices. The individual slices are roughly correlatable with the Humber Arm Allochthon. A detailed map of this area is available from the Canadian Geological Survey Open File (Bostock et. al., in press).

The Northwest Arm Slice is correlative both in age and lithology with the Humber Arm Slice. Its lithologies, however, have been severely disrupted and occur as blocks in a shaly matrix. It is overlain by the Maiden Point Slice, which has a base of pillow lavas, agglomerate, and tuffs. This is overlain by greywackes, slates, and quartz pebble conglomerates. The granites, blue quartz, and metamorphic detritus within the conglomerate suggest a Precambrian basement origin. Sedimentary structures suggest a westerly source. Both sediments and volcanics are cut by gabbros and diorites. The overlying Grandois Slice contains two structurally superimposed units, a lower greywacke and polymict conglomerate, and an upper unit of sandy limestone and brecciated quartzite, siliceous limestone and shale. The Milan Arm melange separates the Grandois and Cape Onion Slice. This contains a wide variety of exotic blocks, including some that are lithologically similar to the Little Port Complex, in a green and black shale matrix. The Cape Onion Slice is similar to the Skinner Cove

Slice in age, chemistry and lithology. Like the Humber Arm Allochthon, the Hare Bay Allochthon is capped with an ophiolite sequence, although not a complete one. The St. Anthony Slice contains mafic agglomerates and pillow lavas, which grade upward both structurally and metamorphically to greenschists and amphibolites and is capped by ultramafics.

Logan, as head of the Canadian Geological Survey in the Mid-Nineteenth Century, recognized the geological importance of Western Newfoundland and employed Richardson to outline the basic geological framework (Billings, 1862; Logan, 1863). With this information, Logan correlated the Western Platform sequences with those of the Quebec and Taconic groups. He explained these groups as deep water sediments, transported over their synchronously deposited shallow water equivalents, and expected this thrust to appear in the Bonne Bay area, which it does. Interpretations for and against this hypothesis flourished during the next century (e.g., Schuchert and Dunbar 1934, Cooper 1937, Betz 1939).

Current understanding of the Western Platform concurs with Logan and began, in part, with a reinterpretation of the Taconics (Zen 1961), the suggestion that both the Taconic and Humber Arm Groups were large klippe that had undergone extensive mid-Ordovician westward transport, and that the uppermost igneous assemblages were included in that transport (Rodgers and Neale, 1963).

The uppermost mafics were recognized as a separate slice in 1968 (Church and Stevens, 1968) and termed ophiolites. As

other ophiolites were interpreted as fragments of oceanic crust (Davies, 1968; Gass, 1968; Reinhardt, 1969), and the similarities between the ophiolites were recognized, the Bay of Islands ophiolites were interpreted as ocean crust (Stevens, 1970; Dewey and Bird, 1971; Church and Stevens, 1971). Recent work on the Bay of Islands has focused on structural and petrologic processes at ocean ridges (e.g., Dewey and Kidd, 1977; Casey, 1978; Rosencrantz, 1978; Karson and Dewey, 1978).

Current Interpretations

The Western Platform is currently interpreted as a Cambrian-Ordovician Atlantic-type continental shelf-margin sequence which became compressed in the Mid-Ordovician during the contraction of the proto-Atlantic (Wilson, 1966), subsequently named Iapetus (Harland and Gayer, 1974). Different schools of thought exist regarding, the type and occurrence of events, the direction of subduction, and the extent of the Iapetus ocean and its relationship to the ophiolites. An Atlantic type, stable continental margin was created by rifting in early Cambrian time. The previously described sedimentary facies were deposited on this margin at increasingly greater depths (Fig. 3).

The question of subduction direction has not been resolved. Dewey (1969) and Bird and Dewey (1970) show the destruction of Iapetus via a west dipping subduction zone. Fragmentation of the ocean and the development of rear arc and intra arc basins have also been suggested (Dewey and Bird, 1971; Dewey, 1974; Bursnall and deWit, 1975; Kennedy, 1975). Protagonists of east

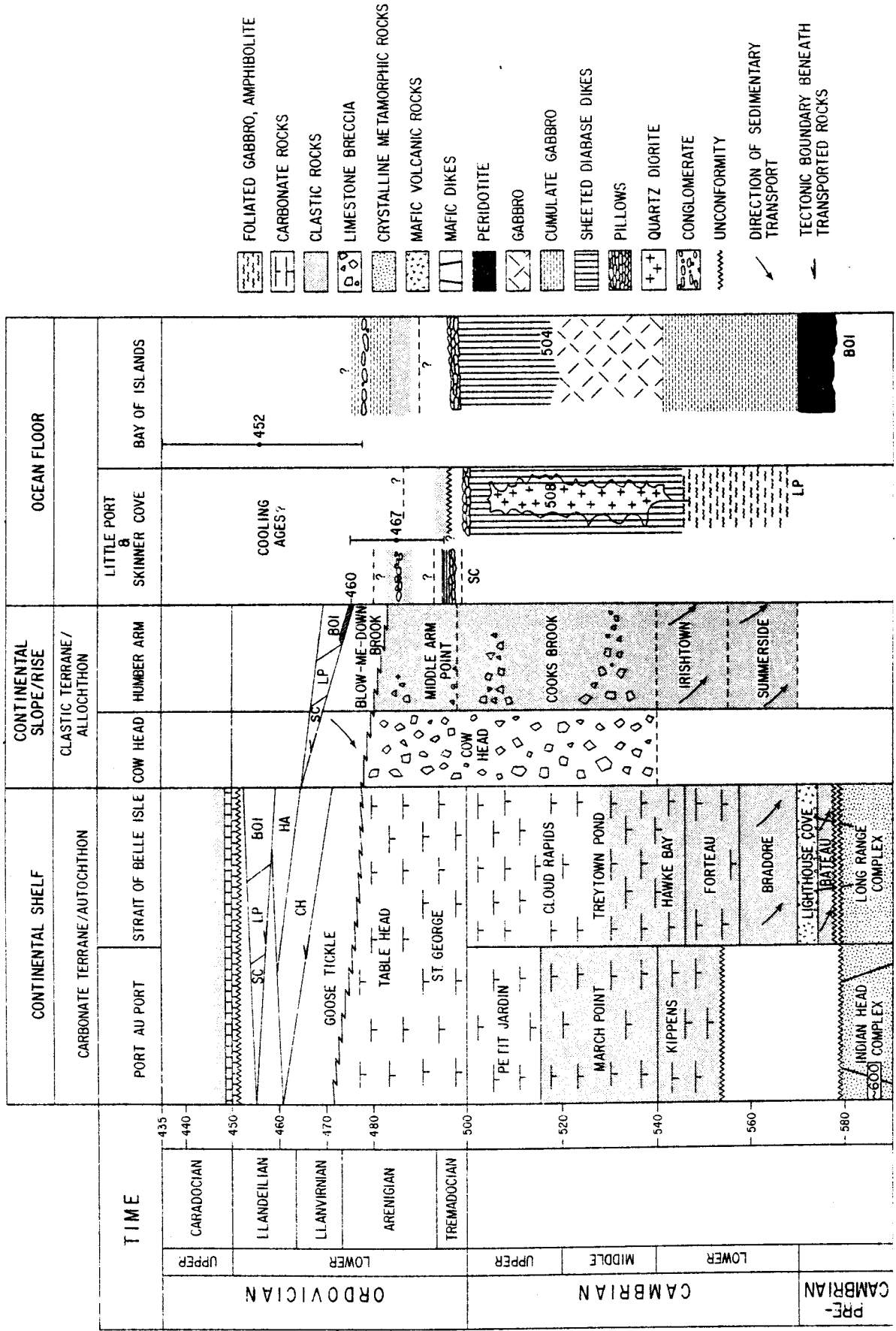


Fig. 3 (from Williams, 1971; Karson, 1975; and Karson and Dewey, 1978) Restored generalized stratigraphic and structural relations of Upper Precambrian to Middle Ordovician rocks of the Bay of Islands area.

dipping subduction (Church and Stevens, 1971) favor a continuous Burlington Peninsula-Western Newfoundland ophiolite sheet, disrupted by tectonism and erosion. Recent investigations in Notre Dame Bay (Nelson and Casey, in review) suggest eastward dipping subduction for that area. Other studies (Kidd, 1977) based on equally convincing evidence favor the opposite westward dipping subduction which may be extended to include all of Western Newfoundland.

Present day subduction patterns in active regions such as New Zealand and Indonesia are complex and variable. In light of this it is certainly reasonable to expect similar complications in Ordovician subduction zones. It is also not clear whether or not the Bay of Islands ophiolites were part of the larger Iapetus ocean or a smaller arc related basin.

A comprehensive suggestion for the Bay of Islands ophiolites and Costal Complex (Karson and Dewey, 1978) suggests formation during the latest Cambrian as part of an earlier Ordovician ridge/ridge transform fault. By Tremodocian time, the oldest parts of the Costal Complex would have passed from the transform segment to the non-transform segment of the fracture zone, and the Skinner Cove Sequence and associated graptolitic shales would have accumulated.

Possibly, during early Arenigian time, reorientation of relative motion vectors for the two plates nucleated oceanic thrusting. By late-Arenigian time these ultramafics had been thrust across the higher level ocean floor rocks producing the basal metamorphic aureole of the allochthon. Compressional

movement proceeded, during which time sedimentation continued on the continental rise in front of the allochthon. The continental shelf may have been uplifted to produce the St. George-Table Head disconformity. The allochthon, most likely consisting of the complete allochthonous assemblage, probably reached the continental shelf by late Llanvirnian time, shedding clastics of the Goose Tickle Formation (flysch) westward over the Table Head Formation (limestones). The complete allochthonous assemblage was in place by late Llandeilian time and deposition of the carbonates of the neautochthonous Long Point Formation began.

CHAPTER III

PETROGRAPHY

Introduction

The mafic suite of Table Mountain is a medium to coarse grained layered assemblage consisting of gabbro, hornblende gabbro, olivine gabbro, troctolite, anorthosite and pyroxenite. These overlie an assemblage of peridotites. Compositional and grain size changes are both sharp and gradational. Over most of the area, grain size is relatively constant. Alteration products indicate an epidote-amphibolite grade of incipient metamorphism.

This section starts with general rock descriptions and is followed by detailed mineral descriptions. Table 1 lists modes and grain sizes for samples of each of the rock types. Fig. 4 shows the sample locations.

Rock DescriptionsGabbro

Medium to coarse grained gabbros make up the majority of the Table Mountain mafic suite. They weather grey-green, the color being dependent upon the relative proportion of plagioclase to clinopyroxene. Because the clinopyroxene is more resistant to weathering than plagioclase, the rocks have a corrugated, rough surface. Cleavage faces may be seen on the larger clinopyroxenes. Plagioclase weathers a chalk white, making layers, dikes and minor structural features, such as folds, easily detectable.

Modal Compositions* From
The Table Mountain Mafic Suite

| Sample Number | Points Counted | % Composition | | | | | | | An | Sub-Area | Comment |
|---------------|-------------------|----------------|----------------|----|-------------|----------------|---------------------------------------|--|----|----------|---|
| | | plag | cpx | ol | hb opaques | chl. | other alter. | | | | |
| 130 | 0 | 99 | | | | | | | 51 | II | Anorthosite, cataclastic areas |
| 169 | 366 | 42 | 19 | 31 | 5 | | 3 | | 67 | I | Gabbro subpolygonal microfolds |
| 171 | 354 | 63 | 25 | | .6 | | 6 | | 68 | V | |
| 188 | 370 | 60 | 30 | | | | 9 | | 65 | V | Subpolygonal |
| 204 | 364 | 34 | 18 | | | 33 | 9 | | 71 | IV | Hornblende gabbro |
| 205 | 604 341 945 | 45 54 48 | 18 14 17 | | 4 1 3 | 25 28 26 | 7--Fine Grain 3--Coarse Grain 6 | | 64 | IV | Hornblende gabbro, rapid grain size change |
| 215B | 325 | 35 | 5 | 52 | | | 7 | | 60 | IV | Troctolite, some plagioclase subgrain and deformation |
| 240 | 347 | 58 | 37 | | .9 | | 5 | | 65 | V | Gabbro polygonal, weak dimensional preferred oriented |
| 253A | 349 | 57 | 16 | 26 | 1 | | | | 70 | V | Olivine gabbro |

*Determined From Point Counting

TABLE I (continued)

| Sample Number | Points Counted | % Composition | | | | | | | An | Sub-Area | Comment | |
|---------------|----------------|---------------|-----|----|----|---------|------|--------------|----|----------|---------|---|
| | | plag | cpx | ol | hb | opaques | chl. | other alter. | | | | |
| 287 | 318 | 51 | 41 | | | 1 | | | 7 | 67 | I | Gabbro |
| 308 | 366 | 32 | 22 | 37 | 2 | | | | 7 | 72 | | Troctolite, large cpx grains |
| 309B | 376 | 59 | 3 | 38 | | | | | 71 | | V | Layered troctolite, some recrystallization, inequant grain size |
| 323C | 471 | 49 | 33 | | 9 | .2 | | | 10 | 67 | VI | |
| 324 | 308 | 29 | 29 | | 39 | 2 | | | 6 | 67 | VI | Hornblende gabbro poikolite, very weak plag. and cpx layering |
| 368 | 362 | 56 | 2 | 38 | | | | | 4 | | IV | Troctolite |
| 594C | 371 | 48 | 17 | | 27 | .3 | | | 8 | 56 | III | Hornblende gabbro, high strain zone |

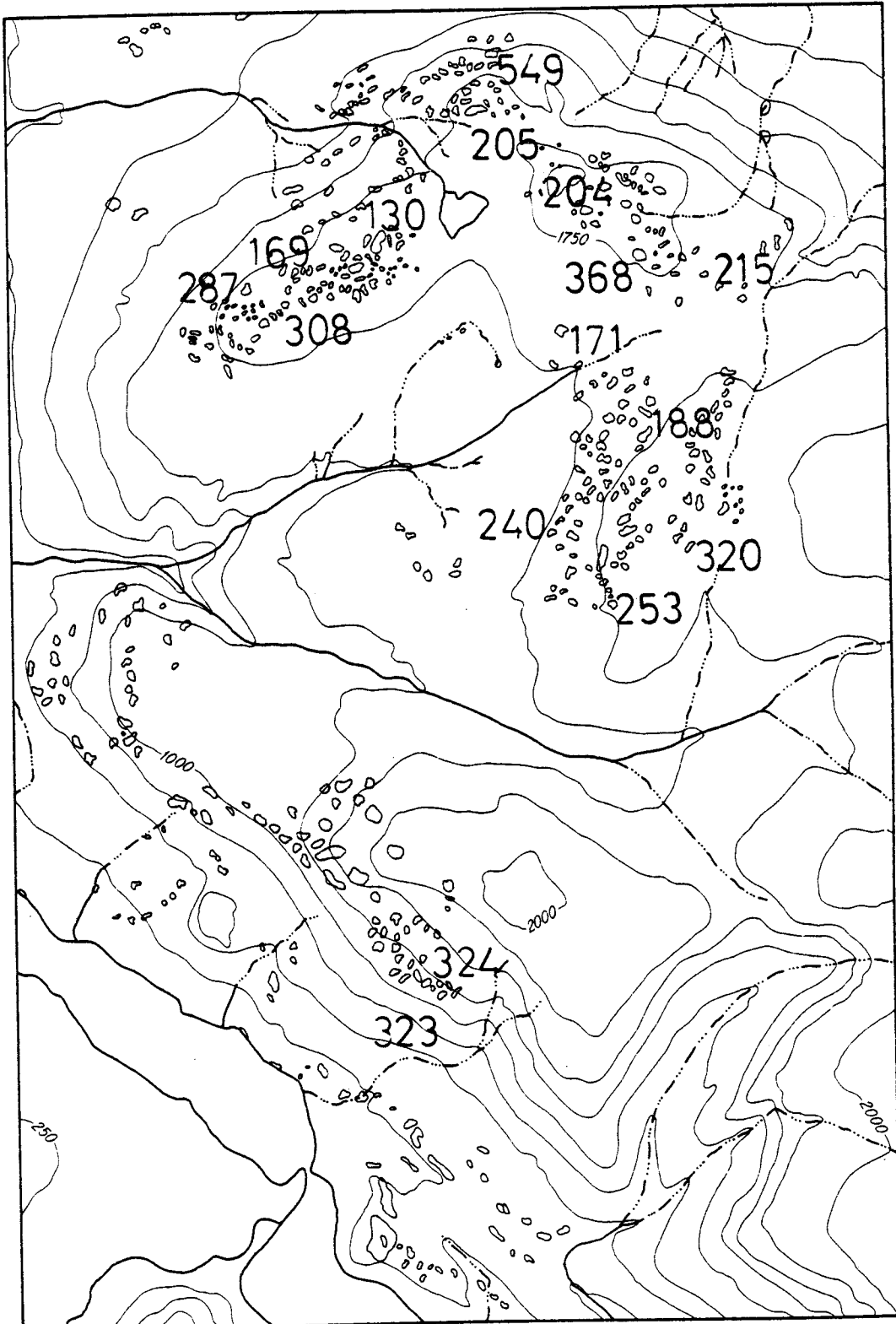


Fig. 4

Location map for modal analysis samples listed in Table 1.

Microtextures are typical of those described as xenomorphic granular, granoblastic or adcumulate.* Grain boundaries between minerals of similar composition are usually straighter than those between mineral grains of different compositions.

Hornblende Gabbros

Hornblende gabbros are present in restricted areas of the Table Mountain massif (see Map III). In hand specimen they are a charcoal grey brown or consist of alternating black and white specks and lines. The coloring is a function of grain size and mineral distribution.

The hornblende grains are shiny black on fresh cleavage faces and dull black on weathered faces. They are accompanied by grey-green pyroxenes. Plagioclase weathers chalky white. Fresh cut surfaces are dark grey green with black flecks.

A very coarse grained variety, containing hornblende crystals 2 - 5 cm. long in a matrix of plagioclase, outcrops at the edge of one hornblende gabbro area. In all but the most fine-grained rocks, hornblende and pyroxene grains have preferred orientation defining a mineral lineation.

The hornblende gabbros may be separated into two groups on the basis of hornblende morphology. Type one contains a

*Adcumulate refers to an originally cumulate crystal which has grown since deposition by the addition of material of the same composition. The growing grains mechanically push out the intercumulus liquid. (Wagner et. al., 1960)

higher percentage of hornblendes, which occur as large (6 - 8 mm.) ophitic grains enclosing sub- and anhedral plagioclase and clinopyroxene. Boundaries between these grains and hornblende are rounded and lobate (Fig. 5). There is no preferred dimensional orientation or layering in the grains within the hornblende.

Type two contains interlocking separate hornblende grains. Hornblende does not surround the plagioclase and pyroxene grains. The distribution appears to be random and a mosaic texture predominates. A weak preferred dimensional orientation and mineral layering is seen in some thin sections. Both a strong lineation and compositional and grain size foliation are observed in hand specimen. Although the hornblendes in Type II are considered primary, the polygonal texture suggests recrystallization. This could have occurred under amphibolite facies metamorphism where hornblendes and pyroxenes may co-exist.

Both types show strain in the form of undulatory extinction, mechanical twins, deformation bands, and intra- and interfolial cracks. Type II contains cataclastic zones.

Olivine Gabbro

Olivine gabbro weathers to both a dark grey-green and an orange-brown-grey depending upon the percentage of olivine. In the field it is often virtually indistinguishable from the more clinopyroxene-rich varieties of gabbro.

Serpentine minerals forming after olivine have obscured many of the primary textures. One sample from a dike which is

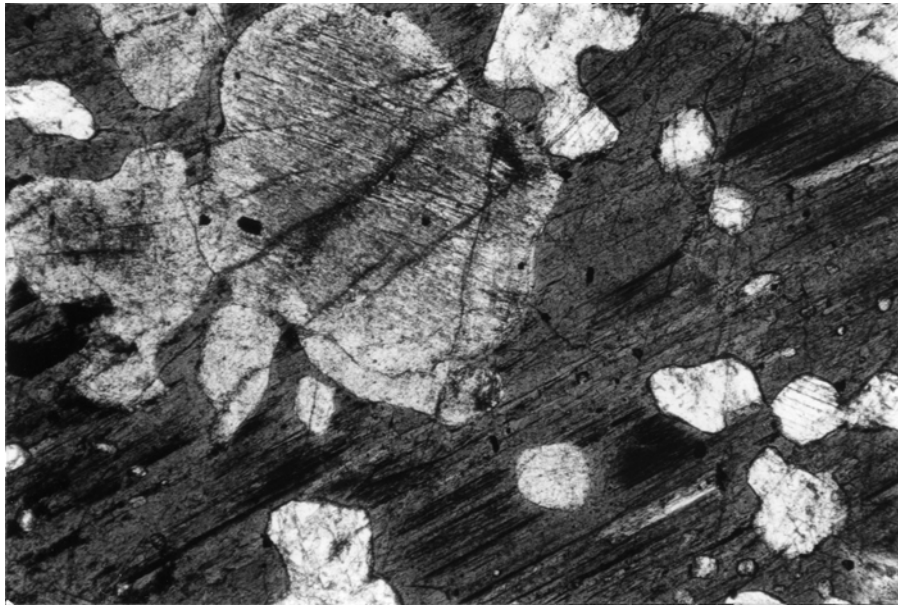


Fig. 5
Ophitic hornblende gabbro containing rounded and lobate plagioclase grains.



Fig. 6
Olivine gabbro with texture indicating simultaneous crystallization of grains.

sub-parallel to layering is remarkably fresh and must have been emplaced post-serpentinization. Throughout this sample, minerals of one composition curve around or fill interstitial spaces of a mineral of a different composition. No consistent sequence or order of crystallization is apparent. In another area, three twinned plagioclase grains, separated by several olivine and clinopyroxene grains, go to extinction at the same time, (Fig. 6). These textures are clearly indicative of simultaneous crystallization and are similar to what might be expected in adcumulate growth such as seen in the Rhum Ultrabasic Complex (Wager and Brown, 1960) or a cumulate with resorption overgrowth, such as seen in the Baie Verte Lineament (Kidd, 1973).

Opaques occur as 'accessory minerals with euhedral to anhedral shapes. They have the same relationship to the rock as a whole, as the other minerals, such as bending around a plagioclase and filling interstitial areas.

Troctolite

Troctolite weathers to a dark-red brown, with white nubs on the surface yielding a very rough texture. The nubs are formed by plagioclase grains which are more resistant to weathering than olivine. The distinction between troctolite and feldspathic dunite is usually placed at ten percent calcic plagioclase.

Troctolite initially occurs as 10 - 20 cm. thick layers and lenses within the gabbros and increases in abundance as the ultramafics are approached. Thick layers (1 - 3 m.)



Fig. 7 (opposite)
Anorthosite layer parallel to layering.



Fig. 8
Anorthosite wedging between troctolite layers.

such as those exposed in the S.E. edge of the map area are usually accompanied by equally thick anorthosite layers.

Mineral layering is observed on the thin section scale. Most samples are extensively serpentized. There is no evidence for either olivine or plagioclase being interstitial. A few small grains and irregular patches of clinopyroxene are present. These may have resulted from an olivine-plagioclase reaction during the rock formation.

Opaques are common but, because of the serpentization, most of them appear secondary. Euhedral and subhedral red chrome-spinel grains are observed in many samples. Most grains are about .3 mm. in size.

Anorthosite

Anorthosite, in association with troctolite, occurs as thick (1 - 3 m.) bands of limited extent in three forms; parallel to layering (Fig. 7), wedging between troctolite (Fig. 8) and engulfed/engulfing troctolite (Fig. 9). It also occurs as thin (2 - 6 cm.) dikes, parallel to and cutting both mafic and ultramafic layering (Fig. 10). Contacts with other rock types are sharp. Anorthosite weathers to a chalk white. In thin section grain boundaries have a mosaic texture suggesting possible adcumulate growth.

Pyroxenite

The pyroxenite is primarily clinopyroxenite and weathers to a stubby, granular avocado green. It occurs mostly as thin layers and dikes within the transition zone mafics and ultra-



Fig. 9 (above)
Troctolite engulfing anorthosite.

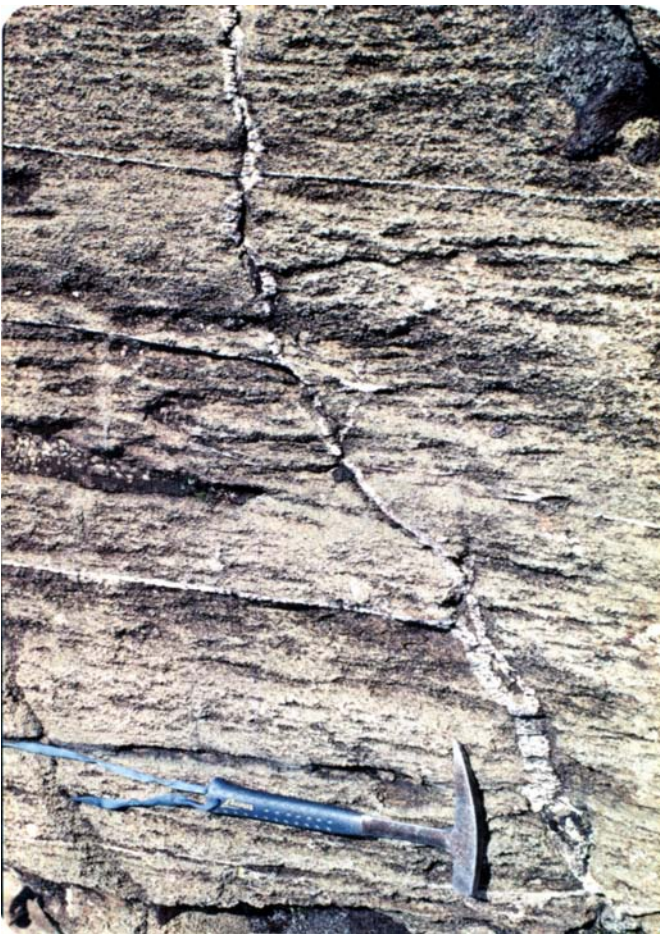


Fig. 10 (opposite)
Anorthosite dikes cutting both
mafic and ultramafic layering.

mafics. A small isolated body approximately 3 m. in diameter occurs at the top of Table Mountain.

In addition to clinopyroxene, minor amounts of orthopyroxene, plagioclase, and interstitial olivine are present. The plagioclase occurs in clusters surrounding some clinopyroxene grains. They are twinned and show almost no undulatory extinction. Some pyroxene grains contain fragments of adjacent pyroxenes (Fig. 11). This is especially, although not exclusively, true where cleavage traces are intersecting at high angles. Some olivines occur as small rounded grains within the clinopyroxenes. Alteration in these rocks is minimal.

Peridotites

Peridotites compose the majority of Table Mountain. They weather orange and red with brown, the color and texture being dependent upon the relative proportions of olivine and pyroxene. Chromitite is also present as thin layers in small areas, usually within dunite bands.

Late Dikes

A fine grained dike material with euhedral phenocrysts of clinopyroxene and plagioclase interfingers with the gabbro (Fig. 12). Very thin chilled margins are present. Flow is apparent by the subparallel alignment of the plagioclase laths.

The dike material weathers to a smooth, dull grey-green. Some of the phenocrysts are fresh, others have completely altered to chlorite. The fine grained matrix shows smectite alteration. The dike intrusion occurred pre-prehnite veining.

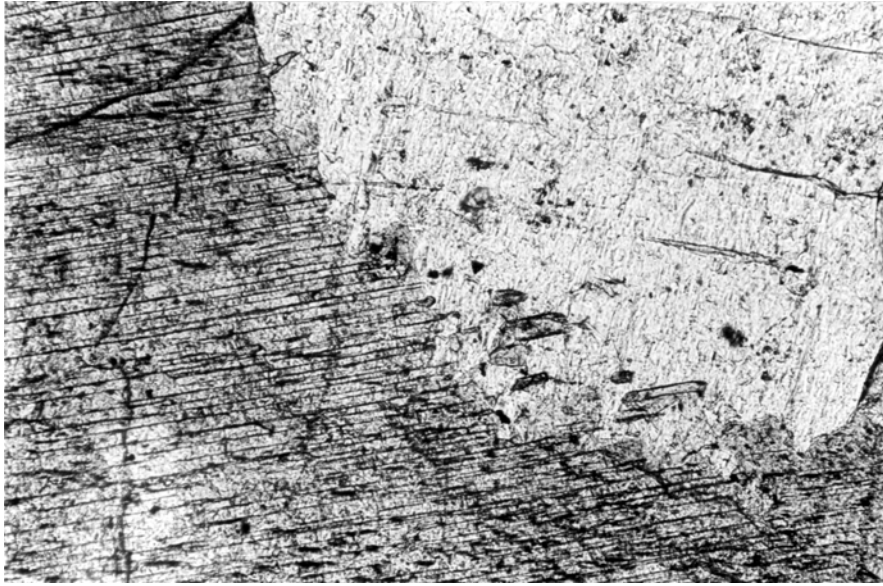


Fig. 11
Pyroxene fragments in adjacent pyroxene grains.

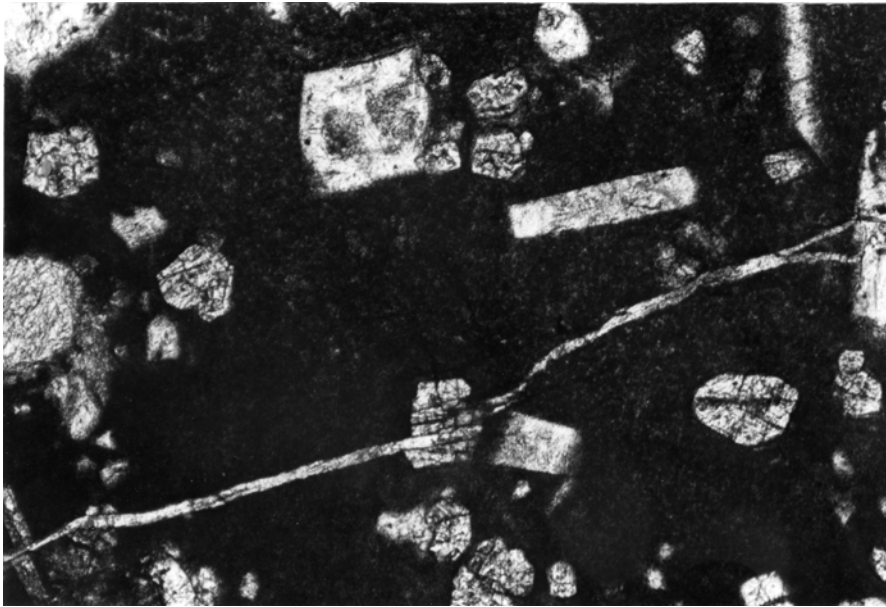


Fig. 12
Fine grained, phenocryst-bearing dike.

Primary Mineral Assemblage

Plagioclase

Plagioclase is the most common mineral. The maximum symmetrical extinction angle on albite twins yield compositions between An₆₄₋₇₁. Smith (1958) determined that the plagioclases were bytownite, An₇₀₋₈₀ with most lying between An₇₀₋₇₅. He does not state what method is used for his determinations. Some samples were analyzed with X-ray powder diffraction. Comparative studies between optic and electron microprobe determinations have shown that optic determinations are frequently five to ten percent lower. This is attributed to the difficulty in finding the largest extinction angle. The plagioclase compositional variation is not systematic within or between rock types from Table Mountain. No optic evidence for zoning is present.

Grain size varies from approximately 0.3 to 3 mm., with most grains being between 1 - 2 mm. Some grains display a weak dimensional preferred orientation. The majority of plagioclase/plagioclase grain boundaries are straight with triple point junctions. A tabular shape predominates. These are similar in appearance to adcumulates from the Rhum Ultrabasic Complex (Wager and Brown, 1967).

Small rounded and lath shape grains are frequently contained in clinopyroxene and hornblende (Fig. 13). In turn, small rounded grains of clinopyroxene, olivine and a few anhedral opaque grains lie within plagioclase grains (Fig. 14).

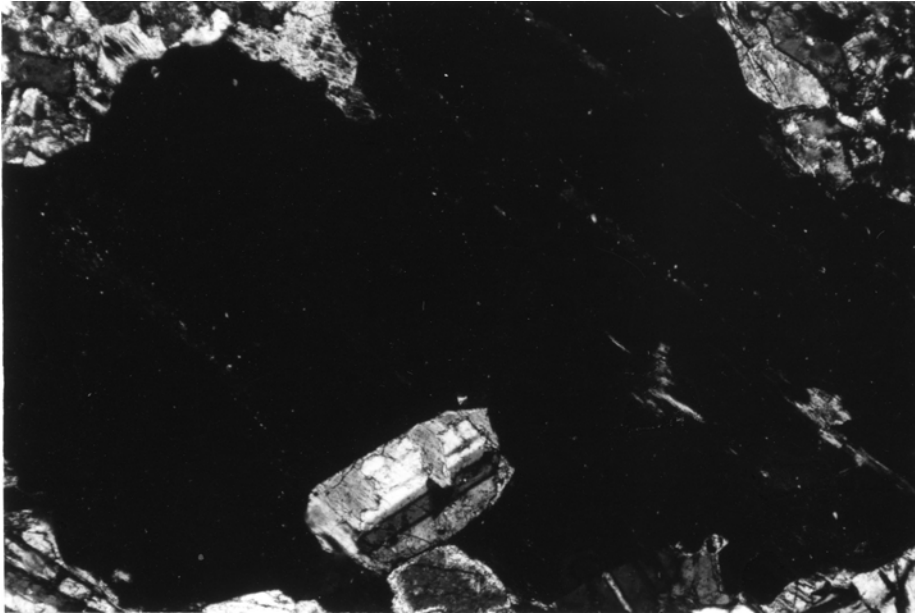


Fig. 13
Twinned plagioclase lath in clinopyroxene grain.



Fig. 14
Rounded clinopyroxene grain in twinned plagioclase.

Growth and mechanical twins¹ are common. Undulatory extinction of varying intensities is present in a large percentage of grains. Randomly-oriented grain microfractures are prevalent, many extend beyond the grain boundary.

Plagioclase alters to epidote, sericite, smectite, and sometimes to a variety of hydrogarnet. The extent of alteration varies widely between samples. Incipient alteration to chlorite is present along grain boundaries, in fractures, and sometimes in random patches within the grain. It is possible that the alteration patches were areas of high strain. There are two lines of evidence for this. One is that the more highly strained grains show a higher percentage of altered areas. This strain, however, may itself be an effect of the alteration. The other evidence comes from mylonite zones. There are few large plagioclase grains in these areas, but in one large tabular grain the alteration has occurred in an almost conjugate fashion. If the grain shown in Fig. 15a is considered to consist of four conjugate wedges, the two compressive direction wedges are less altered than the two extensional wedges which would have had to accommodate the displacement. Another large plagioclase grain oriented at approximately 45 degrees to the layering contains three parallel fractures (Fig. 15b). The alteration in this grain is progressive. The upper third is almost completely altered, the middle third is approximately fifty percent altered, and the

¹The distinguishing criteria between the two types of twins will be discussed under microstructure.

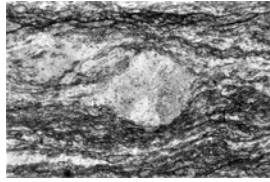


Fig. 15a

Large plagioclase grain in mylonite showing alteration which is preferentially developed in a conjugate pattern in the areas experiencing the most compression.

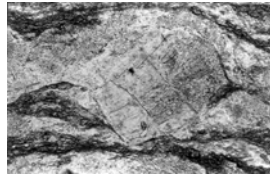


Fig. 15b

Large plagioclase grain showing preferential alteration at the top of the grain which would have experienced the most stress.



Fig. 16

Mosaic texture suggesting recrystallization around the edges of large clinopyroxene grain.

lower third is unaltered. If material were moving around and past the large grain, and principles of fluid mechanics are applied, the upper surface should be experiencing the most force (for both laminae and turbulent flow). Therefore the upper surface should be the most altered which it is.

Clinopyroxene

Clinopyroxene is the second most abundant mafic mineral. In thin section it is an unpleochroic light brown grain usually showing well developed cleavage and/or diallage parting.* It has a diopside-augite composition ($2V \sim 54$, CAZ 45-50, mid and upper second order maximum birefringence). No optically detectable zoning is present, and with the exception of that in pyroxenite, no optic variation was distinguishable between rock types. Clinopyroxene in pyroxenite, however, is more diopsidic and was determined (Smith 1958, Malpas 1976) to be almost pure diopside. Twinning is very rare in all of the clinopyroxenes.

There is a tremendous range in clinopyroxene grain size, from small 0.1 mm. grains included in plagioclase to interstitial grains ranging from 0.5 to 50 mm. across. The clinopyroxenes occur as individual sub- and anhedral grains. Large areas of mosaic texture suggest either adcumulate growth or recrystallization of some of the larger grains. Grains of olivine and plagioclase frequently occur within clinopyroxene grains. These included grains commonly show alteration to

*Diallage is parting only parallel to the front pinacoid (100) and hence may only be accurately determined with the U-Stage (A. Miyashiro, pers. comm.).

serpentine minerals and chlorite around the grain boundary, even when the rest of the pyroxene shows little or no alteration (Fig. 13). The larger grains show the most strain features, having deformation bands, including kink bands, undulatory extinction, and fractures. In some cases, the large grains are surrounded by smaller mosaic texture grains which clearly suggest recrystallization (Fig. 16). Random intragrain cracks are not as frequent as they are in plagioclase.

Clinopyroxene alteration begins along cleavage traces, grain boundaries, kink bands and fractures. Alteration minerals include chlorite, blue-green and pale brown hornblende, actinolite, serpentine minerals, and magnetite.

Hornblende

The distinction between primary and secondary hornblende is subjective. Primary hornblende is here taken to be the poikilitic and granulite facies hornblendes previously described. These hornblendes have their own crystal morphology, i.e., they do not appear to be pseudomorphs after pyroxene, and have a darker red-brown pleochroism than those hornblendes I consider secondary.

The morphology of primary hornblendes has already been described under hornblende gabbro. These hornblendes have $c\wedge z$ between $18-30^\circ$ and $2V \sim 70^\circ$. The hornblende shows varying degrees of alteration, but it is usually relatively fresh. It alters to blue-green hornblende, actinolite and chlorite.

Olivine

Olivine is a major constituent of troctolite and a sig-

nificant ingredient of olivine gabbro. It is slightly more iron rich than olivine in the ultramafics and has a chrysolite composition (Smith, 1958). In most grains the original shape is obscured by serpentine minerals. In the one sample, from a later dike, where olivine is remarkably fresh, it occurs as rounded and anhedral interstitial grains. With the exception of the fresh sample (described in the olivine gabbro section), olivine does not incorporate grains of other minerals within its boundaries. In some troctolite samples, however, several olivine grains may be seen almost surrounding a plagioclase grain.

Orthopyroxene

Orthopyroxene is only present in some pyroxenites. It occurs as an- to subhedral grains with a weak pink pleochroism and $2V \sim 60^\circ$.

Since the pyroxenites are relatively fresh, alteration is only incipient and is the same as that of the clinopyroxenes.

Accessory Minerals

Opaques and chromite are the only accessory minerals. Most of the opaques are magnetite. A few grains of ilmenite have been identified, but no systematic attempt has been made to distinguish them. The opaques occur as eu to subhedral grains within other minerals, along grain boundaries, as exsolution products in clinopyroxene and with serpentine alteration minerals. Euhedral and subhedral grains of a red-chrome spinel are present and range in size from 0.1 to 0.3 mm. They may be cracked and filled with alteration minerals.

Secondary Mineral Assemblage

Chlorite

Chlorite is the most abundant alteration mineral. Several different varieties are present in plagioclase. Anhedral, unpleochroic, pea-green chlorite occurs with epidote along grain boundaries. A fibrous, pale-green pleochroic chlorite forms pseudomorphs after clinopyroxene in many samples (Fig. 17). When this occurs the more well developed chlorite grains are observed in the center of the relict clinopyroxene, whereas the rim appears unaltered. This has been termed atoll-structure (Edwards, 1960) and is attributed to compositional zoning (Rast, 1965).

Large anhedral patches occur in the more severely altered samples. These range in color from strongly pleochroic pale blue to unpleochroic yellow-green and colorless varieties. Birefringence is low and anomalous blue and purple colors are common.

The presence of chlorite along plagioclase grain boundaries indicates that there has been a large degree of element migration.

Epidote

Plagioclase alters in part to epidote. In most instances, the epidote is not well-developed. It is most commonly observed as granular aggregates of high relief within plagioclase grains and is usually accompanied by other alteration minerals.

Sericite

Sericite occurs in patches and often pervades entire plagioclase grains. As mentioned earlier, there appears to be a relationship between strain and at least incipient sericite alteration. In more severely-altered samples, large areas of sericite occur.

Smectite

Fine grained pale brown and yellow smectite replaces some plagioclase. It occurs as a fine dusting on some grains and as large anhedral patches, usually in association with other alteration minerals.

Hydrogarnet

Plagioclase in the troctolites shows some alteration to a milky white weathering variety of hydrogarnet. It is a low T, silica-rich tri-calcium hexahydrate (Malpas, 1976). Euhedral through anhedral grains occur. It is a common alteration mineral of gabbroic rocks where the redistribution of calcium has taken place and frequently occurs in rodingite (Deer, Howie, and Zussman, 1975).

Actinolite

Actinolite and tremolite occur as; fibrous needles randomly oriented in chlorite, growing out of clinopyroxene deformation bands, pseudiomorphs after clinopyroxene, and in large acicular patches often banded by chlorite.

Hornblende

Blue-green hornblende occurs as an alteration mineral of



Fig. 17
Fibrous chlorite pseudomorphs after clinopyroxene.

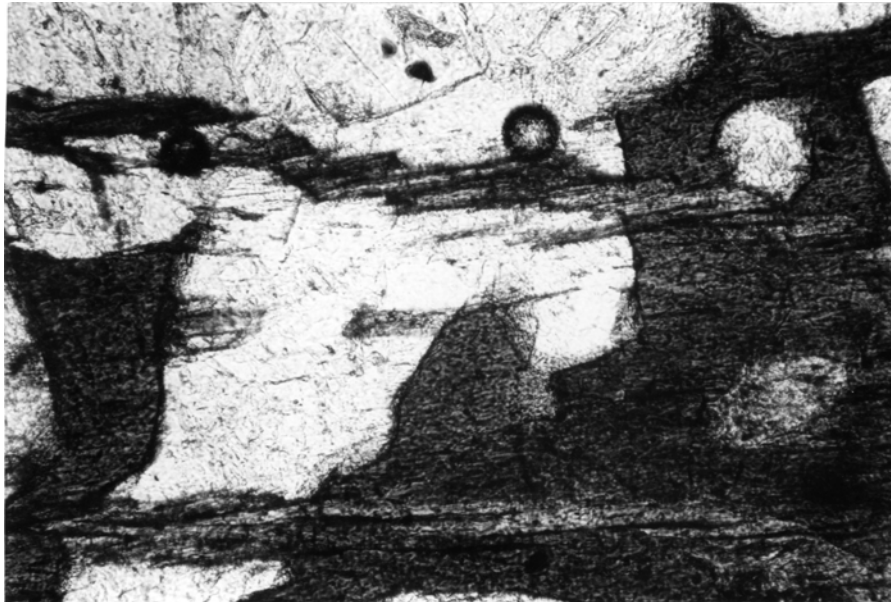


Fig. 18
En-echelon blue-green hornblende laths filling crack in hornblende gabbro.

clinopyroxene and brown hornblende, forming euhedral laths, an echelon along fractures (Fig. 18) and projecting from mafic minerals into plagioclase. It also forms anhedral patches adjacent to actinolite and along grain boundaries.

Brown hornblende occurs in irregular anhedral patches adjacent to clinopyroxene grain boundaries and fractures. In most instances it shows only limited development. It is not clear whether it has a primary or secondary origin.

Serpentine Minerals

Olivine alters to serpentine minerals and magnetite. These form anastomosing areas around the olivine grains, in extreme cases obliterating any relict of the original grain.

Even a small amount of serpentinization produces expansion fractures. These fractures penetrate adjacent grains. If a single olivine grain, such as one in a plagioclase, is being altered, the microfractures radiate in a random circle from the olivine grain. Where the olivine is layered, the cracks are perpendicular to the layering. The expansion fractures serve as conduits for further alteration of the cracked grain. Clinopyroxene is more resistant to fracturing than plagioclase.

Prehnite

Prehnite occurs as a secondary mineral in many of the cross-cutting thin veins and in more intensely altered areas and are sometimes accompanied by zeolites. Reniform globular masses are common. Some of the thicker prehnite veins contain tension gashes with calcite filling.

Zeolites

Small zeolite grains occur with other alteration products and as incipient alteration in clinopyroxene. Most grains are poorly developed and it is not possible to distinguish the individual minerals of this group.

Calcite

Calcite in these rocks is restricted to areas of intense alteration such as the tension gashes mentioned above. It occurs as fine grained aggregates.

Summary

The mafic suite was formed in an environment that permitted some "solid state" adjustment of grain boundaries capable of producing the frequently-observed polygonal grain boundaries. Judging from the mesoscopic "sedimentary structures", the most probable environment was within a flat-floored magma chamber allowing grain deposition and an adcumulate overgrowth. Adcumulate growth is favored by the relatively slow accumulation of the bottom precipitate (Wager et. al., 1960).

Once deposited, these rocks underwent minor deformation of both "soft sediment" or ductile, and more brittle forms. This will be discussed more fully in the structural chapter. The presence of dikes, of similar composition to the main rock, cutting the layering suggests that after solidification, magma was still accessible, possibly through tectonic processes.

Water was present, in at least restricted areas, to form hornblende under primary poikilitic or later amphibolite facies

conditions. The granulite conditions may have been a continuum process, occurring shortly after deposition subsequent to only minor cooling. Further metamorphism and recrystallization occurred under epidote-amphibolite conditions. Mineral mobilization is evident through the extensive development of chlorite in some areas. Further calcium mobilization is apparent at lower T's in the formation of prehnite, the minor presence of zeolites, and very restricted occurrence of calcite.

The primary and secondary minerals are present in ocean floor dredge samples. There is no field evidence to indicate that they are obduction related. They are assumed to have occurred pre-obduction, under oceanic conditions.

CHAPTER IV
PETROGRAPHY OF OCEAN FLOOR GABBROS

Plutonic rocks of gabbroic composition have been recovered from the ocean floor near fracture zones, fault scarps and at spreading centers; from dredge hauls (Shand, 1944; Quon and Ehlers, 1963; Muir and Tilley, 1966; Cann and Funnell, 1967; Bogdanov and Ploshko, 1968; Bonatti et. al., 1970; Melson and Thompson, 1970; Miyashiro et. al., 1970; Miyashiro et. al., 1971; Bonatti et. al., 1975), D.S.D.P. holes (Hodges and Papike, 1976; Helmstaedt and Allen, 1977) and by submersible sampling (Ballard et. al., 1976; Caytrough, in press; Malcolm, 1978; Stroup et. al., 1978).

The mineral compositions cover the full range of the gabbroic suite including olivine gabbros, hornblende gabbros, two pyroxene gabbros, troctolites, norites, anorthosites, and even alkaline and nepheline bearing gabbros (Romanche Fracture Zone - Thompson and Melson, 1972).

Sample condition varies widely from fresh and relatively unaltered to severely serpentized and chloritized, with igneous to mylonitic textures. Grain size within even a single area varies from microgranular to grains larger than one cm. in size.

Plutonic samples are only recovered from areas that have undergone tectonic activity. This suggests additional deformational complexities and the possibility of extensive exposure to sea water and hence low-T alteration. In light of this it is remarkable that fresh samples are recovered

at all. In a comparison of the abundance of rock types recovered from the Romanche and Vema fractures zones, Bonatti and Honnorez (1976), found the following frequency relationships in dredged samples classified as gabbro, metagabbro, amphibolite, and mylonite:

Vema Fracture Zone:

metagabbro > gabbro \approx amphibolite

Romanche Fracture Zone:

gabbro >> metagabbro \approx amphibolite \approx mylonite

In this categorization, however, they do not outline the distinguishing criteria.

In both areas, serpentinite was the most abundantly recovered rock type. This may be due to the misidentification of chlorite and serpentinite which has been demonstrated in samples from the Gibbs Fracture Zone (A. Miyashiro, pers. comm.).

Fresh gabbros* are described with varying textures including poikilitic, cumulate, hypidiomorphic, granophyric, subophitic, and allotriomorphic (Bogdanov and Ploshko, 1968; Melson and Thompson, 1970; Thompson and Melson, 1972; Hodges and Papike, 1976; Helmstaedt and Allen, 1977).

Mineral compositions also vary. Plagioclase composition varies from An₆₋₈₄ in chemically, although not optically zoned grains in Cayman Trough rocks but grains with less than 50% An are clearly altered (Malcolm, 1978), An₉₀₋₈₅ in D.S.D.P. Site 334 (Helmstaedt and Allen, 1977), weakly zoned and around An₇₀

*Gabbros used in the suite sense - not *senso stricto*.

Romanche Fracture Zone (Melson and Thompson, 1970) and labradorite to bytownite at 24° and 30° N. (Miyashiro et. al., 1971). Mafic minerals include orthopyroxene, clinopyroxene, olivine and brown hornblende. All of the analyzed orthopyroxenes were hypersthene, many with augite exsolution parallel to (100) indicating original crystallization as orthopyroxene. Others show (100) and (001) augite exsolution indicating original crystallization as pigeonite with subsequent inversion to orthopyroxene. The (001) exsolution augite shows a tendency to form blebs, and with mild deformation to break into granular aggregates. (Hodges and Papike, 1976).

Clinopyroxene occurs as unzoned and weakly zoned augite (Romanche Fracture Zone - Melson and Thompson, 1970), diopside (Romanche Fracture Zone - Bonatti et. al., 1970) and diopsidic-augite (D.S.D.P. Site 334 - Hodges and Papike, 1976), frequently with orthopyroxene exsolution parallel to (100). Some augite grains exhibit a second more poorly developed (001) orthopyroxene exsolution (Hodges and Papike, 1976).

Olivine is not very abundant. Where present, compositional ranges include Fo_{72-84} in gabbros and Fo_{82-88} in troctolites from the Cayman Trough (Malcolm, 1978) and Fo_{87-88} in D.S.D.P. Hole 334 olivine gabbros (Hodges and Papike, 1976).

Distinguishing primary and secondary amphiboles poses the difficulties previously discussed. Many petrologists are convinced that primary magmatic amphiboles do occur. Only brown hornblende is likely to be primary. Cann (pers.

comm.) believes that they can be distinguished chemically. Magmatic hornblendes have TiO_2 contents above 0.4. Petrographically they can be distinguished by their brown color and location such as brown patches and rims within and around clinopyroxenes (A. Miyashiro, pers. comm.).

Accessory minerals include opaques, sphene, apatite and zircon. Many apatite grains may be secondary (F. Malcolm and D. Stakes, pers. comm.). Almost all the samples show at least mild deformation in the form of undulatory extinction and mechanical twins in plagioclase.

The primary mineral assemblage of the Table Mountain ophiolites to a first approximation contains a mineral assemblage similar to that of ocean floor mafics. The major differences are the presence of orthopyroxene, pigeonite and well-developed exsolution textures in the oceanic samples, indicating a more limited amount of Ca for the available Mn and Mg in oceanic samples. Plagioclases from both areas are within the same calcic range so the calcium is not combining with extra aluminum. Whole rock analysis (Malpas, 1976) indicate alkali enrichment and magnesium depletion relative to oceanic gabbro, although still within the relative ocean gabbro compositional range. Some of the change may have occurred during late stage alteration. It is more likely, however, that they indicate a less tholeiitic magma and possibly formation in an environment that allowed any less calcic pyroxenes which formed to completely change to clinopyroxene. The adcumulate texture of these samples suggests relatively

slow accumulation, so the change would have to occur prior to deposition.

A large percentage of gabbros dredged from the ocean floor show signs of metamorphism (Cann and Funnell, 1967; Miyashiro et. al., 1971; Ponatti et. al., 1975). These samples have probably been subjected, in varying degrees, to complex interactions of dynamic, contact, and thermal metamorphic conditions. Because of different and complex histories, traditional, regional, metamorphic facies classification criteria may not be valid.

This is a problem that has not been resolved and has only been partially investigated, particularly the aspects involving tectonics and hydrothermal circulation alteration.

To deal with this an attempt has been made to separate ocean floor metamorphics into two groups; one that may be classified according to "burial" metamorphic criteria (Coombs, 1961) with the emphasis on the lack of a tectonic foliation, and another group that has undergone contact, cataclastic and hydrothermal metamorphism (Miyashiro et. al., 1971). The most clear cut distinction between these two groups is an absence of tectonic foliation in the "burial" metamorphics. The term ocean-floor metamorphism may be the most appropriate to describe both types post-magmatic changes. Thus denoting that additional and/or different factors have produced the same mineral and compositional changes in ocean floor rocks that are observed in orogenic belts.

There is also the further question of low T metamorphic

alteration versus sea water alteration. Can and should a distinction be made? And if so where should the boundary be drawn. This is a problem which has only been recently addressed. One-hundred °C has been suggested as an arbitrary boundary, but the chemical and petrographic distinctions at this boundary are unclear.

Unfoliated oceanic metamorphic rocks have been classified into two groups on the basis of the extent of alteration and thereby the presence of the initial igneous composition (Miyashiro, et. al., 1971). This classification has not been widely adopted. Group I rocks are virtually unchanged from their initial composition and texture. Group II rocks have been intensely altered. The alteration minerals of Group I and II identify the facies classification. Metagabbros from Group I lie within the greenschist and amphibolite metamorphic facies. Some have undergone retrogressive changes in the zeolite facies. The group is characterized by the presence of calcic plagioclase (labradorite and bytownite) and the absence of epidote. Even when the mafic minerals show considerable alteration the high calcic plagioclase remains intact.

Group II includes zeolite and greenschist metamorphic facies. Many of these also retain gabbroic textures but there is a loss of C_2O and an increase in H_2O , leading to chlorite enrichment and the formation of some albite.

There is no classification system for deformed ocean floor rocks. Their mineral assemblages permit them to be

classified by the same criteria as the non-tectonic metamorphic facies and this is done although often with reservation (Bonatti et. al., 1975; Cann and Funnell, 1967; Hodges and Papike, 1976). The extent to which tectonic factors affect the composition has not been determined. There is considerable variation in the extent and variety of deformed samples.

Dredge hauls from 24° and 30° N. on the Mid-Atlantic Ridge (Miyashiro et. al., 1971) recovered metagabbros with banded structures suggesting granulation and recrystallization. The banding was accompanied by minute grains of brown hornblende produced by interstitial recrystallization. Granulated pyroxene samples from 06° N. (Bonatti et. al., 1975) contained banded amphibolitic metagabbros. Mineral layering on the scale of 1 mm. was present and strain was apparent in the undulatory extinction and frequently bent polysynthetic twins in the plagioclase, xenoblastic quartz grains and altered mafic minerals. The fine banding is attributed to either dynamic metamorphism during dike injection or shearing along upper ocean crust fault planes (Bonatti et. al., 1975).

A metagabbronorite (sic) from D.S.D.P. Hole 334 is intensely deformed along a restricted narrow shear zone, which contains large augen-shaped porphyroclasts with long recrystallized tails (Helmstaedt and Allen, 1977). Brown hornblende mylonites have been recovered from St. Paul's rocks (Thompson and Melson, 1972).

The differences in composition and texture between ocean

floor gabbro samples are attributed to strain rate, temperature, pressure, and the influence of volatiles.

In light of the extensive variability in sample composition and texture, comparative petrography between ocean floor and Table Mountain gabbro shows numerous similarities and differences. Such a spectrum could possibly be obtained between almost any "cumulate" suite of gabbros. Certainly numerous pro and con comparisons have been made with layered intrusions. An important comparison should involve geochemical and petrological data, but such data is not currently available for this suite.

There are several significant differences between ocean-floor and land or regional metamorphism; the lack of epidote and hence the epidote-amphibolite facies in Group I metamorphics, the resistance of calcic plagioclase to alteration, and the lack of carbonates being important examples. These differences may be indicative of very low P with relatively high heat flow, such as would occur near an ocean ridge magma chamber (Miyashiro et. al., 1971). However epidote is developed in metabasalt so other complicating parameters such as the extent of hydrothermal circulation and the oxidation environment may be involved. It may also be that it is easier for apatite than epidote to form as a secondary mineral in some oceanic regimes, such as the hydrothermal conditions in the Galapagos spreading center, and hence become the calcium sink (D. Stakes, pers. comm.). This however is unlikely in this rock suite because there is no additional source of PO_4 .

More extensive metamorphism, such as that of Group II, and deformation, could accompany transform domain tectonism involving high strains, reheating and increased hydrothermal circulation, but still at relatively low confining P.

Table Mountain gabbros all show some degree of alteration. Most of the alteration is similar to that described for Group I; i.e., chlorite, calcic plagioclase, actinolite, with very little carbonate and the later development of lower T metamorphic facies. An important difference between the two groups however, is the incipient development of epidote and the lack of accessory minerals, particularly apatite gabbros. This may be related to obduction, but is more likely the result of a continuation of the ocean-floor metamorphism.

There are numerous possibilities for the incipient development of epidote and lack of apatite. It may be that the hydrothermal circulation and tectonic conditions away from transforms are conducive to the development of incipient epidote and not apatite. We also know very little about most oceanic areas, particularly the initial stages of ocean formation and back arc basins. Both of these areas may be the site of pre-obduction ophiolites.

Any correlations between ophiolites, dredge hauls and the majority of ocean crust should be drawn with the realization that both dredge hauls and ophiolites may be sampling unrelated and anomalous bits of ocean crust. Nevertheless the known chemical, petrographic, and metamorphic comparisons bear substantial similarities indicative of some common parentage.

CHAPTER V
STRUCTURAL GEOLOGY

Mesosopic Relationships

The Northern exposure of Table Mountain consists of a base of ultramafic rocks capped along a roughly horizontal contact with mafic rocks, which include gabbro, hornblende gabbro, olivine gabbro, troctolite, feldspathic dunite, and anorthosite. A layering and a lineation are present in both the mafic and ultramafic suites.

The layering is primarily defined by a compositional variation between the layers, although some grain size variation is present. Layers range from approximately 1 cm. to several meters in thickness. Most layers are between 1 and 10 cm. thick in the mafics (Fig. 7). In the transition zone area, however, the layers are commonly .5 to 1 meter thick, with thin bands of pyroxene or chromitite within the ultramafic layer. The layers are discontinuous over distances of less than 100 meters. The presence of sedimentary structures and adcumulate textures suggest that at least the primary layering is sedimentary.

A lineation, defined by the alignment of mineral aggregates is present in most outcrops and lies within the foliation plane. Because of differential weathering, the pyroxene lineation is more detectable and hence was the one that was measured. Where grain sizes were small or no differential weathering was present, a lineation was not observed. The aligned grains appear to be individual minerals showing varying degrees of

deformation and do not appear to be boudinaged.

Close to the transition zone or mafic-ultramafic contact, there are small ultramafic pods. They have both elongate and rounded shapes, but the elongate shape predominates. The layering within the pods is usually parallel with that of the surrounding gabbro, although the boundaries are not. They occur in areas which have undergone extensive macroscopic folding. Similar mafic pods are not observed in the ultramafics. Several interpretations are possible. The ultramafic material may have been deposited at the same time as and within the mafic material. This would help to create an instability (probably due to density contrast) which resulted in folding. Alternatively, folding may have occurred, squeezing the ultramafic material into the mafic material with the subsequent development of a foliation. In the latter situation, the foliation could be parallel, or close to parallel, with the primary layering. Neither explanation addresses the question of why mafic pods do not appear in the ultramafic layers.

Although some criteria have been outlined by structural geologists (e.g., Hobbs, Means, and Williams, 1977, pp. 156-159), it is often difficult and even impossible to distinguish between tectonic and sedimentary structures in metamorphosed and deformed rocks, especially when features such as a cumulate origin or transposition are involved. The distinction is sometimes made on lithological basis. This however, cannot be applied to ophiolite complexes which have igneous and metamorphic lithologies, yet display sedimentary features. In layered intrusions, such as the Skaergaard and Bushveld Complexes,



Fig. 19
Irregularities in mafic layering suggesting small channels.



Fig. 20
Cross lamination in gabbro channel structure.

many features have a sedimentary origin (Wager and Deer, 1967).

Five types of sedimentary features were recognized in the Table Mountain mafic suite. They will be discussed in two groups. The first group consists of those features indicating transport and deposition, such as channels, cross-lamination, and graded bedding. The second group contains those features that indicate post-depositional, or soft-sediment style deformation and includes a variety of slump features such as folds and faults. Both groups of sedimentary features may have undergone subsequent deformation.

Throughout the mafic suite, layers show abrupt compositional change. Many of the contrasting layers cut the layering and are clearly dikes. Others parallel the layering and may be either depositional layers or igneous sills. A third type of variation, however, suggests minor winnowing, forming small channel-structures, and continued deposition. Such an example is shown in Figure 19. Both leucogabbro, anorthosite, and olivine rich channel fill are present. The channel truncates the gabbro layering. Within the channel, the layering is not strictly parallel with that of the host gabbro, and a compositional variation suggests cross-lamination.

The single most convincing example of sedimentary transport and deposition during the formation of the ophiolite complex is shown in Figure 20, where cross-lamination in a leucogabbro abuts a layered gabbro channel structure. Other examples of channel structure and cross lamination are not as clear, e.g., Figure 21, which shows anorthosite-leucogabbro compositional changes at a steep angle of repose with regular layering



Fig. 21
Cross lamination in leucogabbro with a steep angle of repose.

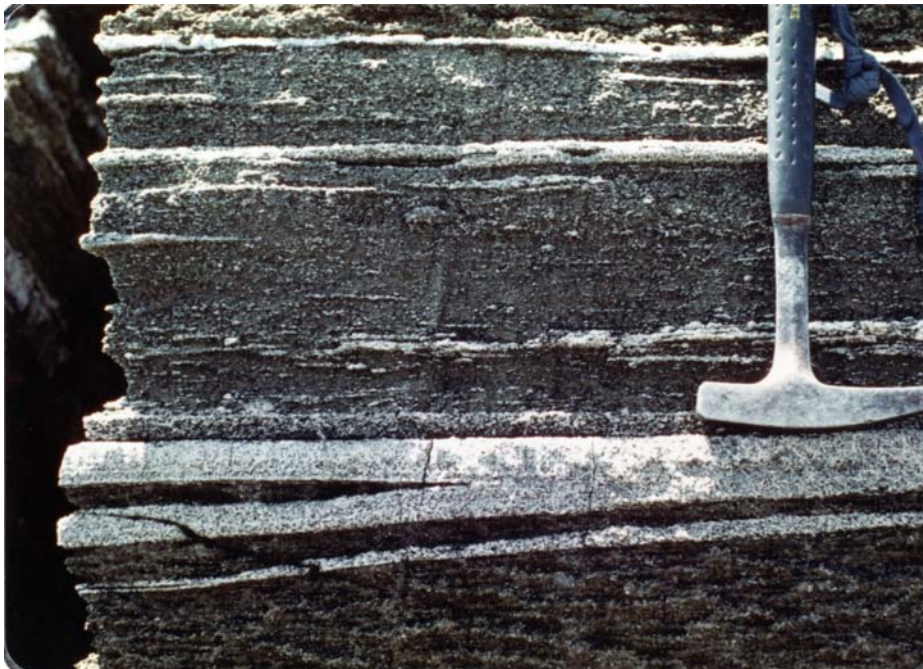


Fig. 22
Weak size grading in an anorthosite layer with the appearance of a pseudo-fold.

above and below the cross lamination and equant grain size.

Graded bedding is poorly developed in the Table Mountain mafic suite. Figure 22 shows one of the few examples of weak size grading, in this instance occurring in one of the anorthosite-leucogabbro layers. The absence of size grading suggests that the formation processes allowed only a very narrow range in grain size. In a convecting magma chamber this may relate to the size and rate of movement of a convecting cell, as well as viscosity.

The second groups of sedimentary features, folds and faults, can be associated with slumping, and are indicative of mechanical instability. Two styles of intrafolial folds are present in the Table Mountain mafic suite; symmetric, tight, or isoclinal isolated folds (Fig. 23), and asymmetric, multiple and single hinge folds, mostly with and S-symmetry (Fig. 24). Some fold limbs have undergone thinning. Most of the folds occur on flat one-dimensional surfaces, making pitch and plunge measurements extremely difficult. Half-wavelengths varied between 6 and 20 cm. Larger folds also exist. As seen in Figure 25 on a surface where the limbs are exposed, the anorthosite looks like layering. At roughly right angles to that surface however, the layer appears to be folded. No axial surface foliations are developed, suggesting that folds formed prior to lithification. This assertion is further supported by the undisturbed appearance of the overlying layers. However, folds such as those in Figure 23 have feldspars which indicate possible tectonism, and post-lithification deformation cannot be ruled out.



Fig. 23
Symmetric intrafolial fold.

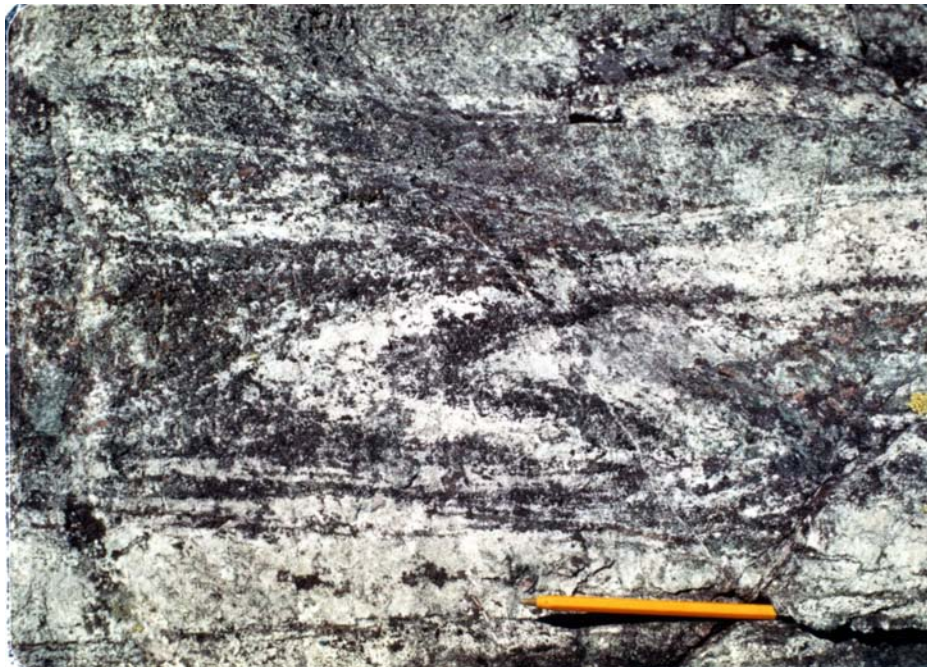


Fig. 24
Asymmetric, S-style, intrafolial fold.

A third style of folding, non-intrafolial, shown in Figure 26, contains several convoluted layers suggesting a more thorough mixing. These folds may be the result of slumping in the magma chamber, such as in response to a slight change in dip or tectonic activity. In marine sediments, a dip of even one degree is estimated to be sufficient to cause large scale slumping. Slump folds described in the sedimentary literature, however, usually present a more chaotic and disrupted appearance than is observed in those of Table Mountain. The influence of solidification in an igneous regime has not been assessed, and may aid in the restrained quality of these folds.

A fold style, here termed "pseudo-fold" is also present. This feature appears to represent the low angle intersection of two dikes, or a dike and a layer of similar composition. It is most easily observed when the pseudo-fold material is plagioclase rich. The intersecting angle may be sharp, as observed in Figure 22. In this example, the presence of graded bedding in only one of the limbs rules out the possibility that it is a fold. Other examples are not as clear. Figure 27 shows the more rounded intersection of an anorthosite dike and layer, or two anorthosite dikes. The widening of the "limbs" at the pseudo hinge area is interpreted to be the result of the confluence of the two dikes.

One of the most clear pieces of evidence for soft-sediment deformation is shown in Figure 28. In a solid block, an area of layered anorthosite and gabbro has been down dropped and tilted. The edges are offset and diffuse. Gabbro is present



Fig. 25
Large fold in two dimensions showing limbs with the appearance of layering.



Fig. 26
Multiple folds in transition area.

where an anorthosite layer would be expected. No layering or lineation is present in the gabbro fill. The faulting or slumping must have occurred before rigid fault lines could be maintained. The lower anorthosite layer is approximately 30 cm. thick in the unfaulted block. It is less than half that and decreases at an angle in the faulted block. Therefore it appears that, as observed on this surface, anorthosite was removed during faulting. Only a few cm. above and below the fault area, the block shows a continuous gabbro layer suggesting that the effects of the deformation were restricted to a narrow zone.

Such a situation might develop where cooling to a solid occurred shortly after deposition under a steady state regime for a magma of gabbroic composition. The introduction of a thick anorthosite layer may have introduced an instability through either rapid accumulation or a different cooling rate, i.e., some mechanism which created a layer which was unable to withstand the subsequent loading or was more easily disturbed by minor tectonism.

Literature on experimental soft-sediment deformation is sparse and extrapolation to an igneous magma chamber is difficult. A majority of the work appears to have been done by Rettger (1935). The deformation mechanism usually could not be determined from the end deformation structure. Intrafolial folds and slump features were produced by all of the types of deformation except falling objects. During subaqueous slumping, intrafolial folds formed perpendicular to the direction of the moving mass. In cases of differential movement, intrafolial



Fig. 27

Pseudo-fold caused by the intersection of an anorthosite dike and anorthosite layer or two anorthosite dikes.



Fig. 28

Pre-lithification slumping in anorthosite-gabbro block.

folds, showing a consistent sense of direction formed with the dip of the axial plane almost 45° toward the dip of the moving face. The larger the load the thinner the deformation zone. Intrafolial folds produced during differential loading dipped towards the loading plane. If the loading plane was uneven, faults as well as folds formed. The faults had diffuse boundaries and were down thrown on the less weighted side. Minor bend folds were observed along some of the faults.

The development of the previously described sedimentary features, and adcumulate texture indicate that a magma chamber existed for at least part of the formation of this ophiolite suite, and that both transport and prelithification deformation occurred within the magma chamber. Convection coupled with tectonic activity could produce the observed sedimentary features. The extent and style of the resulting structures would depend upon: 1) the rate, size, and shape of the convection cell, which in turn is related to the temperature, temperature gradient, viscosity, and size and shape of the magma chamber; 2) the rheology of, and viscosity contrast between, the magma and crystals; and 3) the presence and extent of tectonic activity.

Dike injection and further deformation occurred post consolidation. Dikes of dunite, pyroxenite, anorthosite, and combinations of these minerals intersect, parallel, and cut the layering of both mafic and ultramafic rocks. Feldspathic dikes, 1-3 cm. wide are the most common occurring in both the mafic and transition zone suites. They frequently contain

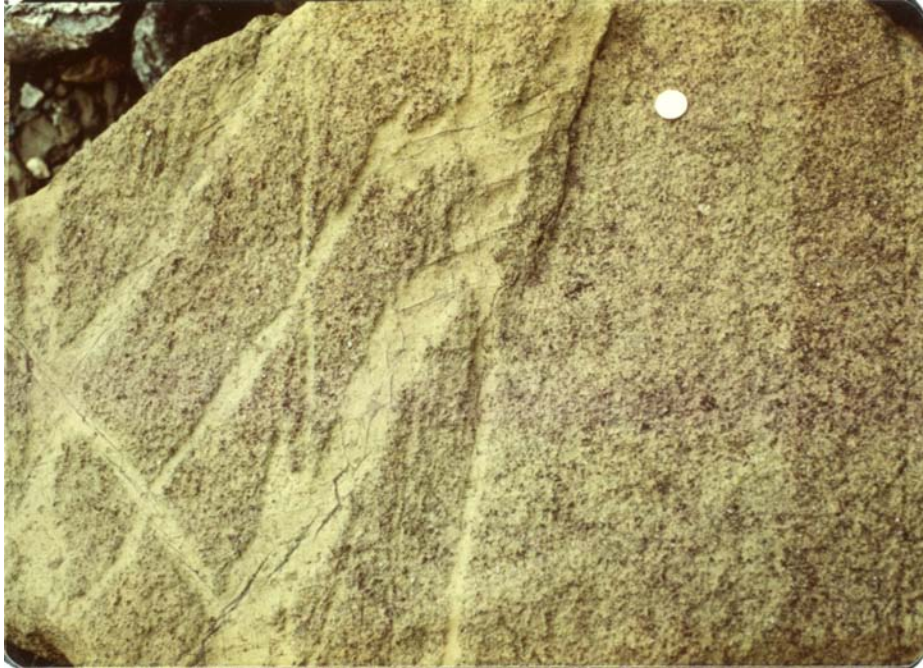


Fig. 29
Intersecting dunite dikes in layered ultramafic rock.



Fig. 30
Dunite dike in layered mafic rock.

minor amounts of pyroxene and sometimes hornblende. No chilled margins were observed in any of the dikes. Dunite dikes are also common, particularly, in the ultramafic part of the transition zone where they form frequent intersections (Fig. 29). They also occur in the mafics, but, as with the anorthosite dikes can only be ascertained for certain where they cut the layering as in Figure 30. Like the anorthosite dikes they are usually a few cm. wide. In the example shown, the dunite dike terminates against a coarse grained gabbro layer. These coarse grained layers increase in frequency towards the transition zone. Most were parallel to the layering, but a few, particularly the thinner ones, cut the layering. Hornblende has formed around the edges of some of these pyroxenes, indicating the presence of water and suggesting later stage magmatic injection.

One curious feature of the Table Mountain ophiolite suite is the presence of large pyroxenes. These are mostly found (in a single area) close to the hinge of a macroscopic fold. In some outcrops the large pyroxenes are abundant (Fig. 31). In other outcrops, only a single large pyroxene is present (Fig. 32, shown in greater detail in Fig. 33). In the multiple pyroxene area, many grains have augen shapes and tails. Adjacent layering conforms to the grain outline. Some grains appear compressed and to varying degrees. In thin section the grains show the effects of considerable deformation and recrystallization. This suggests that deformation occurred after the pyroxene was present and that it had a different rheology than the surrounding gabbroic layers. It is difficult,



Fig. 31
Multiple large pyroxene grains in layered gabbro.



Fig. 32
Single large pyroxene grain in layered gabbro.

however, to explain the varying amount of flattening in the pyroxenes over such a small area.

Where the single pyroxene is present, the grain does not appear to be as deformed as those in the multiple pyroxene area. Cleavage traces are roughly perpendicular to layering. The underlying olivine gabbro layer is slightly compressed, but flattening is absent in the pyroxene grain. The overlying layer contains a fine grained material which roughly parallels the pyroxene grain and fills the irregular parts of the surface. The coarse grained gabbroic material, which makes up the majority of the overlying layer is only slightly deflected by the presence of this large pyroxene grain. If a sedimentary origin is invoked, a large crystal could have formed, been transported, and then deposited. Once deposited, some continued growth and minor deformation may have occurred in situ.

Not all features, however, can be attributed to sedimentary style deformation. Post-lithification deformation, or deformation in a more solid state, is observed in the form of offsets in dikes, deformation of the layering and lineation, and the presence of high strain zones and mylonites. (The high strain zones and mylonites will be discussed later in a section dealing with cataclastic rocks.)

Figure 34 shows an area of medium-grained well layered gabbro which is bent and then truncated by a finer grained homogeneous gabbro. A ridge of material has formed along the abutting plane which roughly parallels the nearby layering. In Figure 35, a feldspar lineation, on the right hand side of the photograph



Fig. 33
Large pyroxene grain of Fig. 32 shown in greater detail.



Fig. 34
Deformation of layered gabbro terminating against homogeneous gabbro.



Fig. 35

Deformation of feldspar lineation.

is deflected from a high angle to subparallel to a thin anorthosite dike. On the left, the dike is offset and the feldspar lineation maintains a constant orientation. A possible interpretation is that the dike was in the lower position and that the right hand (now upper) side moved, compressing, and deflecting the feldspar lineation.

Macroscopic and Geometric Relationships

The mapped area has been divided into six subareas which are shown in Figure 36. Poles to layering and lineations for each subarea have been plotted on an equal area net and contoured using the Braun (1969) method. Some of the subareas have similar geometric patterns and will be discussed together in the following sequence: IV and V; I and II; III; and IV.

Subareas IV and V

Poles to layering in subarea V have a 22% per 1% area maximum concentration, lying within a pi circle (Fig. 37a). The distribution is skewed or appressed to the S.W. suggesting an asymmetric fold with either more extension or more exposure along the N.E. limb. This is borne out by the map distribution in which more of the N.E. limb is exposed. There is no significant or consistent change in dip.

The pi axis lies at 50 → 34 and is only 4° away from the area of maximum lineation concentration (Fig. 37b). The lineations lie along a great circle, strongly skewed to the east. The strong concentration at 50 → 32, as with the poles to layering, is a function of the outcrop exposure and not necessarily the folding process. For example, the lineation roughly

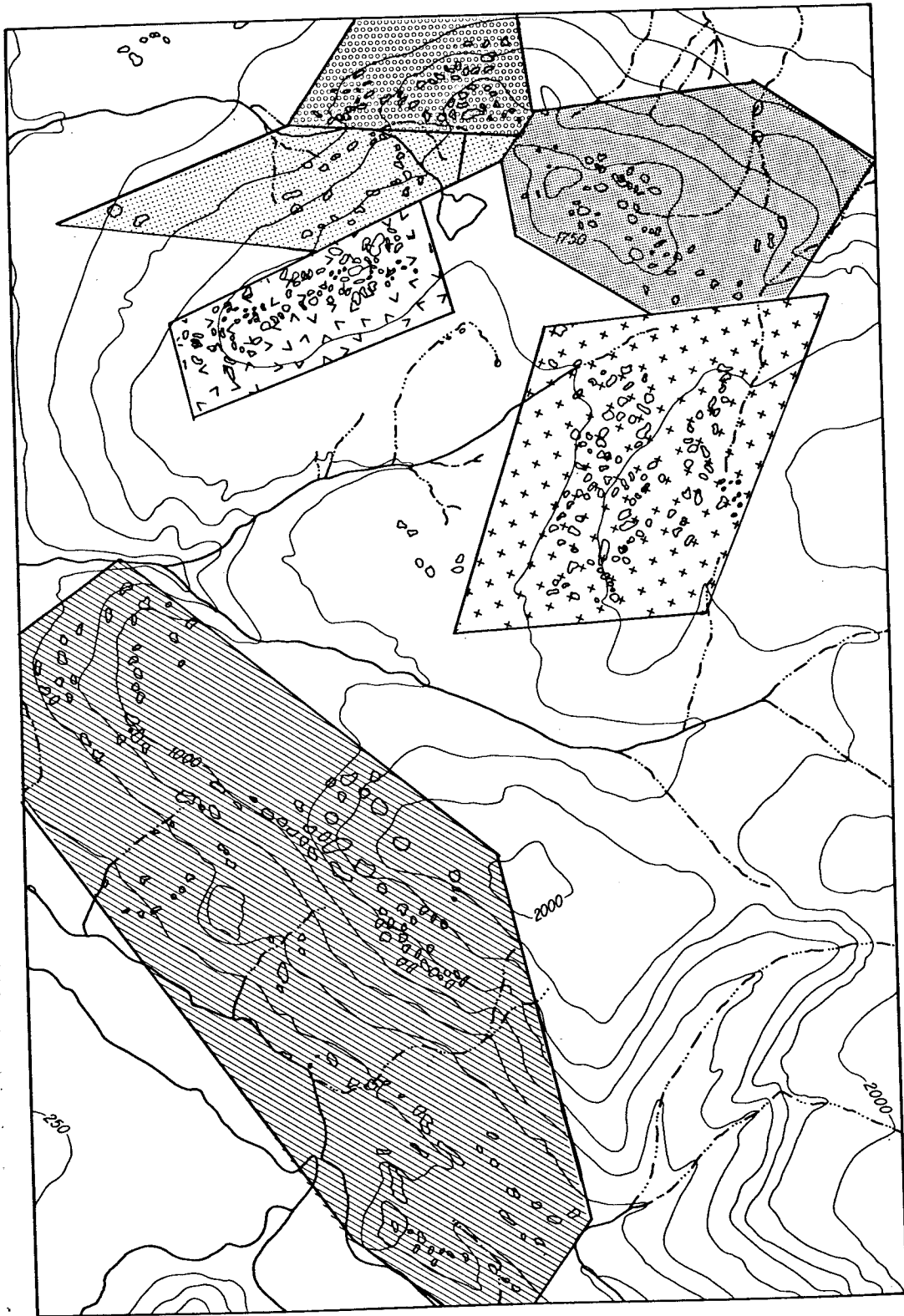
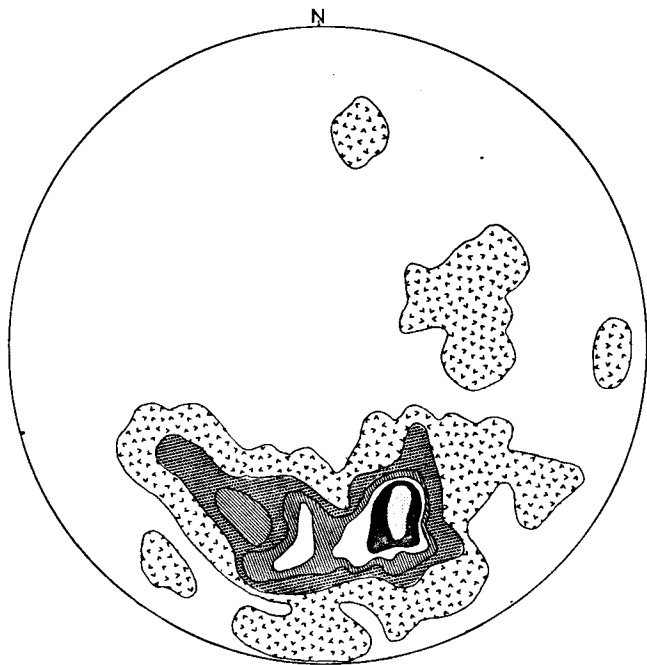
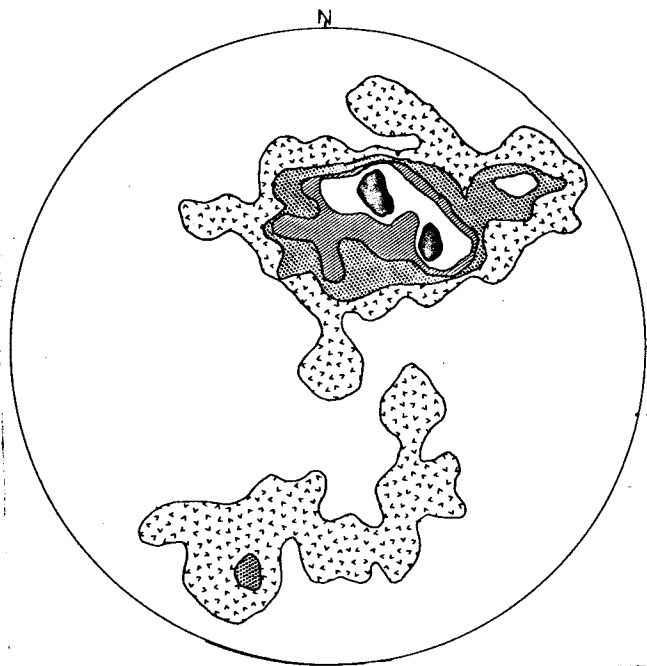


Fig. 36
Six subareas of Table Mountain.



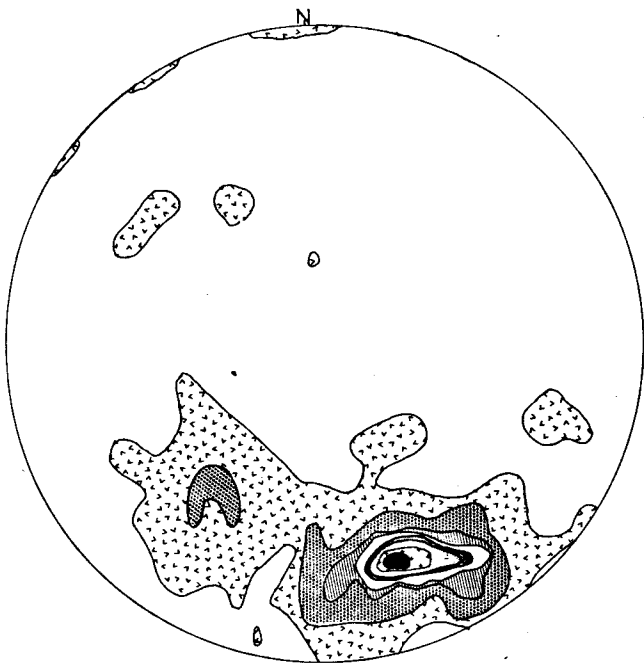


A. Poles to Layering, 59 Points

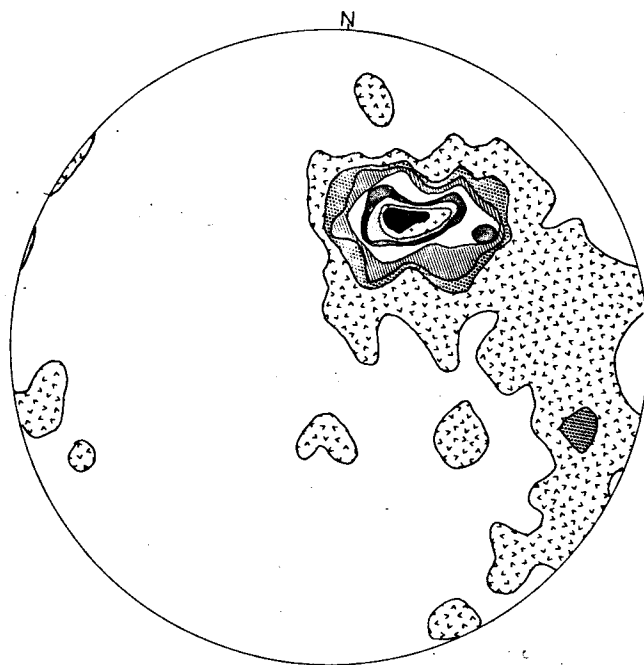


B. Lineations, 49 Points

Fig. 37, Subarea IV



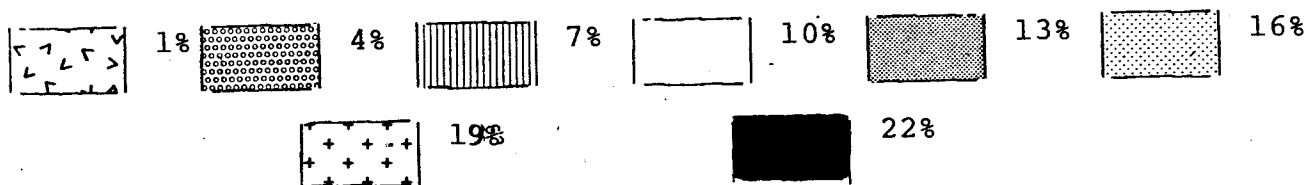
A. Poles to Layering, 97 Points



B. Lineations, 77 Points

Fig. 38, Subarea V

CONTOURED STEREOGRAPHIC PROJECTIONS - % AREA



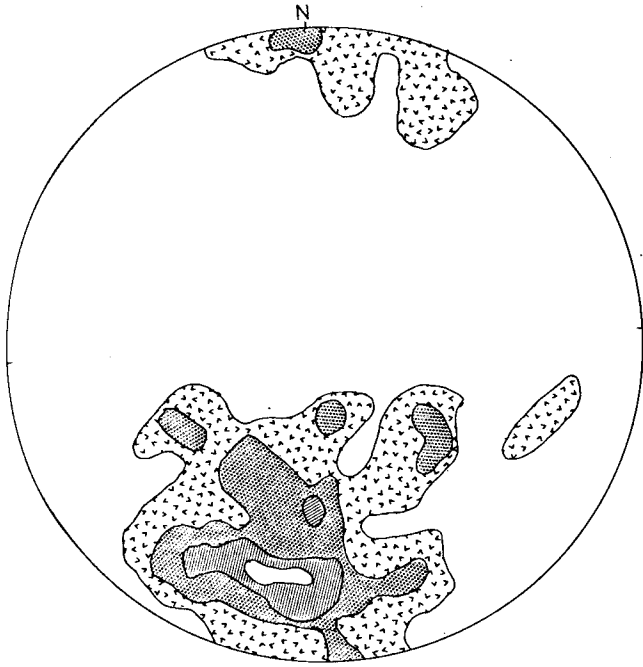
parallels the pi axis, but at the fold hinge the lineation follows the fold form and is actually perpendicular to the fold axis. This suggests a pre-folding lineation which maintained a constant relationship with the folded layers.

The poles to layering in subarea IV also lie along a pi circle skewed to the S.W. and away from the area of maximum concentration. The pi axis lies at the point of maximum concentration. The lineation concentration, however, is not as strongly skewed along a great circle as in subarea V. The map pattern is not straight forward. There is considerably more outcrop along the N.E. end of the limb and the hinge area is not as tight or as well defined as in subarea V. In the central area there is a considerable disruption of the layering, hornblende gabbro, a porphoritic mafic dike, and high strain zones are present.

Subareas I and II

Subareas I and II present the most complicated map pattern suggesting numerous small fold and faults. Poles to layering in subarea I define a thick pi circle with two submaximums of 7% and 13%. The pi axis at 05 → 93 lies adjacent to the area of maximum lineation concentration (Fig. 39a and 39b). The great circle, defined by the lineation concentration differs by less than 10° from axial plane. In a relatively flat lying fold, such as that defined by the equal area net small perturbations in the layering and folding would be especially apparent.

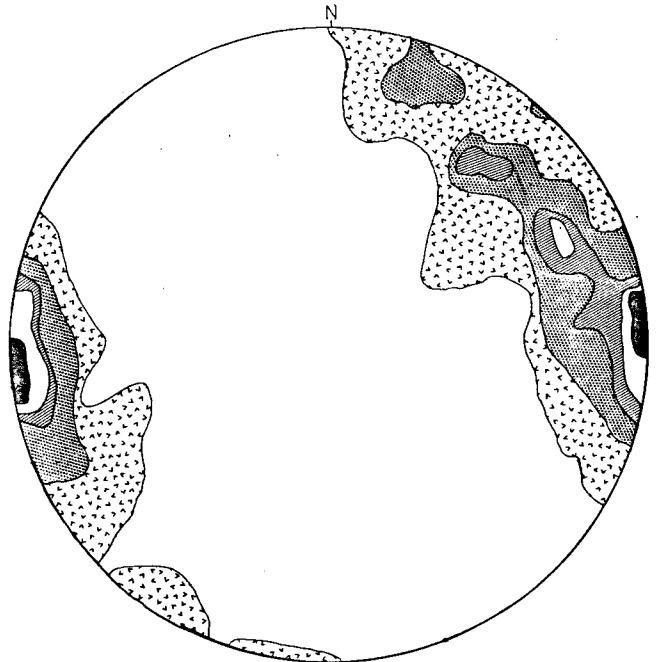
Subarea II S-poles plot with a maximum concentration of 10%, but do not define a clear pi circle. Instead the geometry



A. Poles to Layering, 63 Points

B. Lineations, 20 Points

Fig. 40, Subarea II



A. Poles to Layering, 99 Points

B. Lineations, 70 Points

Fig. 39, Subarea I

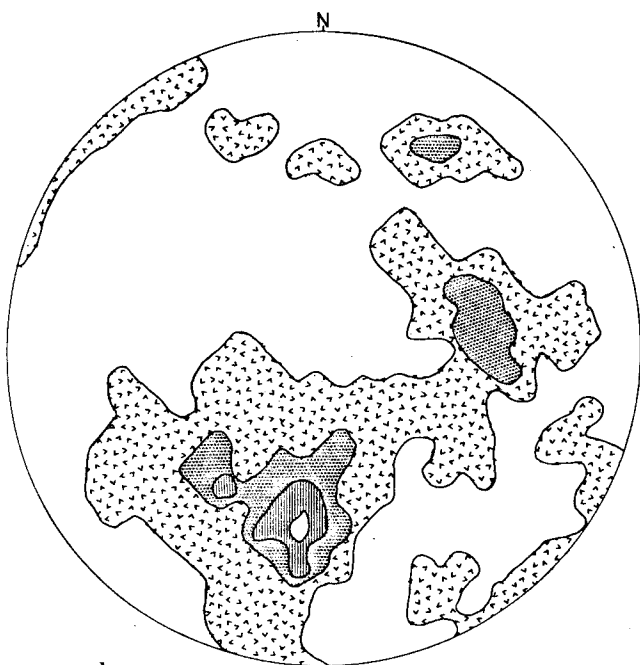
suggests a rather poorly defined steeply plunging fold limb. Only twenty lineations were measured in the area. These plot in an irregular elliptical form on an almost horizontal plane with a maximum concentration at $03 \rightarrow 100$. This is very close to the maximum lineation concentration of the overlying gabbro ($0 \rightarrow 80-90$). The lineation then lies roughly parallel with the mafic/ultramafic contact.

Subarea III

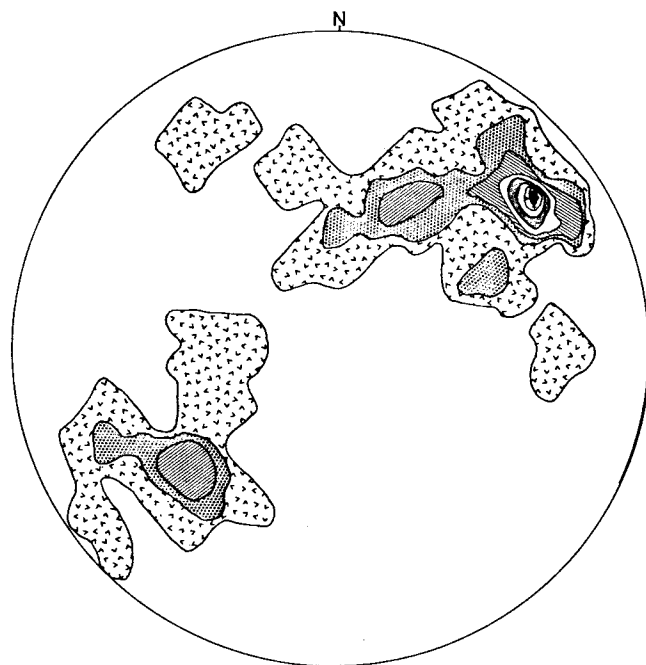
No geometrically simple form is apparent in the pi diagram of subarea III. Two areas of major concentration lie within an irregular 1% per area concentration. A great circle through this area gives a pi axis of $30 \rightarrow 321$ (Fig. 41). This does not lie within the great circle defined by the lineation. Along a great circle the maximum lineation concentration and pi axis are separated by 90° . The outcrop distribution suggests a predominantly N.W. trending, moderately dipping layering which becomes folded, faulted, and deformed in a series of high strain zones which increase in density toward the hornblende gabbro area. The petrography indicates that the hornblende was present before deformation. Possibly, the presence of water in the hornblende facilitated the deformation in this area.

Subarea VI

This area spans the greatest relief and has the widest range of lithologies. A weak pi circle can be drawn from the S-poles giving a vertical pi axis. The axis approximately coincides with the maximum lineation concentration (Fig. 42a and 42b).

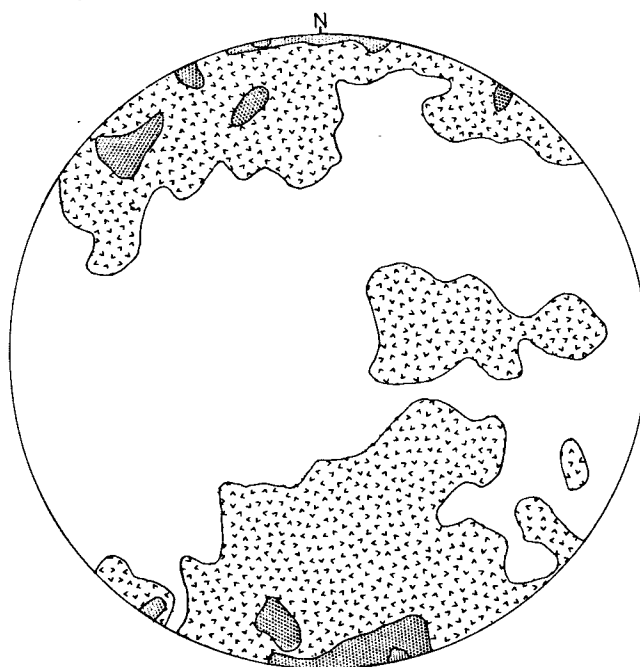


A. Poles to Layering, 55 Points



B. Lineations, 31 Points

Fig. 41, Subarea III



A. Poles to Layering, 139 Points



B. Lineations, 90 Points

Fig. 42, Subarea VI

Within this area two large blocks of gabbro and one large block of troctolite/anorthosite/and gabbro mixture are present in the ultramafic rocks. The two blocks do not appear to be deformed. They lack high strain zones and have a regular steeply dipping, N.E. trending layering. The underlying ultramafics are serpentized obscuring any deformation features which may have been present. The mixed composition block, however, contains several small high strain zones. The origin of these blocks is unclear. They may be glacial erratics, part of a block which became separated during obduction or during the formation of the Trout River Fault, or part of the primary crustal structure.

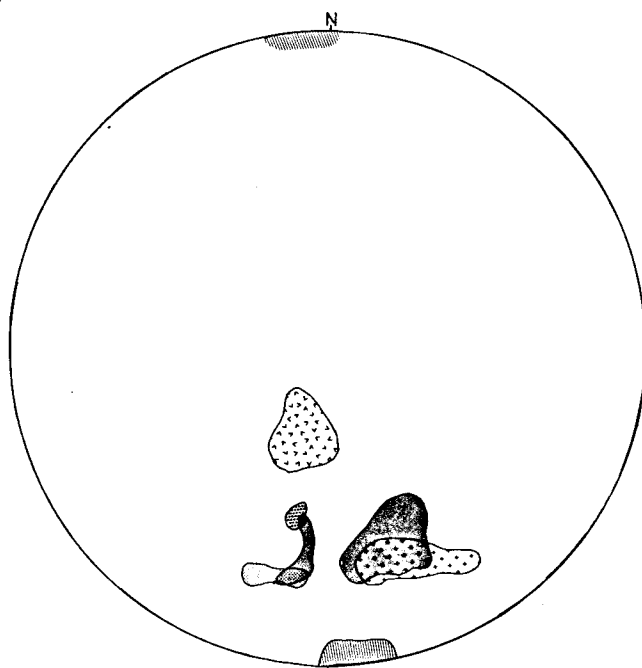
On a composite net, the ten percent per area concentration for S-poles and lineations for all six subareas has been plotted (Fig. 43). The S-poles plot in a moderately to steeply south plunging direction slightly skewed to the east. This agrees with the generally N.W. trending foliation found in the other Bay of Islands massifs. The lineations lie in three distinct groups: Subareas V, I, and III moderately N.E. plunging; Subareas I and II horizontal and east-west trending; and Subarea VI steeply N.W. plunging. One possible explanation for the homogeneity in S-poles and heterogeneity in lineations may be different styles of folding.

The Dewey/Kidd model predicts S-shape folding of the gabbro layer during differential subsidence. In this model some of the highest angles of repose are expected at the layer two/layer three interface. This coupled with the density contrast

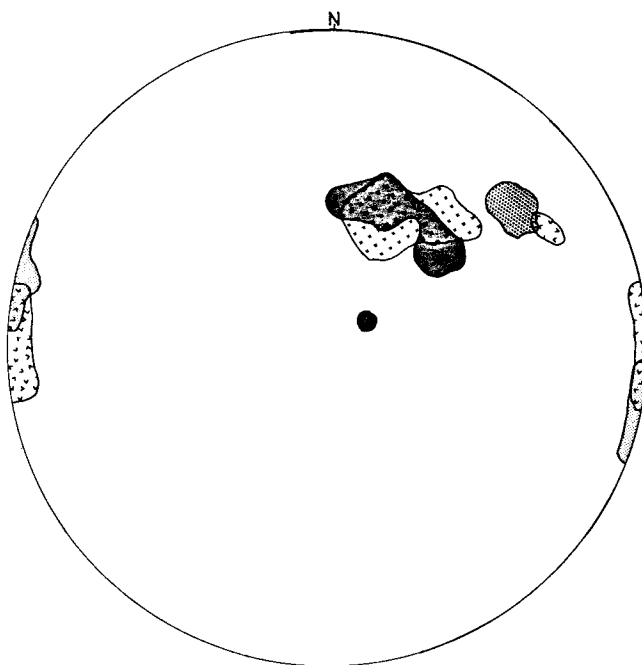
between mafic and ultramafic layers, and possible accumulation rate differences suggest that this would be a very unstable area and subject to large scale slumping. Compression of the slumped material as it moved away from the spreading center could maintain and enhance the primary layering and accentuate lineation differences, particularly if the lineation had changed orientation during folding.

In summary, the development of the Table Mountain mafic suit may be considered to have occurred in the following sequence:

- 1) Deposition of the mafic and ultramafic material along a differentially subsiding floor, as depicted in the Dewey and Kidd model, within a convecting magma chamber, capable of forming sedimentary style structures.
- 2) Injection of dikes, possibly with an increasing water content.
- 3) Folding of the material on a macroscopic scale which resulted in complex geometric patterns and some deformation of the material.
- 4) Formation of high strain zones (these may have begun in response to the folding but continued after the major phase of folding subsided).
- 5) Formation of mylonites, possibly in response to obduction.



Composite Poles to Layering - Contoured at 10 % Area for Subareas



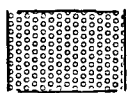
Composite Lineations - Contoured at 10% Area for Subareas



I



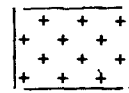
II



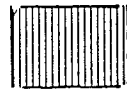
III



IV



V



VI

CHAPTER VI

MICROSTRUCTURE

General Introduction

Although the optical scale microstructures of deformed rocks have been described since the work of Sorby (1853), Sander (1930), and Harker (1932), our understanding of these features and their relationship to larger scale strains is very limited. Microstructures are largely concerned with the role of crystal defects in deformation processes and the ways in which the arrangement of crystal defects may be influenced by the thermal history (Hobbs, Means, and Williams, 1976).

Many early experimental investigations were conducted on metals (Cahn, 1953, 1954; Pratt, 1953; Hall, 1954) which have higher symmetry and give less ambiguous results. More recent work has been aided by the use of the transmission electron microscope, allowing a higher resolution of the microdeformation structures. The majority of experimental investigations, however, are conducted on monomineralic rocks, particularly quartz or olivine. Extensions to gabbroic rocks are scarce.

Nevertheless, some experimental work has been done on the two primary mineral constituents of gabbro; plagioclase and pyroxene. This work, and its relationship to the features observed in the Table Mountain gabbros, will be discussed.

Plagioclase

Introduction

Plagioclase has a triclinic symmetry. Despite its abundance

in crustal rocks, it has received little experimental attention, especially when compared with investigations of quartz and olivine deformation. Among those who have conducted experimental plagioclase deformation studies are; Muggie and Heide (1931), Laves (1965), Borg and Handin (1966), Seifert (1968), Borg and Heard (1967, 1969, 1970), White (1975), Marshall et. al. (1976), and Seifert and Ver Ploeg (1977).

Plagioclase deformed under both experimental and natural conditions contain deformation lamellae, kink bands, slip lines, twins and fractures. Experimental results give an indication of the conditions under which these different features develop. Figure 44 shows the relative development of cataclasis, deformation lamellae, and twinning, at different temperatures and pressures, for experimentally deformed anorthite. Other compositions of plagioclase broadly show the same deformation mechanisms under experimental conditions. The relationship with naturally deformed plagioclase is not as clear, in particular, the effects and interdependence of strain rate, work hardening, and temperature.

Slip features and microfractures are not observed in undeformed plagioclase, and hence are interpreted as a fairly straight forward indication of strain. Twinning is more ambiguous, since twins are observed in both deformed and undeformed plagioclases. Unlike other silicates such as quartz, subgrain development is very poor in plagioclase.

Deformation Lamellae

Deformation lamellae are narrow planar and subplanar

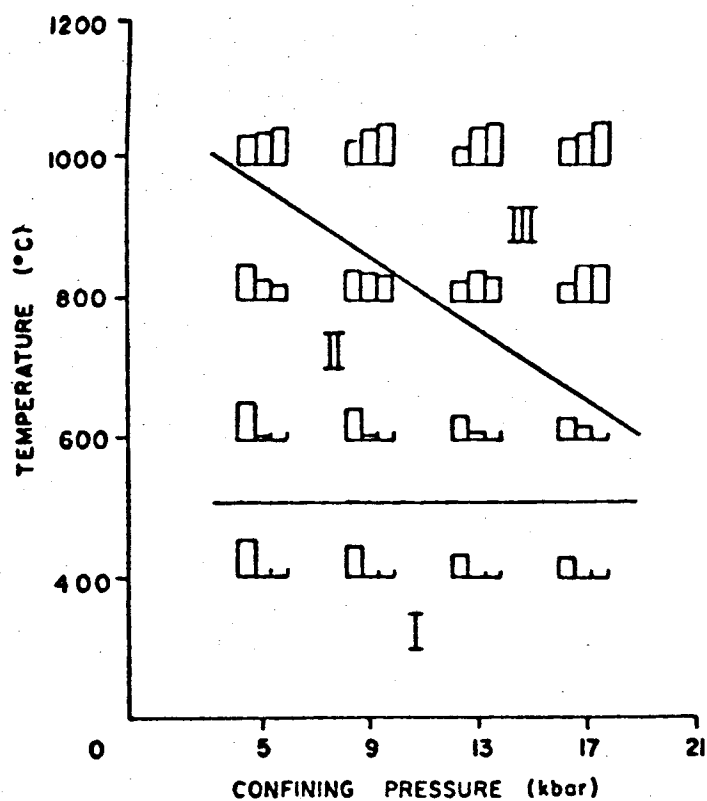


Fig. 44 (from Seifert and Ver Ploeg, 1977)

Deformation mode diagram showing the average percentage of each mode of deformation at each temperature and confining pressure. The three columns in each histogram represent, from left to right, percent cataclasis, percent deformation lamellae, and percent deformation twinning. The three columns do not add up to 100% so that it is possible to observe the relative amounts of the different modes of deformation at a given temperature and confining pressure and changes in the amount of deformation with changes in temperature and confining pressure. For scale the column in the lower left corner histogram equals 63%. Deformation fields I, II, and III are distinguished on the basis of different relative proportions of the three modes of deformation

features that develop within single grains. They have a slightly different refractive index to the host grain, (Hobbs, Means and Williams, 1976), and are attributed to planar arrays of locked-in slip dislocations creating a stress field. They are useful in determining active slip systems (Raleigh, 1968), and are especially common in quartz deformed at low temperatures.

Deformation lamellae have been experimentally produced in triaxial compression tests in plagioclase at temperatures above 600°C at all confining pressures, (Borg and Heard, 1969, 1970; Seifert and Ver Ploeg, 1977), and in shock deformation experiments (Robertson et. al., 1968). They have a diffuse planar appearance and often show varying orientations within a single grain (Seifert and Ver Ploeg, 1977). There is no strict crystallographic control on their formation, but they often occur oblique to unique crystallographic planes of low indices. They are localized within the host grain and have not been observed to cross grain boundaries. In anorthosite triaxial compression tests, the percentage of crystals with deformation lamellae showed a positive correlation with temperature (Seifert and Ver Ploeg, 1977), ranging from 1% to 30% at 600°C, to 15% to 80% at 1000°C. They are restricted to untwinned sections of the plagioclase grains (Borg and Heard, 1970).

No deformation lamellae were observed in the Table Mountain plagioclases. If twinning occurred either during or shortly after crystallization and persisted throughout the temperature range at which deformation lamellae could form, it may

have interfered with their development. This, however, does not explain the lack of deformation lamellae in untwinned grains. Possibly they have been obscured by undulatory extinction and alteration, or are out of the resolution range of the optical microscope used in this investigation.

Deformation Bands

Deformation bands are planar intragrain regions that have undergone a different kind of deformation than the host grain (Hobbs, Means, and Williams, 1976) and are frequently inclined at high angles to active glide planes (Seifert, 1965). They may contain deformation lamellae.

Magnified over 400 x's, albite deformation band boundaries were shown to consist of a continuous series of small connected cracks (Seifert, 1965). The consistent position of these bands at high angles to (010) and the position of (010) and optics within the bands, suggests that movement has occurred along (010) planes as they bent during formation of the deformation bands, possibly along composition planes of albite twins (Seifert, 1965).

When the boundary between adjacent parts of the grain is sharp, a special type of deformation band, a kink band, is formed (Hobbs, Means, and Williams, 1976) and should be describable by axes of external and internal rotation (Seifert, 1965). Kink bands are observed in both experimentally (Borg and Heard, 1969, 1970), (Seifert and Ver Ploeg, 1977) and naturally (Seifert, 1965) deformed plagioclases of widely varying compositions, and often accompany slip and twinning.

Kink bands in the plagioclase grains of the Table Mountain mafic rocks are only observed where they are bending twins. Some of the grains show areas of slight deformation band development. They are accompanied by undulatory extinction. The grains in which deformation bands are visible are relatively unaltered. If alteration is aided by deformation (White, 1975; Seifert and Ver Ploeg, 1977) a higher percentage of the grains may have contained deformation bands which are now obscured by alteration products.

Slip

Intragranular slip or glide usually occurs along crystallographic planes and in crystallographic directions which have low Miller indices and dense ion packing. The plane and direction define a slip system which is temperature dependent. In complex crystals it is often possible to predict slip on simple geometric grounds. This is especially true for macroscopic slip which may even occur on non-crystallographic planes (Nicolas and Poirer, 1976).

In plagioclase, the development of intragranular slip is hindered by high Peierls force, the 11^* superlattice, and twins (White, 1975). In triaxial compression tests, plagioclase grains unfavorably oriented for twinning slip along (010) in the $[010]$ direction at 200°C and 5 Kb, and 800°C and 10 Kb. The slip was accompanied by kinking and up to a 7° rotation of the active slip plane (Borg and Heard, 1969, 1970).

Optically, slip results in thin closely-spaced planes. Only one photomicrograph was given (Borg and Heard, 1969) and

no distinguishing criteria. From the photomicrograph it would be difficult to distinguish a slip plane from a thin deformation twin or even cleavage. Therefore its optical distinction in the Table Mountain plagioclase grains was not made, It is very likely, however, that such slip did occur.

Twinning

At least seven different types of twins have been distinguished in plagioclase. Only two of these, albite and pericline, are commonly produced mechanically. In a detailed optical investigation of twinning from Broken Hill mafic gneisses Vernon (1965) found that 46% of the mechanical twins conformed to the albite law and 42% conformed to the pericline law. Thus they are mechanically produced in almost equal number, but pericline twinning makes up less than 10% of igneous twins.

There has been some literature discussion about which twins form first. Lawrence (1970) found pericline twins bent by albite twins suggesting an earlier formation for the pericline twins. Vernon (1965), however found no systematic variation in sequence of twin development. White (1975) found that pericline twins only occurred where albite twins were already plentiful. These variations may be a function of orientation with respect to the principal stress directions or temperature, pressure, and strain rate conditions. The importance of orientation was made clear in an experiment by Borg and Heard (1967), in which a plagioclase containing a large albite twin was deformed. One side of the deformed twin contained mechanically produced albite and pericline twins, the other side was twin

free. Table II lists the important criteria for the formation of twins by the albite and pericline laws and the multiple terminology used for the criteria.

The direction of pericline twinning is (010) with the glide plane parallel to the Rhomb Section. Albite twinning direction is irrational and dependent upon composition. It is the line of intersection of (010) with a plane defined by $b + b^*$. The glide plane is parallel to (010). When the grain is properly oriented both twins will form in the same grain. This orientation will occur when; 1) both slip planes are in a position of high resolved shear stress, i.e. K_1 and N_1 for both twins are about 45° from C.; 2) the sense of movement is positive, i.e. right and left lateral slip so that the shear directions don't interlock; and 3) the critical resolved shear stress for the two processes is similar (Borg and Heard, 1970).

The process by which mechanical twins are produced is not clear. Dislocation structures at the tip of the twin terminations suggest that they are produced by dislocation mechanisms similar to those which operate during the rapid deformation of metals (White, 1975). Twins were produced at 800°C and pressures of 8 to 10 Kb with strain rate of $10^{-4}/\text{sec}$. and $2 \times 10^{-5}/\text{sec}$. Seifert (1968) found that by 900° and 1000°C twinning was occurring at 1 and 2 Kb.

The ease of mechanical twinning at elevated temperatures may be attributed to the increased structural disordering which occurs at elevated temperatures, and the greater ease of bond breaking. Laves (1952), Starkey (1964), Seifert and

Table II

Albite and Pericline Twin Laws in Plagioclase

| Twin Law | Twin Axis | K_1 Twin/Composition Plane (also glide or slip plane) | η Twin Direction (slip plane) | Reference |
|-------------------------|--------------|---|--|-------------------------------------|
| Albite (normal) | $\perp(010)$ | (010) | | Deer, Howie, and Zusseman, 1975. |
| | | (010) | | Kerr, 1959 |
| | | (010) | irrational | Nicolas and Poirier, 1976. |
| Pericline (parallel) | $[010]$ | {010} | irrational | Borg and Heard, 1969. |
| | | (k0l) rhomb section | | Deer, Howie, and Zusseman, 1975. |
| | | in zone (010) | | Kerr, 1959. |
| | | irrational, near (001) | [010] | Nicolas and Poirier, 1976. |
| | | rhomb section | $\langle 010 \rangle$ | Borg and Heard, 1969. |

Ver Ploeg (1977), Borg and Heard (1969), describe styles of experimentally-produced mechanical twinning, which support the descriptions from naturally-produced mechanical twins (Vance, 1961; Seifert, 1964; Vernon, 1965). Twins with irregularly defined margins, lenticular twins, twins with irregular twin lamellae, very thin twins, and twins which increase in abundance around grain boundaries are considered mechanical. There may be some difficulty distinguishing between very thin twins and cleavage planes because they are subparallel. Lenticular twins are the most clearly mechanical and are observed in experimentally deformed metals (Cahn, 1953, 1954; Pratt, 1953; Hall, 1954), and in calcite (Turner, Griggs, and Heard, 1954).

All other twins are considered to be growth twins. This, however, is not strictly true since "growth" type twins have been experimentally produced (Borg and Heard, 1969). Twins which form abrupt terminations on angular steps in the composition plane are the most likely to have been produced by shear during growth or later annealing (Vernon, 1965). They terminate along irrational planes and have been experimentally produced during solid state growth in face centered cubic metals (Vernon, 1965), and in zone refined lead (Bolling and Winegrad, 1958). They are produced by stacking faults which form at grain corners, producing twin interfaces that expand as the grain grows. A simple twin will form if no later stage stacking faults are produced. Lamellae twins form when stacking faults re-establish the original orientation (Burke, 1950). The stress involved in forming such terminations by strictly

mechanical means would be unrealistically large.

Both mechanical and growth twins are present in the Table Mountain mafic rocks. In addition to the distinctions between growth and mechanical twins already mentioned, a further distinction between these two types may be given by the presence of inclusions. In the samples examined from Table Mountain those twins which fit the morphological criteria for growth twins, pass unchanged through inclusions of other grains while those twins which appear to be mechanical terminate against inclusions. This is best seen in Figure 14, where a rounded inclusion of olivine lies in the center of a thick albite growth twin. Thinner mechanical pericline twins taper towards the albite twin, terminating at the intersection. Those twins which intersect the olivine grains prior to the albite twin, terminate against the olivine.

Both bent and kinked twins are present in Table Mountain plagioclase grains. Bending as shown in Figure 45 is a gentle flexure of the twins. In this example it is interesting that mechanical twins are developed on what would be considered the compressive side. This is a further indication of their mechanical origin.

The kinked example is more difficult to see, Figure 46 shows an example of polysynthetic twins which, taper and bend. A similar feature in a polysynthetic twin pictured in Borg and Heard (1970), is attributed to a 7° kink band where the twins end.

In addition to their interesting morphology, plagioclase twins should theoretically be able to yield important information



Fig. 45
Bending in plagioclase twin.

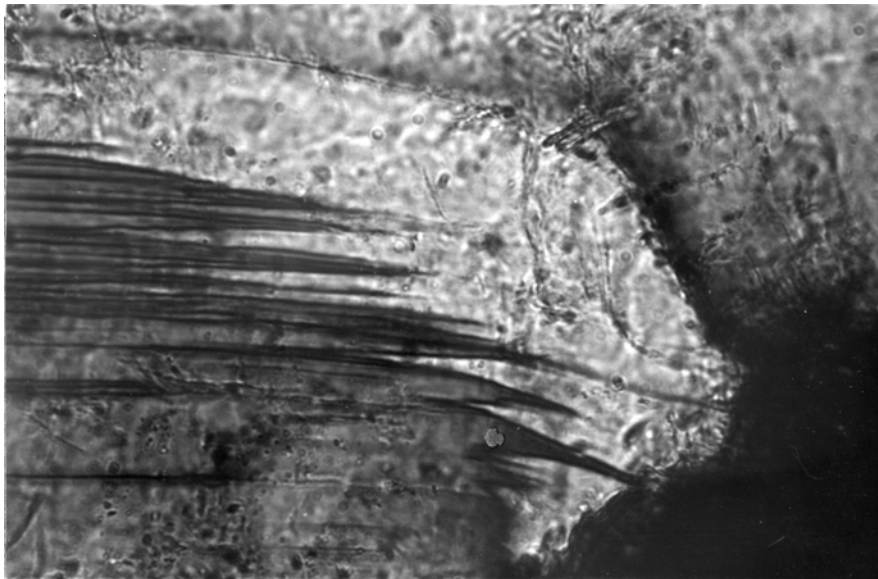


Fig. 46
Tapered and bent plagioclase twin, possibly due to kinking.

about conditions of deformation, such as temperature and possibly stress directions.

Twinning in calcite has been used to determine principle compressive stress directions (Turner and Weiss, 1963). Plagioclase twins are also theoretically suitable for determining principal directions of compressive stress. Lawrence (1970) using naturally deformed plagioclase with an average composition of An_{20} from a hypidiomorphic granular gneiss, made stress determinations using albite twins. An unusual feature of these twins was the bending of pericline in the presence of straight albite twins, which suggest to him a later formation for the albite twins.

To determine the direction of principal compressive stress, the poles to (010) and (001) were obtained using the Universal-Stage from the composition planes or cleavages from twinned grains. Optical and crystallographic directions are close at An_{20} , so optical directions were substituted when crystallographic directions couldn't be determined. This enabled each twinned grain to be measured. Fifty measurements were taken from each oriented thin section. Points were plotted at 45° to the pole to (010) and in the plane containing both the pole to (010) and to (001). If the cleavage angle with the untwinned portion of the grain could be accurately determined, the points were identified as C (compression) and T (tension).

C is plotted as the obtuse angle (93°) between the pole to (010) and pole to (001). T is plotted as the acute angle (83°). C and T are difficult to distinguish in most grains especially when lamellae are very thin, so most grains retain

a 90° ambiguity and are labeled 0.

The samples were taken from near a fault. As the fault is approached, the plagioclases elongate parallel to their a-axes. Because of the fabric few or no grains are oriented in positions that would give C, T, or O points near the lineation and hence only a partial stress field is revealed.

An important comparison with stress and percentage of twinning in calcite, is that, in calcite twins, the center of concentration of C points is also the point of highest twinning. This center area is considered maximum stress for the entire plot. Lawrence (1970) also estimates percentage twinning and found that this does not occur with plagioclase twins, thereby emphasizing the inhomogeneity of deformation on the scale of individual grains.

Borg and Heard (1970) take advantage of the combined albite and pericline twins to apply the Turner and Weiss (1965) stress determinations from twins. Unfortunately, they do not have a large enough sample to determine the accuracy of their method. Because of the difficulty of measuring the Rhomb Section, Borg and Heard (1970) recommend measuring the (010) and (001) planes which, for the purposes of investigation, are close. Although the angle between the Rhomb Section and (001) varies widely in Low T plagioclases: from $+35^\circ$ for An_0 , to -17° and -20° for An_{100} , variation in high T forms is always between $4 - 6^\circ$. For Table Mountain compositions the variation is approximately $4 - 10^\circ$. The (010) \wedge (001) ranges from $90^\circ 3\frac{1}{2}' An_0$ to $83^\circ 54' An_{100}$. The situation might be visualized as in Fig. 47

This page is missing from both the archive and library shelf copies of the thesis (probably was Fig. 47, which is also not present)

C' is considered the bisector of the acute angle between (001) and (010). The angles used, however, are small and therefore inaccuracies due to Universal-Stage wobble may be significant. Further inaccuracies may be introduced because twinning is affected by local stress inhomogenities, such as impurities and adjacent minerals. A further important question that has not been addressed experimentally, is the behavior of a twin formed under gradually cooling conditions in a changing stress regime. Which temperature and stress will the twins represent?

In ophiolite rocks, an effective measure of the major compressive axis would be significant in understanding accretion processes. These rocks contain a layering, but are predicted to change lithologies parallel to the compositional strike (Greenbaum, 1972; Dewey and Kidd, 1977). If this is true and, if twinning occurred after deposition as the wedge moved out of the magma chamber and away from the axial singularity, then the major compressive axis would be at some oblique angle to the layering. The obliqueness of the angle should depend upon the amount of rotation undergone by that part of the magma chamber floor. An especially nice aspect of this, is that material at the base of the magma chamber would probably be still warm enough to undergo mechanical twinning. Samples from Table Mountain contain a large number of polysynthetic albite and pericline twins.

For this investigation layered gabbroic rocks were examined with the Universal Stage. Sections were cut perpendicular to the foliation. The (010) and (001) composition planes were measured for every section which contained both

twins when the twins fit the "mechanical twins" criteria previously discussed. Poles to the planes were plotted on a Schmidt net. C' was taken as the acute bisector. When the angle was 90° no C' measurement was made. The number of grains in the six samples measured varied from 4 to 36.

The distribution was contoured using the Braun (1969) method. The orientation of the layering in thin section was plotted. The results are given in Table III. The angle the area of highest concentration made with the layering was measured. The obliquity varied from 5 to 42° . The only troctolite sample measured has the highest angle, while the olivine gabbro has the lowest. This sample, however, was the dike rock noted for its extreme freshness.

The orientation of the layering was then plotted on a stereonet. The samples were unoriented, so to relate the highest percentage of compression concentration determined from the twinning, great circles were drawn at that angular distance from the layering. The lineation was plotted. No consistent relationship between the three factors could be ascertained. In light of the lack of a relationship between the factors, and the absence of an independent test to verify the validity of this method in determining maximum compression direction, it is impossible to use it as a test of a differentially subsiding accretionary wedge.

Subgrains

Subgrains are low angle lattice misorientation grains. They are common in deformed quartz but rarely occur in plagi-

TABLE III

Angle between compressive stress direction and layering determined from twin orientations.

| Sample Number | Layering | Lineation | Number of Points | Highest % Concentration | Angle to Layering | Rock Type | Subarea |
|---------------|-----------|-----------|------------------|-------------------------|-------------------|----------------------|---------|
| 119 | 100, 21SW | ----- | 20 | 15% | 25°-40° | gabbro | I |
| 171 | 135, 50NE | 15 → 118 | 4 | ----- | 50°-65° | gabbro | V |
| 188 | 85, 80NW | 36 → 43 | 16 | 13% | 7°-20° | gabbro | V |
| 240 | 125, 76NE | 05 → 117 | 22 | 22% | 25° | hornblende gabbro | IV |
| 253A | 70, 64NW | 47 → 23 | 36 | 19% | 5°-10° | olivine gabbro | V |
| 320B | 70, 68NW | 46 → 14 | 19 | 21% | 33°-42° | troctolite | V |

class. White (1975) attributes this to the presence of the 11^* superlattice and possibly to twins, both of which hinder the movement of dislocations and hence the planar alignment of dislocations to form subgrains of these two factors. The 11 superlattice structure seems to be the most influential. Dislocations in superlattices increase the disorder in the form of anti-phase boundaries and hence the internal energy of the grain. To minimize the energy, another dislocation of the same sign is formed opposite the anti-phase boundary thus producing a super dislocation, which severely inhibits cross slip and climb and thereby recovery. Superlattices however have a critical disordering temperature. The thermal influence is supported by the formation of subgrains in upper amphibolite grade metamorphic andesines and labradorites (White, 1974). Albite, however, does not form a superlattice and therefore should form subgrains more easily. This is discussed in relation to dislocation distributions by Lorimer et. al. 1972.

Some subgrain formation was observed in Table Mountain plagioclases in the fresh olivine gabbro sample. They form in untwinned grains. This suggests that at elevated temperatures in grains unsuitably oriented for twinning subgrains may form.

Recrystallization

Three major processes have been proposed in materials science for the nucleation of primary recrystallization. All of these methods appear applicable to some examples of plagioclase recrystallization. The processes are: 1) Nu-

cleation and growth of discrete grains (Burke and Turnbull, 1952; White, 1975), 2) Formation and growth of subgrains with progressive misorientation produced either by coalescence of subgrain boundaries or by subgrain rotation (Li, 1962; Hu, 1963; Vernon, 1975; Marshall and Wilson, 1976) and 3) Bulging of pre-existing high angle boundaries between two points that are pinned by other defects (Bailey and Hirsch, 1962; Vernon, 1976).

Recrystallization of plagioclase under experimental conditions has only been documented once and then in a peristerite (Marshall et. al., 1976). In this experiment conducted in a Griggs apparatus at 850°C at 10 Kb. with a strain rate of $10^{-5}/S$, recrystallization occurred by the nucleation and growth of discrete grains scattered through a strongly deformed matrix. No chemical change was mentioned.

In naturally deformed and recrystallized oligoclase White (1975) found a change of An_{29-31} to An_{20-27} in a microprobe analysis from primary to recrystallized grains. This was in keeping with the lower metamorphic grade at which recrystallization occurred. Vernon (1975) also found a slight decrease in calcium content in recrystallized plagioclase grains, which appeared to form from subgrains. This may indicate that at least a small compositional change is necessary for recrystallization to occur (Vernon, 1976).

In a large andesine (An_{40}) single crystal from a granulite facies terrain in Central Australia, partial recrystallization has preferentially occurred along narrow zones and in local patches of relatively high strain. Bulges, which

may have formed from the local migration of deformation band boundaries, appear to have acted as nuclei for new grains. Other deformation bands, however, pass into diffuse patches of apparent subgrains that could also eventually give rise to new grains (Vernon, 1976).

Where recrystallization has been documented, the crystallographic orientation of the new grains is close to that of the original grain. This suggests that, as with quartz and olivine, a host-new grain relationship controls the intragranular recrystallization of plagioclase (Vernon, 1976).

As mentioned earlier, many of the Table Mountain plagioclase grains have the low-energy triple point boundaries indicative of either adcumulate growth or recrystallization. In most non-cataclastic samples, definitive evidence for recrystallization is small. In areas where two distinct grain sizes exist, the smaller grains often have a mosaic texture. This is the situation shown in Fig. 48. Twinning is present in both sizes although in the larger grain they show more of the mechanical twinning morphology. Possibly two periods of deformation are represented; an earlier and probably higher temperature period in which recrystallization or some degree of grain boundary adjustment occurred, and a later period of either lower temperature or higher strain rate deformation during which twins formed. The two periods do not necessarily represent a major hiatus in time. Alternatively the twinning and recrystallization may have occurred simultaneously. The growth like twins in the smaller grains may have been induced by the same stress regime which caused the recrystallization

and mechanical appearing twins in the larger grain.

Cataclasis

Cataclasis, consisting of inter and intragranular fractures, crushing and undulatory extinction, is the dominant form of deformation at all temperatures and confining pressures in an experimentally deformed anorthosite (Seifert and Ver Ploeg, 1977). The extent of cataclasis shows a weak negative correlation with temperature and a strong negative correlation with confining pressure. The percentage of cataclasis ranged from 40 - 75% at 5 Kb. to 25 - 50% Kb.

Below 600°C, there are no active slip or twin glide systems, so cataclasis is the only form of deformation (Borg and Heard, 1969, 1970). Fractures often accompany the more ductile forms of deformation, forming adjacent to twins, along the margins of deformation bands, and at grain boundary intersections.

Most Table Mountain samples show some evidence of grain-scale cataclasis, in the form of small intragrain microfractures, and some larger fractures that extend beyond grain boundaries. Alteration minerals commonly occur along the microfractures which probably served as conduits for alteration material. The orientation of cracks both inter and intragranular appears to be random and bears no relationship to the presence or absence of more ductile deformation features. Figure 49 shows microfractures forming in a single large plagioclase grain surrounded by cataclastic material.

Long fractures, termed transverse fractures, are present

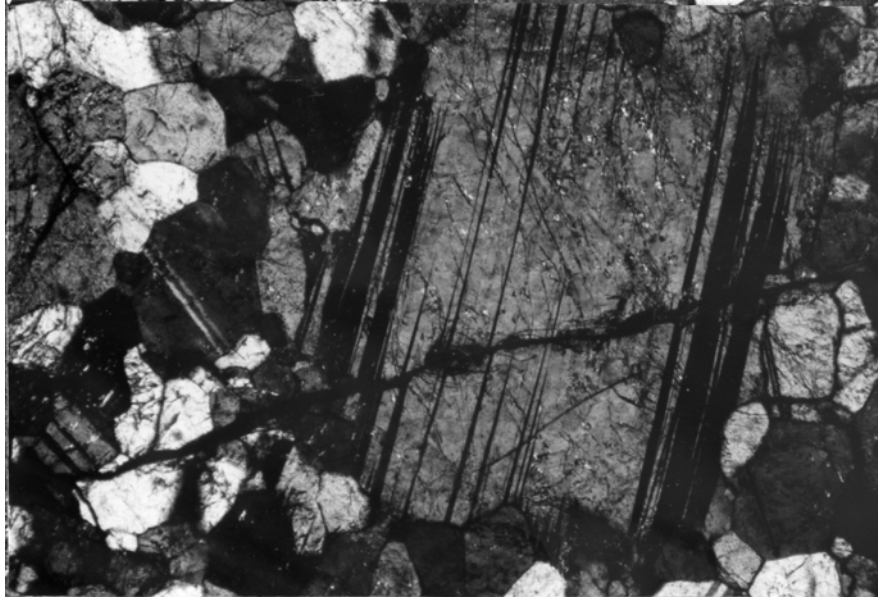


Fig. 48
Recrystallization in plagioclase grains showing mosaic texture in smaller grains.

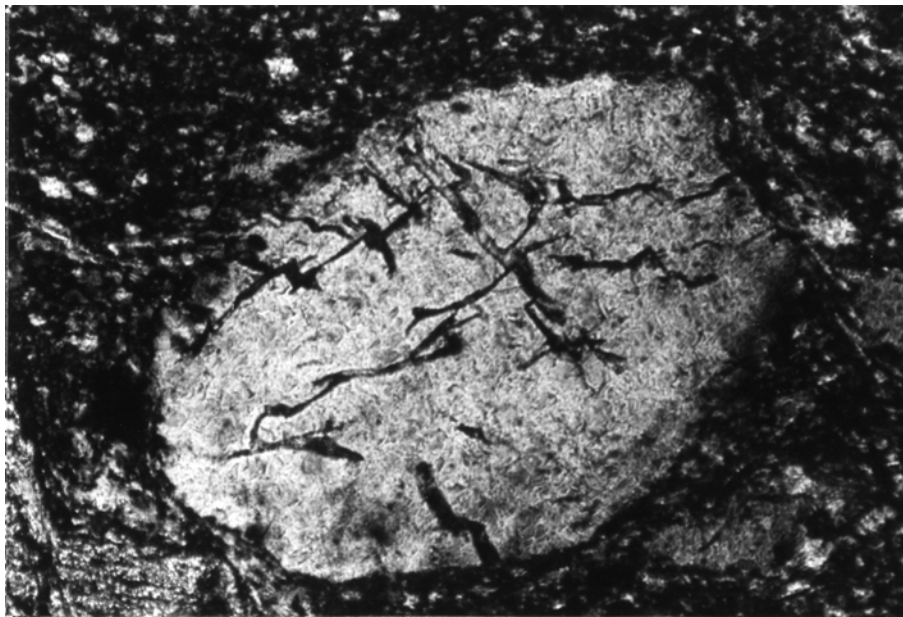


Fig. 49
Microfractures forming in a single large plagioclase grain surrounded by cataclastic material.

in some samples and cut the plagioclase grains, usually unaffected by grain boundary interference. These are often filled with minerals such as prehnite and are sometimes accompanied by more extensive brittle deformation such as grain fragments, and offsets of earlier, smaller fractures.

Diopside

A majority of the attention given to experimental and natural pyroxene deformation studies have been focused on orthopyroxene, particularly in relation to mantle peridotites and the enstatite - clino-enstatite inversion. Some of the deformation processes are also applicable to clinopyroxene.

Clinopyroxenes have monoclinic symmetry. Griggs et. al. (1960) were the first to experimentally deform diopside. At 5 Kb. and 500°C in a triaxial compression test; diopside deformed by twinning on (100) [100] and on (001) [100]. Further investigations by Raleigh (1965) and Raleigh and Talbot (1967) showed that at higher temperatures and lower strain rates slip on (100) [001] and twinning on (100) [100] prevailed over (001) [100] twinning. Slip becomes important above 1000°C for strain rates of $5 \times 10^{-5} \text{ s}^{-1}$ and only one slip system has been reported. Twins formed on (001) [100] are wider, more widely spaced, and more discontinuous than (100) [001] twins. Both sets of twins formed where the resolved shear stress on the twin glide system is high. In a large number of grains the compression axes most favorably oriented for twin gliding are sub-parallel to the direction of maximum compression in experiments. Compression axes determined for naturally deformed

diopside from a faulted region in the Eastern Mount Lofty Ranges, South Australia agree with the compression directions deduced from faulting.

At more elevated temperatures and lower strain rates e.g. 1050°C and $10^{-3}/s.$ or 750°C and $10^{-6}/s.$, (100) [001] twin gliding gives way to translation gliding or slip on many systems (Ave'Lallemant per. comm. in Carter, 1976). Kirby and Kronenberg (1978) in triaxial compression experiments found a similar sequence of deformation mechanisms in clinopyroxenite with increasing temperature and decreasing strain rate, temperatures ranged from 400° - 1000°C and strain rates from $10^{-3}/s.$ to $10^{-7}/s.$ at a confining pressure of 15 Kb. Temperature and strain rate fields over which the mechanisms operate overlap but the general trend was: 1) cataclasis, 2) (100) and (001) mechanical twinning 3) (hk0) <001> slip and associated kinking and undulatory extinction and 4) multiple slip and associated relatively homogeneous strain and subgrain formation. Under conditions 1 and 2, the flow stress ($\sigma_1 - \sigma_3$) shows little sensitivity to temperature and strain rate. Flow stress under conditions which promote slip, however, show considerably more sensitivity to temperature and strain rate.

One means of recovery in clinopyroxenes is by polygonization with polygon walls having the appearance of straight sharp kink band boundaries separating optically homogeneous domains. Polygonization in clinopyroxenes requires higher temperatures and/or lower strain rates than needed for orthopyroxene or olivine.

Experimental recrystallization of pyroxene has been difficult. Carter et. al. (1972) recrystallized compacted powders of diopside at 15 Kb. and 1000°C at a strain rate of $7.8 \times 10^{-7}/s$. A strong [010] preferred orientation developed parallel to σ_1 . The remaining crystal and indicatrix axes form a girdle in the $\sigma_1 - \sigma_3$ plane. Few clinopyroxene fabrics have been determined in peridotite tectonites and no steady state mechanical data are available for clinopyroxenite.

Table Mountain clinopyroxenes occur in two distinct size groups, as large grains up to 50 mm. across and smaller equant grains about equal in size with the plagioclase. Deformation has been accomplished primarily through slip and fracturing. No mechanical twinning was observed. The individual deformation features are most easily observed in the larger grains. This may be because, unhindered by grain boundaries, they are able to store larger quantities of strain and therefore the deformation features are more extensively developed.

Movement has occurred parallel to the axis of cleavage traces or partings. Universal-Stage determinations were not done. Optic axes figures and extinction angles indicate that the slip plane is probably (100), which fits with experimental results. Kinking at high angles to the cleavage (Fig. 50) and fracturing perpendicular to the cleavage (Fig. 51) are frequently observed, especially in the larger grains.

In cases of more extensive deformation, fracturing disrupts the grain and long thin pyroxene pieces are rotated to an oblique angle to the cleavage (Fig. 52). The shortness

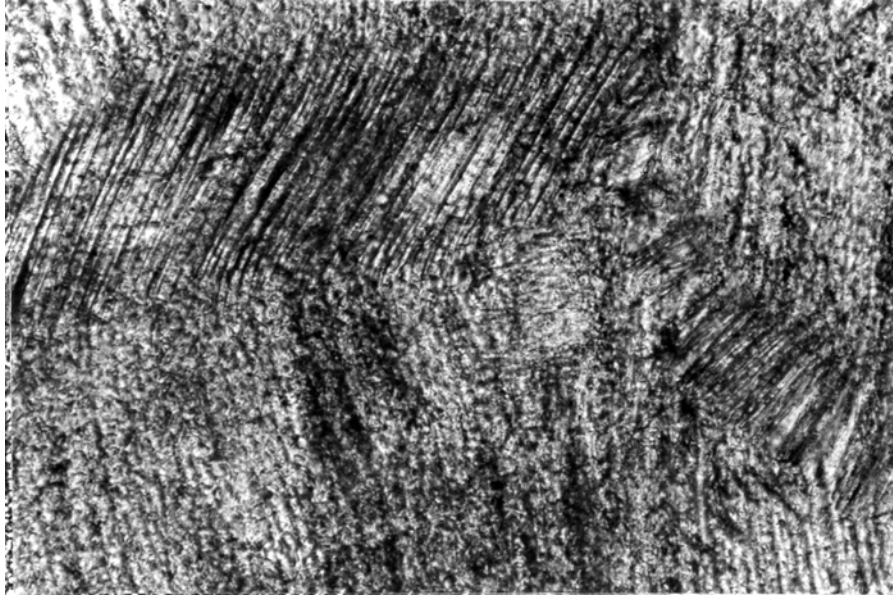


Fig. 50
Kinking in diopside at high angles to the cleavage.



Fig. 51
Fracturing in diopside perpendicular to the cleavage.

of the perpendicular to cleavage fractures suggests the release of smaller strain accumulations and/or the difficulty of propagating a crack perpendicular to cleavage. Such difficulty might arise where slip and fracturing are occurring simultaneously. A fracture propagating through the grain would abut a surface where active glide was occurring and its strain energy would be dissipated.

Deformation bands are also present. These are irregular bands that appear to be compositionally the same as the host grains but extinguish at a different position, and are therefore best observed under crossed polarizer with part of the grain at extinction. They vary in width from approximately .1 mm. to .01 mm. and widen when they encounter an inclusion or another deformation band. They frequently thin and pinch out adjacent to the grain boundary.

Fractures having a random orientation with respect to cleavage occur in many of the grains. They become especially prevalent as cataclastic areas are approached. One grain contains an especially interesting fracture (Fig. 53). It extends from the grain boundary, well past the center of the grain where it branches at a high angle. The fracture edges (Fig. 54) are irregular and contain both lobed and straight segments. Plagioclase fills the fracture and actinolite needles radiate from the pyroxene boundary into the plagioclase. The fractured grain is surrounded by smaller plagioclase and clinopyroxene grains. This fracture is further evidence for at least some melting or magmatic activity postdating the onset of brittle deformation.

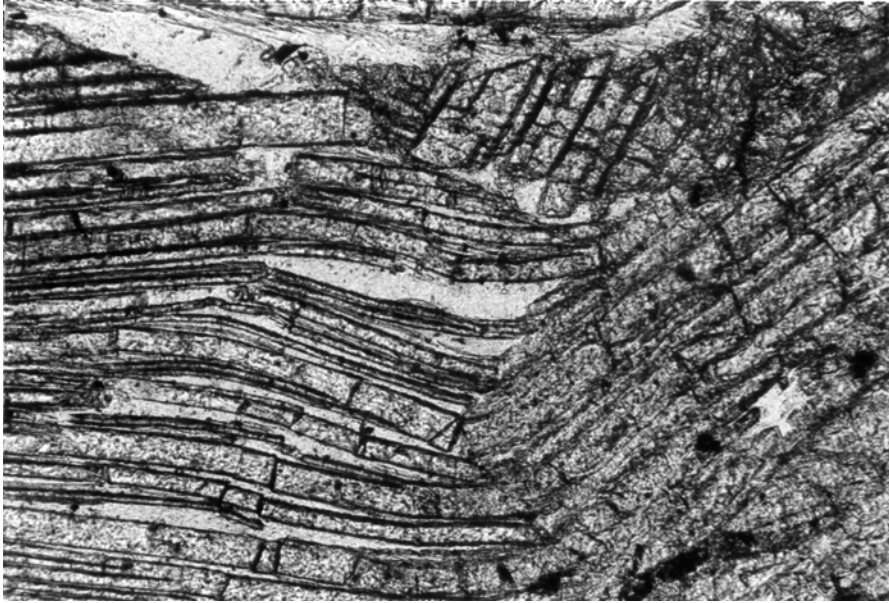


Fig. 52
Rotation of pyroxene fragments.



Fig. 53
Plagioclase and actinolite filling large fracture in diopside grain.

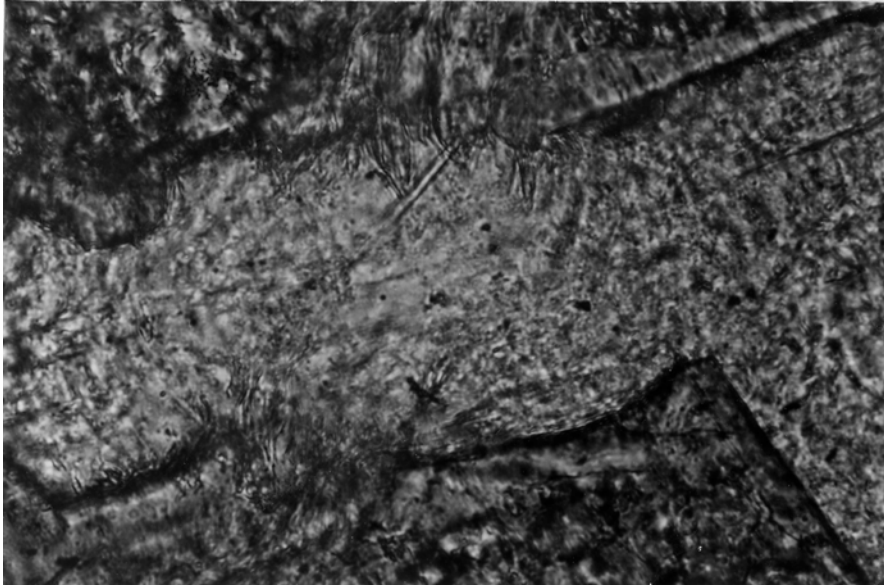


Fig. 54
Plagioclase and actinolite filling large fracture in diopside grain.

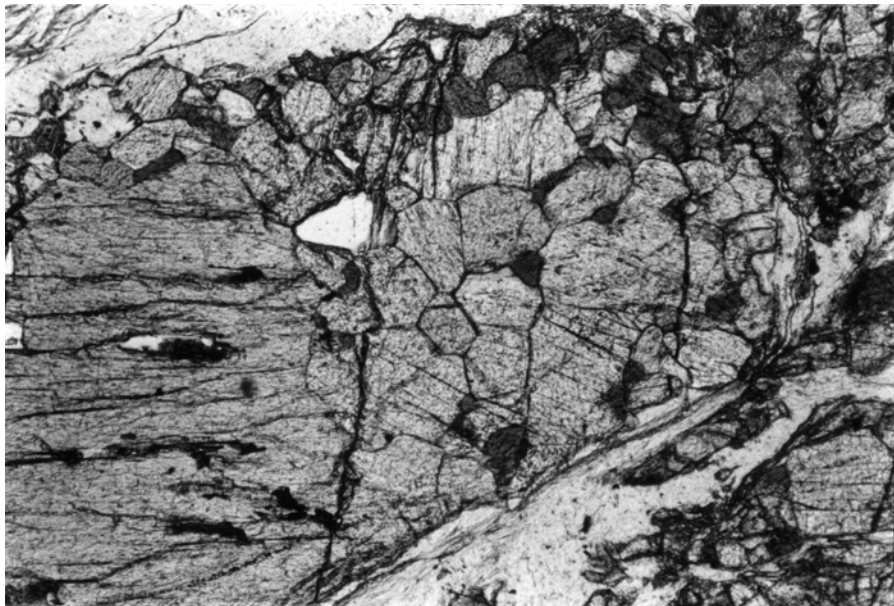


Fig. 55
Incipient recrystallization in diopside grain.

As mentioned in the petrography section, many of the clinopyroxene grains appear to have undergone recrystallization as shown by the polygonal grain boundary junctions in large rounded clumps of clinopyroxene (Fig. 6). In some grains which appear to have undergone recrystallization, the new grain boundary forms between the highest concentration of opaque inclusions. The presence of such inclusions must favorably affect recrystallization, possibly by increasing the disorder and hence strain energy in the host grain. The incipient recrystallization as shown in Figure 55 suggests that grain nucleation and growth has not played a significant role. Therefore recrystallization probably occurred through subgrains or the bulging of pre-existing high angle boundaries. No data is currently available to see what chemical change accompanied recrystallization.

Summary

The majority of the Table Mountain mafic samples have been deformed at elevated temperatures and/or low strain rates. This is seen from the microstructures in the abundance of mechanical twinning in the plagioclase and slip, kinking and recrystallization in the pyroxenes. Stress determinations from albite and pericline twins in the plagioclase indicate that the compressive axes to the stress were at moderately oblique angles to the layering.

Strain post-dating the plastic deformation was accommodated by intragrain microfracturing and the minor development of transverse fractures that bisect grain boundaries. Some of the

transverse fracturing was accompanied by hornblende injection. Most of the transverse fractures however, are filled with prehnite, smectite, and sericite, low grade metamorphic minerals. All of these secondary minerals and deformation features are found in ocean dredge samples and could therefore have formed in the oceanic as well as the land part of the ophiolite history.

CHAPTER VII
CATACLASTIC ROCKS

Introduction

Developmental processes and even terminology of cataclastic rocks are neither well understood nor well formulated. Two major morphological divisions of cataclastic rocks exist determined by the presence or absence of a cataclastic foliation, termed fluxion structure. Higgins (1971) has clarified and extended the classification to include cohesion, recrystallization and grain size (Table IV)

In all cases cataclasis involved high strain and grain size reduction. The development of each specific type of cataclastic rock depends on the temperature, pressure, strain rate and the mechanical properties of the mineral undergoing cataclasis. Microscopic deformation mechanisms include microfracturing, frictional sliding, dislocation glide and climb, volume and grain boundary diffusion and grain boundary sliding (J. Tullis, 1978). Of the two major groups, those with fluxion structure, the mylonites, have received the most attention within experimental and descriptive literature.

Cataclastic rocks with and without fluxion structure are present in Table Mountain. Those lacking fluxion structure are found in small high-strain zones; those with fluxion structure are well-developed mylonites and ultramylonites associated with the Trout River Pond Fault.

Classification of Cataclastic Rocks

Porphyroclastic, protoclastic, diaphthoritic, pseudotachylitic, polymetamorphic, polycataclastic, phyllitic, and other terms are used as modifiers.

| | | | |
|--------------------------------|--|--|--|
| Rocks without primary cohesion | Rocks with primary cohesion | | Approximate size of most porphyroclasts in rocks with fluxion structure, or Approximate volume percent fragments in rocks without fluxion structure. |
| | Cataclasis dominant over neomineralization-recrystallization | Neomineralization-recrystallization dominant over cataclasis | |
| Fault breccia | Rocks without fluxion structure | Rocks with fluxion structure | Visible to naked eye |
| | Microbreccia | Proto-mylonite | |
| Fault gouge | Cataclasite | Mylonite | >0.2 mm |
| | | Ultra-mylonite | <0.2 mm |
| | | Phyllonite (variety) | |

ALL ROCKS ARE GRADATIONAL

Non-Foliated Cataclastic Rocks

High-strain zones do not appear to be as abundant or as well developed on Table Mountain as they are on the other Bay of Island massifs. They are most prevalent in the hornblende gabbros on the NE side of the field area. In outcrop and in thin section, the high-strain zones accompany areas of extensive microfracturing at many angles to the layering plane, and form irregular and interfingering boundaries with the less deformed areas (Fig. 56).

Offsets and bending of the lineation and layering occur adjacent to the microfractures. Where the fractures are numerous and intersect, the deformation of the intrafracture material increases. The fractures themselves vary in morphology from very thin (2 mm.) linear features to 50 cm. wide zones of braided deformation. The braiding is best seen on polished surfaces. The braiding usually pinches out before intersecting the narrow linear fractures.

Although fractures are found to occur throughout wide areas and are especially predominant in the hornblende gabbro, the individual fractures have very limited extent and rarely extend beyond 10 cm. Grain size does not appear to influence the development of microfractures.

The thin section deformation observed was discussed under microstructure. The only addition to that discussion would be, that in areas where a linear zone of cataclasis has developed, tension gashes have been observed to form perpendicular to the linear trend of the cataclasis (Fig. 57).

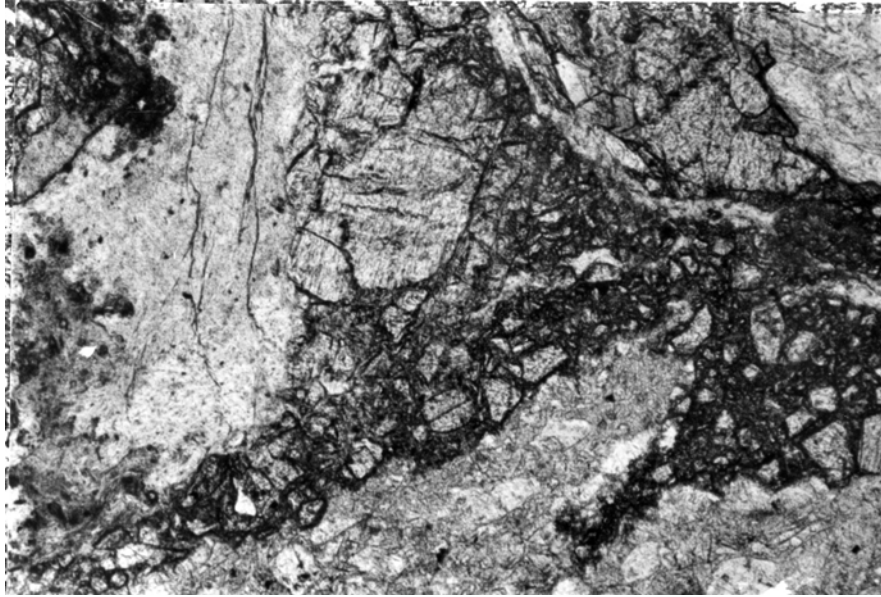


Fig. 56
Irregular and interfingering boundaries of cataclastic material in host rock.

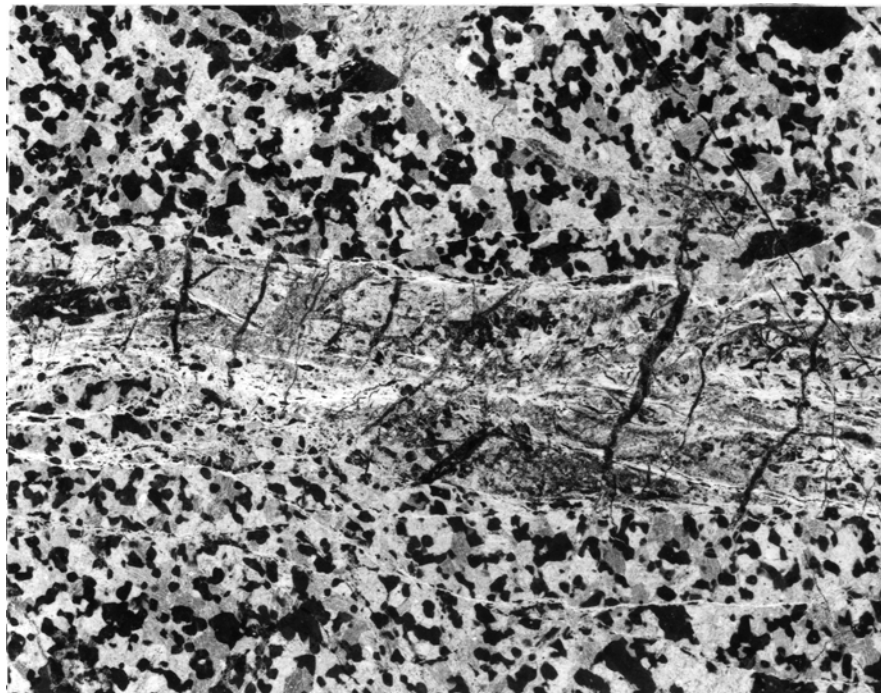


Fig. 57
Tension gashes forming perpendicular to a high strain zone.

Foliated Cataclastic Rocks

Mylonites are thought to form in at least three different ways: 1) at low temperature and high strain rates where the rocks are brittle and deform principally by microfracturing, which can be analogous to ductile deformation or translation gliding; 2) at higher temperatures where the rocks are more ductile and the deformation mechanism is principally by dislocation glide aided by recovery and recrystallization, and boudinage and necking are common; and 3) at even higher temperatures and low-stress conditions where the most easily recrystallized mineral recrystallizes into small grains and deformation proceeds superplastically by grain boundary sliding (Higgins, 1971; Bell and Ethridge, 1973; Boullier and Gueguen, 1974; Allison and La Tour, 1977; J. Tullis, 1978).

Mylonites outcrop along a steep cliff paralleling Trout River Pond. They have a north-northwest trending gently north-east dipping foliation. The mylonite is in contact along its upper surface with gabbro which appears relatively undeformed. The transition is sharp. The lower bounding surface has been eroded away (Fig. 58). Bell and Ethridge (1973) have noted gneissic rocks which appeared undeformed in hand specimen have significant mylonitic deformation in thin section. Unfortunately none of the nearby rocks are available for thin section study in this investigation.

In outcrop the mylonites have a grey-green color and a strong although not strictly parallel foliation. Grain size



Fig. 58
Mylonite in contact with gabbro.

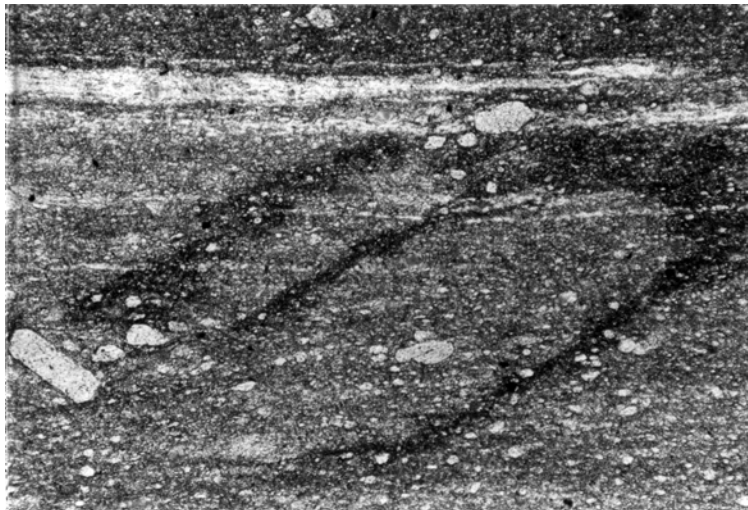


Fig. 59
Large euhedral plagioclase grain in mylonite.

variations are apparent, but they are mostly too fine to measure. The most obvious distinction is between layers with and without grain clasts larger than the host matrix. Grain clasts usually have an augen or flattened shape.

In hand specimen, the mylonites are cut by small fractures. Fractures perpendicular or subperpendicular to the foliation occur within the clast layers. They die out within the clastless layers. Low and moderate angle fractures occur in the clastless layers. In several instances larger fractures at about 45° to the foliation will parent smaller conjugate fractures. Offsets are minor.

Microscopic observations show brittle and ductile deformation features. The plagioclase appears to be almost completely recrystallized and consists of small, equant, anhedral grains. The grains are capable of flow between the less ductile pyroxene layers. It is not clear whether it behaved plastically or pseudoplastically. One relict plagioclase clast was observed (Fig. 49). This grain shows intense undulatory extinction, is cut by microfractures, and is surrounded by cataclastic and recrystallized small plagioclase grains.

In the thin sections studied, only one plagioclase grain has grown considerably larger than the adjacent grains. This one grain has an euhedral shape oriented at about 35° to the foliation and about 110° to an area of more intense deformation (Fig. 59).

The pyroxene grains have deformed in a wide variety of

ways which include boudinage, fracture, kinking, bending, sheaving, folding, slip, and recrystallization. Many of these processes appear to be simultaneous. They show some dependence upon the orientation of the cleavage to the foliation plane, the proximity of plagioclase, and grain size.

In Figures 60 and 61, the cleavage in a large pyroxene grain is oriented perpendicular to the mylonite foliation. The cleavage at the end of the grain is bending into parallelism with the foliation. This is being accomplished by kinking between "subgrain" areas (more clearly evident under crossed polarizers), and extension parallel to the cleavage as it approaches parallel with the mylonite foliation. In Fig. 62, the pyroxene grains appear to have sheared parallel to the foliation which is also parallel to the cleavage trace. Fig. 63 shows the sheared Fig. 62 pyroxene reconstructed to its pre-shearing state. In Figures 64 and 65, another pyroxene grain is separated by what appears to have been kinking with a loss of the kinked fragments. Some minor extension may also have occurred parallel to the cleavage trace.

Small pyroxene grains or fragments undergoing mylonite deformation appear to be influenced by the more ductile behavior of plagioclase, and form boudins. In Figure 66, a small pyroxene fragment is separated from a larger pyroxene grain by a thin layer of plagioclase. Shown enlarged in Fig. 67, the fragment has been boudinaged by what appears to be tight kinking and extension parallel to the edge of the large

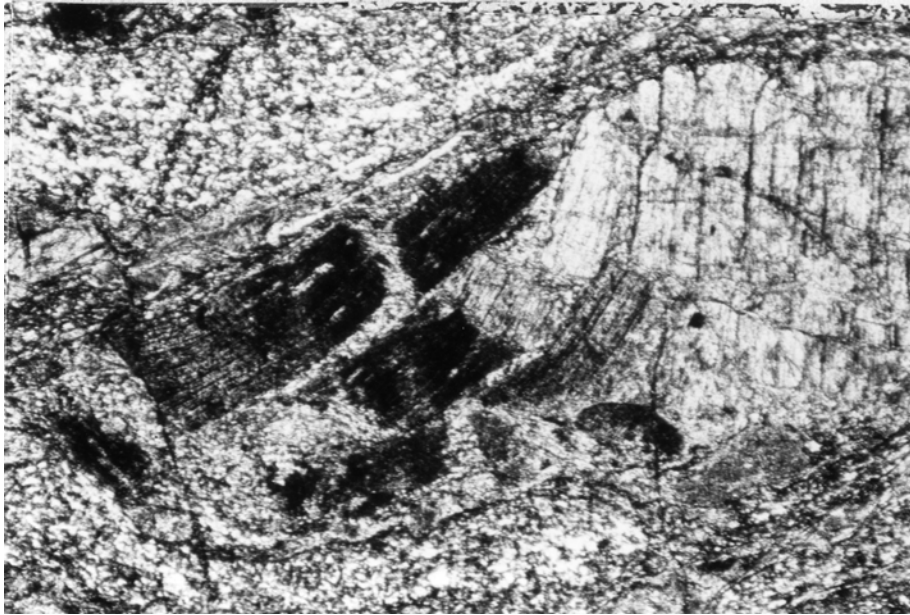


Fig. 60
Deformation of large pyroxene grain (crossed-polarizers).



Fig. 61
Deformation of large pyroxene grain (uncrossed-polarizers).

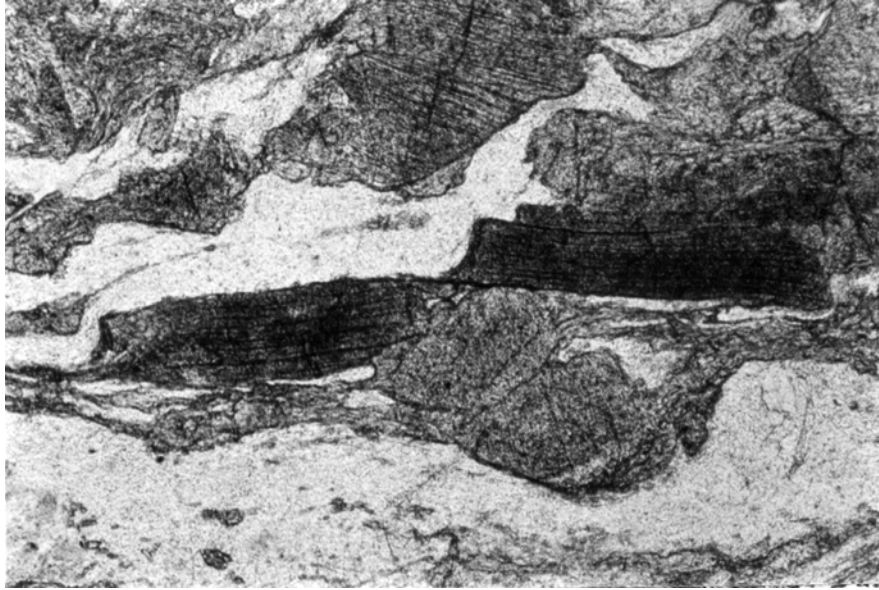


Fig. 62
Pyroxene sheared parallel to cleavage trace and mylonite foliation.

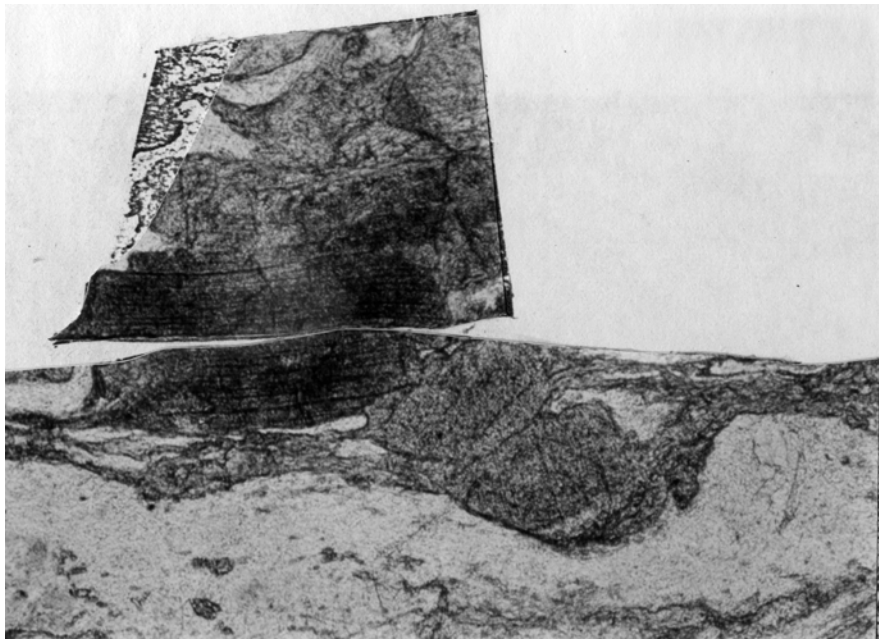


Fig. 63
Reconstruction of Fig. 62 pyroxene.

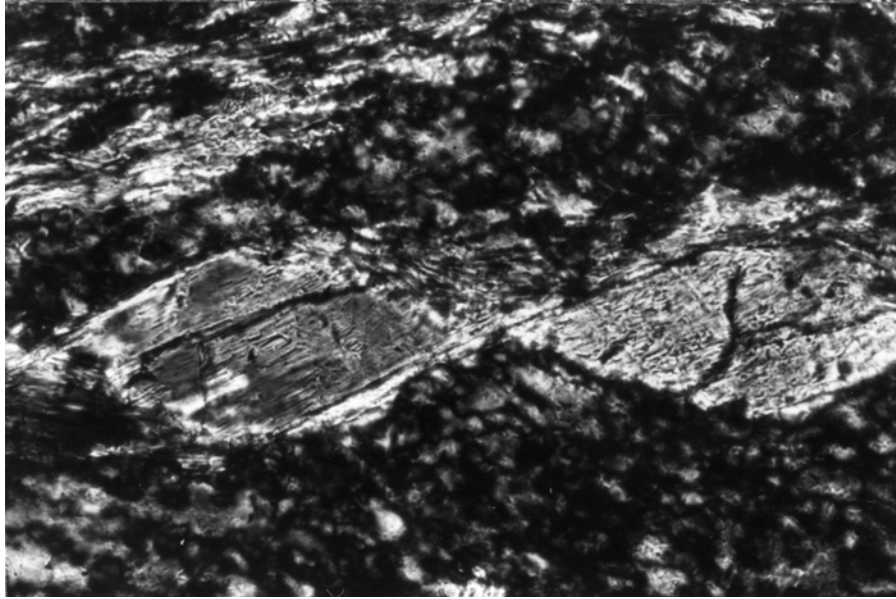


Fig. 64
Pyroxene with sheared appearance probably due to kinking and loss of kinked fragments (crossed-polarizers).

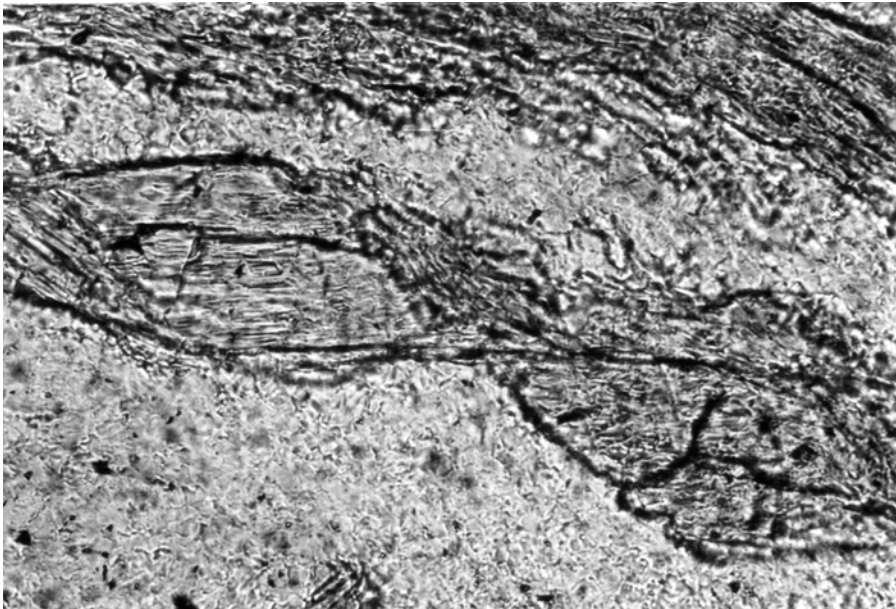


Fig. 65
Above Figure with uncrossed polarizers.

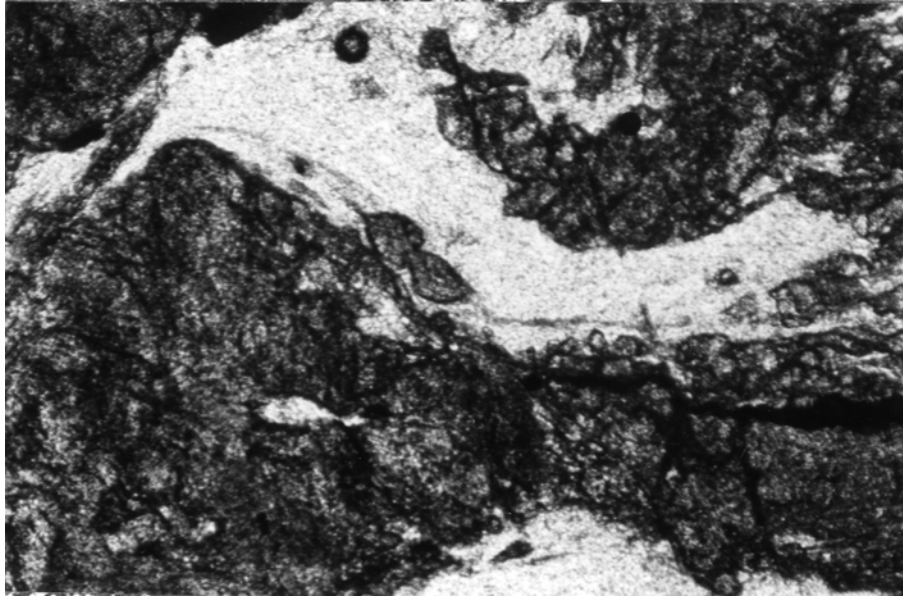


Fig. 66
Boudinaged pyroxene fragment separated from larger pyroxene by a thin layer of plagioclase.

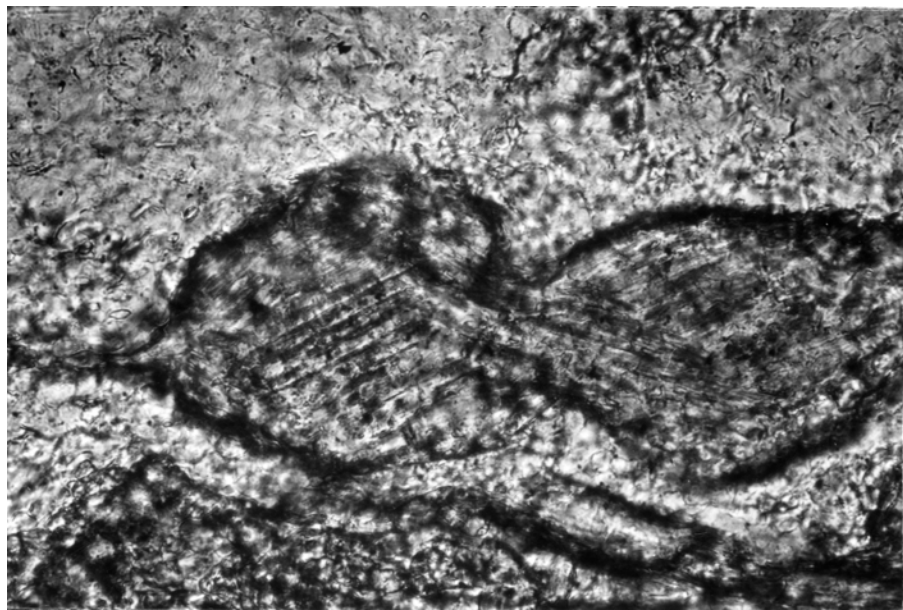


Fig. 67
Detail of boudin from Figure 66.

adjacent pyroxene grain. Figures 68 and 69 show boudins which are more formed by either much tighter kinks or fractures and are clearly fragments of the larger pyroxene.

Folding of the mylonite foliation occurs where both the pyroxene and plagioclase grains are small and grain size variation is minimal. The folding, as shown in Figure 70 is best developed at the plagioclase/pyroxene interface.

Large and small fractures, both inter and intra grain occur throughout the mylonites. In individual pyroxene grains fractures often develop between 30° and 45° to the foliation, especially if the cleavage is approximately 45° to the foliation. These fractures probably developed during mylonitization. Intergrain fractures of varying widths have developed. Some of the thinner fractures do not propagate through the plagioclase areas. Other fractures with more diffuse boundaries, and accompanied by alteration, are primarily in the plagioclase (Fig. 71). The larger cross-cutting fractures are not bent or deformed and probably formed after the mylonitization was completed.

From the observations available it is not clear if the fineness of the mylonite grain size is a function of the initial grain size or degree of deformation. Rough estimates using a method of strain analysis discussed in the next section suggest that the finer grain size does reflect more intense deformation.

Strain Analysis

From these samples it appears that mylonitization has

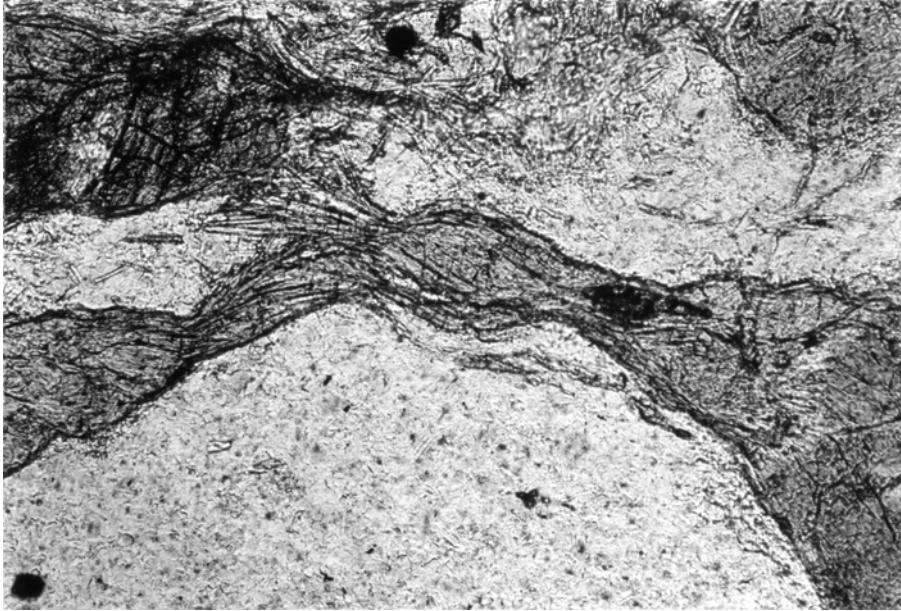


Fig. 68
Two generations of boudins in pyroxene.

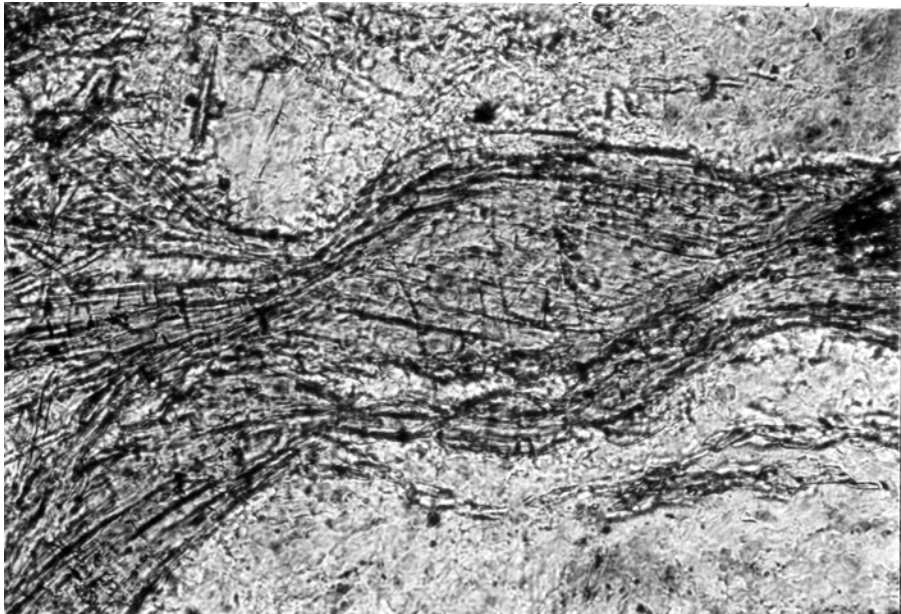


Fig. 69
Detail of boudin from Figure 68.



Fig. 70
Folding of mylonite foliation.

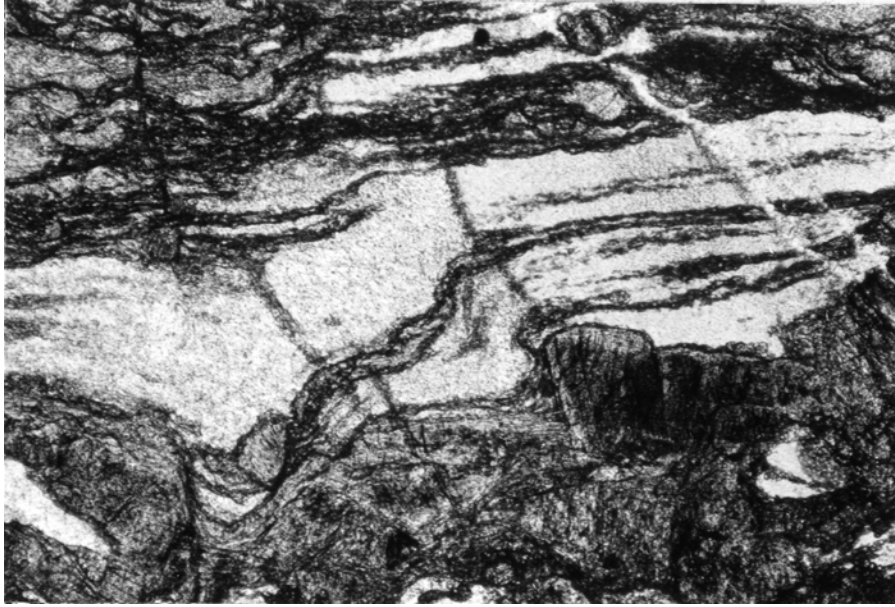


Fig. 71
Fractures oblique to mylonite foliation.

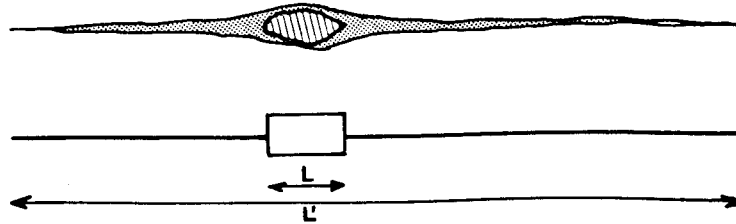


Fig. 72 (from Boullier and Gueguen, 1975)

Strain analysis using formula: $\text{strain} = (L' - L)/L$.

occurred through both brittle and ductile deformation processes. The deformation processes are dependent upon grain composition, size, and orientation, as well as temperature, pressure, and strain rate. Boullier and Gueguen (1975) take a grain (L) and the length to which the grain has extended through deformation (L'). The initial length is somewhat arbitrary and is taken as the area where the grain does not appear recrystallized. Longitudinal strain is then determined by the formula -- $\text{Strain} = (L' - L)/L$ (Fig. 72). Using orthopyroxene for a marker grain in mylonitic peridotite nodules from kimberlites, they found the average strain to be 840%.

The reliability of this method depends upon how the strain is averaged and over what scale, and the principal deformation process. This method is most reliable where deformation is by superplastic flow. Where deformation has involved boudinage or fracturing, only a minimum strain will be measured because the strain may be accommodated by the fracturing and by the movement of the marker fragments to a point where the initial relationship is obscured.

The Table Mountain mylonites have undergone extensive fracturing and boudinage. It is difficult to determine where one grain begins and another ends. Some pyroxenes have been recrystallized or do not have a measurable tail. In most pyroxenes the tail was considerably and consistently better developed on one side of the deformed grain. Only six suitable grains were found. These were grains which had a

large central clast and tails of approximately equal length. The initial length was taken as the large rounded clast area. Three of these grains were from an area which still contained large clinopyroxenes. Strain measurements were 230%, 270% and 300%. Two grains were from an area of finely foliated pyroxene and plagioclase. Both strain measurements from this area were 940%. In an area showing intermediate grain size, strain was measured in a single grain and found to be 660%. Thus, the marker grain method (Boullier and Gueguen, 1975) agrees at least in a rough way with the microscopic observations, and the degree of deformation, expressed as the extension of a pyroxene grain, increases with increasing strain.

Center Point Method

The center point method for strain analysis was developed by Ramsay (1967, p. 195). It is ideally suited for homogeneous strain in rocks that have suffered pressure solution, but is generally applicable to rocks in which there are two distinct grain sizes and the grains had an initially equal or known unequal distribution.

The distance (d) between centers of adjacent large grains, i.e. non-matrix are measured. These measurements are plotted against the orientation of the line measured from some known azimuth in the section. These points would be scattered over a linear distance M in undeformed equally distributed material (Figures 73 and 74). In deformed material, however, the points plot along a bell curve (Figures 75 and 76). The high and low points mark the areas of maximum and minimum

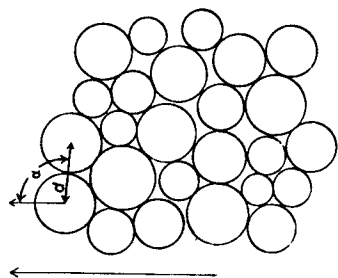


Fig. 73 (from Ramsay, 1967)

Section through a rock made up of an aggregate of undeformed spheres.

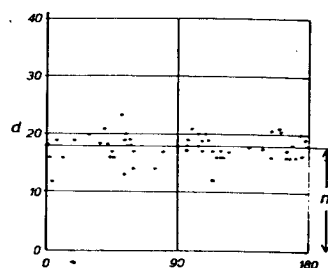


Fig. 74 (from Ramsay, 1967)

Plot of d against α for the material of Fig. 73.

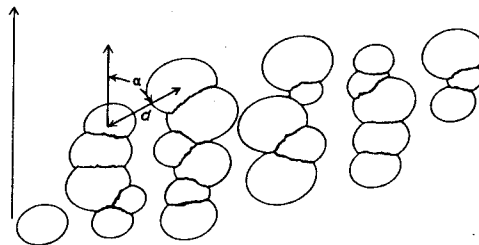


Fig. 75

Section through a deformed aggregate of partially deformed spheres which have undergone partial pressure solution along their mutual contacts.

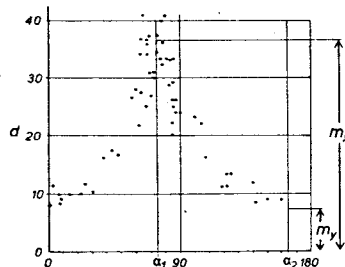


Fig. 76

Plot of d against α for the material of Fig. 75.

extension which are taken as MX and MY. The MX/MY ratio is equal to the ratio of principal strains. If the original distance M is known or the original size and distribution of the grains, then it is possible to calculate the two principal quadratic extensions. Like the marker grain method, the center point method only gives a minimum strain estimate.

Assuming an initially random igneous fabric with roughly equal distances between minerals, Helmstaedt and Allen (1977) used this method to estimate strain in a "metagabbro norite" (HLR-4) from DSDP hole 334. The ratio of maximum to minimum length was 4.1:1.

Application problems, similar to those of the marker grain method were encountered, in using the center point method to determine strain in the Table Mountain mylonites. It was not possible to determine the extent of a grain in the coarser pyroxene area so no measurements were taken. In a finely foliated area with small grains, similar to the 940% strain area, 21 measurements were made and plotted. The distribution of points was random, so no ratio of maximum to minimum elongation was made (Fig. 77).

The random distribution may be a function of multiple splitting of grains, a large shearing component during deformation, or inhomogeneous strain, all of which are likely. Because no ratio was obtained with the center point method, a comparison could not be made between the two methods.

Summary

Some of the areas of the Table Mountain mafic suite have

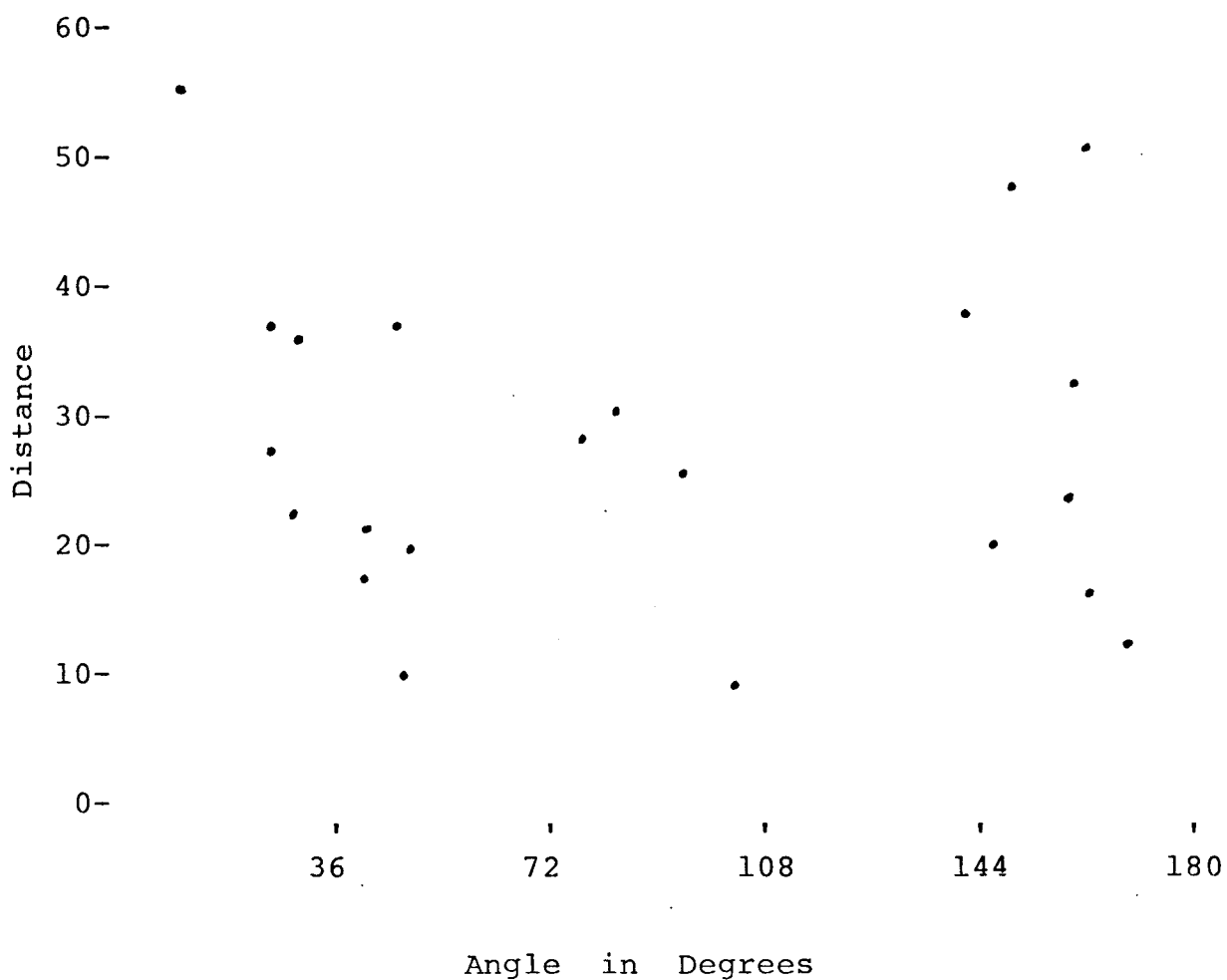


Fig. 77

Random distribution of 21 points in attempt to apply Ramsay's (1967) Center Point Method for strain analysis to a Table Mountain mylonite

been subjected to intense deformation. The deformation is expressed as linear high strain zones and as mylonites. Extrapolating from the strain percentages measured in the mylonites for the different degrees of pyroxene cataclasis, the high strain zones have experienced much smaller strains. The two major compositional minerals, plagioclase and pyroxene, were more equally deformed when the strain is lower. When the strains are higher, plagioclase appears to accommodate more of the strain through granulation which allows it to behave in a ductile and even superplastic fashion. This difference, however, may be a function of the other parameters involved in producing deformation such as strain rate, temperature, pressure and the influence of water.

CHAPTER VIII

SUMMARY AND CONCLUSIONS

Drawing from the previously described field relationships, geometric interpretations, and petrographic investigations, the following sequence of events can be distinguished from Table Mountain:

- A. igneous layering, sedimentary, structures, and mineral lineation (?),
- B. dikes and veins,
- B. large scale folding of cumulate banding,
- B. hornblende gabbro,
- C. faulting and other high strains.

The first four events (A and B), probably occurred prior to complete solidification.

The igneous layering and sedimentary structures show mineral deposition under conditions which promoted adcumulate growth, were capable of transporting the mineral grains, and were subjected to at least minor tectonic activity during the initial stages of formation. Such conditions can be explained by deposition on a flat floored magma chamber in which convection is also occurring. The direction of flow within the convection cell may have influenced the orientation of plagioclase grains with respect to the cumulate banding and therefore the subsequent folding. The tectonic activity could have resulted from minor adjustments to subsidence as well as in response to large scale faulting.

Beginning shortly after the initial deposition, the igneous material was intruded by dikes and veins of plagioclase, olivine, pyroxene, and a fine grained, phenocryst bearing mafic material. These dikes parallel, cut, and are folded with the sedimentary layering. Only the fine grained mafic material shows chilled margins. The mafic dikes are intruded close to tectonically disturbed areas and are apparently later than the other dikes.

The relationship and timing of the hornblende gabbro in the formation sequence is unclear, in part because the relationship has been obscured by the close proximity to intense deformation. The layering in the hornblende gabbro and the hornblende lineation, approximately parallel many of the contacts with the host gabbro, but there is no strictly consistent relationship between them.

Macroscopic folding has been determined from the geometric analysis of the six subareas. The lineation consistently parallels the fold axis. Three different orientations have been determined for these fold axes:

- A. For subareas I and II, an east-west horizontal axis.
- B. For subareas IV and V, a northeast trending, moderately plunging axis.
- C. For subarea VI, a vertical axis.

The parallelism of the lineation and fold axis suggest that the lineation is either tectonically introduced during the deformation that produced the folding, or that it is a primary,

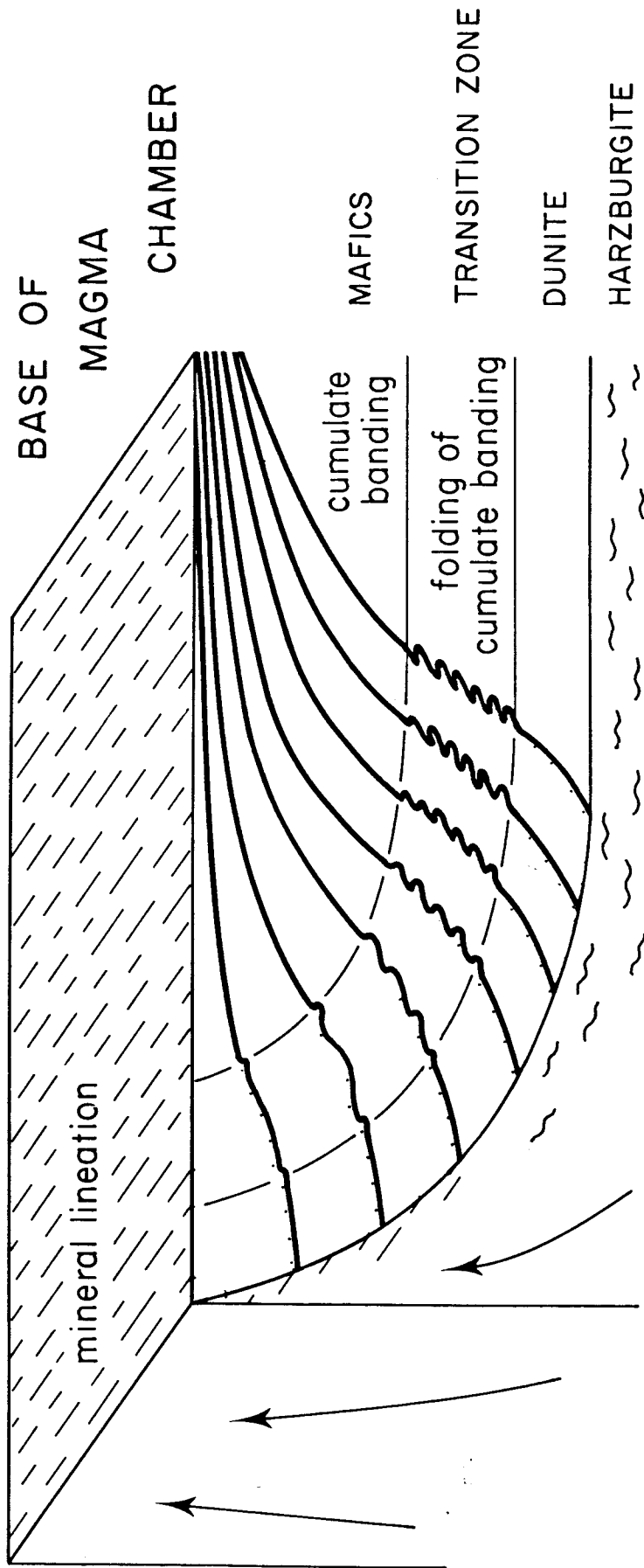


Fig. 78 (after Dewey and Kidd, 1977)

Development of lineation and folding in cumulate banding through differential subsidence of the material at the base of the magma chamber.

sedimentary style features, that was perpendicular to the compressive stress direction producing the folds. Figure 78 (after Dewey and Kidd, 1977), depicts this situation. A sedimentary mineral lineation is produced at the base of the magma chamber. Assuming a differentially subsiding wedge, folding would occur as the angle between the wedge and the base of the magma chamber increased. Folding would be especially prevalent along the transition zone were different mineral densities and accumulation rates, and the steepness of the cumulate banding would increase the instability and enhance folding. The different fold orientations can be produced by rotation and/or faulting of the crustal blocks outside of the magma chamber. Faults have been observed on many scales in submersible studies of the ocean floor. Alternatively, the blocks may have been faulted and/or rotated into their present orientation with each other during obduction.

The last event recorded, produced the cataclastic rocks described in the previous chapter. The cataclasis is particularly well developed near the hornblende gabbros, suggesting that the presence of water may have aided in the deformation. The cataclastic zones formed at widely varying angles to the layering, dikes, and veins. No lineation is developed. It is not clear if the cataclasis occurred in response to obduction or non-obduction ocean crust processes. Experimental evidence for at least some of the deformation structures favors a high temperature environment. Extrapolating from laboratory to natural strain rates however, is subject to considerable qualification. Therefore, it is possible for the deformation to have occurred during obduction.

The study of ophiolites is an integral part in understanding the formation and development of ocean crust. Table Mountain, on a macroscopic scale, is a relatively simple ophiolite complex, one that would seem to easily fit the seismic stratigraphy that defines lower oceanic crustal structure. Yet, on a smaller scale it shows complicated structural and petrological variations. These observed variations, coupled with samples and observations from the ocean floor, have begun to shed some light on processes through which ocean floor is created, and may eventually lead to an understanding of the mechanisms behind the lateral movements of the sea floor.

BIBLIOGRAPHY

- Allison, I., and LaTour, T.E., 1977, Brittle deformation of hornblende in a mylonite: a direct geometrical analogue of ductile deformation by translation gliding: Canadian Jour. Earth Sci., v. 14, p. 1953-1958.
- Bailey, J.E., and Hirsch, P.B., 1962, The recrystallization process in some polycrystalline metals: Proc. Roy. Soc. (London), Ser. A 267, p. 11-30.
- Ballard, R.D.; Bryan, W.B.; Heirtzler, J.R.; Keller, G.; Moore, J.G.; and Van Andel, T.J., 1975, Manned submersible observations in the FAMOUS area: mid-Atlantic ridge: Science, v. 190, p. 103-108.
- Bell, T.H., and Ethridge, M.A., 1973, Microstructure of mylonites and their descriptive terminology: Lithos, v. 6, p. 337-348.
- Betz, Fr., Jr., 1939, Geology and mineral deposits of the Canada Bay area, northern Newfoundland: Geol. Survey of Newfoundland Bull. #16.
- Betz, Fr., Jr., 1943, Late paleozoic faulting in western Newfoundland: Geol. Soc. America Bull., v. 54, p. 687-706.
- Billings, E., 1862, Further observations on the age of the red sand rock formation (Potsdam group) of Canada and Vermont: Am. J. Sci., 2nd ser., v. 33, p. 101-137.
- Bird, J.M., and Dewey, J.F., 1970, Lithosphere plate-continental margin tectonics and the evolution of the Appalachian orogen: Geol. Soc. America Bull., v. 81, p. 1031-1060.
- Bogdanov, Y.A., and Ploshko, V.U., 1968, Igneous and metamorphic rocks from the abyssal Romanche depression: Dokl. Akad. Nauk. S.S.S.R., v. 177, p. 173-176.
- Bolling, G.F., and Winegrad, W.C., 1958: Jour. Inst. Metals, v. 86, p. 492.
- Bonatti, E., and Honnorez, J., 1976, Sections of the earth's crust in the equatorial Atlantic: Jour. Geophysical Res., 81, #23, p. 4104-4116.
- Bonatti, E., Elter, P., and Ferrara, G., 1970, Equatorial mid-Atlantic ridge: petrologic and sr-isotope, evidence for an Alpine assemblage: Earth Planet. Sci. Lett., v. 9, p. 247-256.

- Bonatti, E., Honnorez, J., Kirst, P., and Radicoti, 1975, Metagabbros from the mid-Atlantic ridge at 06°N. contact-hydrothermal-dynamic metamorphism beneath the axial valley: *J. Geol.*, v. 83, p. 61-78.
- Bottinga, Y., and Allegre, C., 1976, Geophysical, petrological, and geochemical models of the oceanic lithosphere: *Tectonophysics*, v. 32, p. 9-59.
- Borg, I., and Handin, J.W., 1966, Experimental deformation of crystalline rocks: *Tectonophysics*, v. 314, p. 249-368.
- Borg, I.Y., and Heard, H.C., 1967, Further studies on experimentally deformed plagioclase in rock deformation and the deformation mechanisms in torsion tests: *Air Force, Cambridge Res. Lab. Rept.*, A.F.C.R.L.-67-0308.
- Borg, I.Y., and Heard, H.C., 1969, Mechanical twinning and slip in experimentally deformed plagioclase: *Contrib. Mineral. Petrol.*, v. 23, p. 128-135.
- Borg, I.Y., and Heard, H.C., 1970, Experimental deformation of plagioclase: In *Experimental and Natural Rock Deformation*, Paulitsch Ed., Springer, Berlin, p. 375-403.
- Bostock, H.H., Cumming, L.M., Williams, H., and Smyth, W.R., 1976, Geologic map of the strait of Belle Isle region: *Geological Soc. Canada Open File*.
- Boullier, A.M., and Gueguen, Y., 1975, SP-mylonites. Origin of some mylonites by superplastic flow: *Contrib. Mineral. Petrol.*, v. 50, p. 93-104.
- Braun, Gunther, 1969, Computer calculated nets for petrofabric and structural analysis: *Neues Jahrbuch für Min. (Monats)*, Hefty, p. 469-476.
- Buddington, A.F., and Hess, H.H., 1937, Layered peridotite laccoliths in the Trout River area, Newfoundland: *Am. J. Sci.*, v. 33, p. 380-388.
- Burke, J.E., 1950, The formation of annealing twins. *Trans.: Amer. Inst. Min. Met. Eng.*, v. 188, p. 1324.
- Burke, J.E., and Turnbull, D., 1952, Recrystallization and grain growth: *Prog. Metal Phys.*, v. 3, p. 220.
- Burnsnall, J.T., and DeWitt, M.J., 1975, Timing and development of the orthotectonic zone in the Appalachian orogen of northwest Newfoundland: *Canadian Jour. Earth Sci.*, v. 12, p. 712-722.

- Cahn, R.W., 1953, Plastic deformation of α -uranium; twinning and twinned crystals: *A CTA Metallurgica*, v. 1, p. 49.
- Cahn, R.W., 1954, Twinned crystals: *Advances in Physics*, v. 3, p. 363.
- Cann, J.R., 1974, A model for oceanic crustal structure developed: *Royal Astron. Soc. Geophys. Jour.*, v. 39, p. 169-187.
- Cann, J.R., and Funnell, B.M., 1967, Palmer Ridge: A section through the upper part of the ocean crust?: *Nature*, v. 213, p. 661-664.
- Carter, N.L., 1976, Steady state flow of rocks: Review of *Geophysics and Space Physics*, v. 14, #3, p. 301-360.
- Carter, N.L., Baker, D.W., and George, R.P., Jr., 1972, Seismic anisotropy, flow, and constitution of the upper mantle: In *Flow and Fracture of Rocks*, Geophys. Monograph Ser., edited by H.C. Heard, I.Y. Borg, N.L. Carter, and C.B. Raleigh, A.G.U., Washington, D.C., v. 16, p. 167-190.
- Carter, N.L., Griggs, D.T., and Christie, J.M., 1964, Experimental deformation and recrystallization of quartz: *J. Geol.*, v. 72, p. 687-733.
- Casey, J.F., 1978, Complex upper and lower boundaries of the coarse grained plutonic rocks of the North Arm Mountain massif, Bay of Islands ophiolite complex, western Newfoundland: *N.E. Sec. Geol. Soc. America Bull. Abst.*, v. 10, #2, p. 3.
- Ballard, R., Bryan, W., Davis, K., deBoer, J., DeLong, S., Dick, H., Emery, K.O., Fox, P.J., Hempton, M., Malcolm, F., Melson, W.G., Spydell, R., Stroup, J., Thompson, G., Wright, R., Uchupi, E., 1978, Geological and geophysical investigation of the mid-Cayman rise spreading center: initial results and observations: *Ewing Symposium, Implications of Deep Drilling Results in the Atlantic Ocean*, v. II.
- Church, W.C., and Stevens, R.K., 1968, Crustal evolution of the western margin of the Newfoundland Appalachians: *Program Annu. Meet. Geol. Soc. America, New Mexico*, p. 53.
- Church, W.R., and Riccio, L., 1974, The sheeted dike layer of the Belts Cove ophiolite complex does not represent spreading: discussion: *Canadian Jour. Earth Sci.*, v. II, p. 1499-1502.
- Coombs, D.S., 1961, Some recent work on the lower grades of metamorphism: *Australian J. Sci.*, v. 24, p. 203-215.

- Cooper, J.R., 1936, Geology of the southern half of the Bay of Islands igneous complex: Newfoundland Dept. Nat. Res., Geol. Soc. Bull., v. 4, p. 62.
- Comeau, R.L., 1972, Transported slices of the costal complex, Bay of Islands - western Newfoundland: unpub. M. Sc. thesis, Memorial University of Newfoundland, p. 105.
- Dallmeyer, R.D., and Williams, H., 1975, $^{40}\text{Ar}/^{39}\text{Ar}$ release spectra of hornblende from the metamorphic aureole of the Bay of Islands complex western Newfoundland: timing of ophiolite obduction at the ancient continental margin of eastern North America: Geol. Soc. America Abs., v. 7, no. 6, p. 75.
- Davies, H.L., 1968, Papuan ultramafic belt: XXIII Internat. Geol. Congr., v. 1, p. 209-220.
- Deer, W.A., Howie, R.A., and Zussman, J., 1975, An Introduction to the Rock Forming Minerals, Longman, London, p. 528.
- Dewey, J.F., 1974, Continental margins and ophiolite obduction Appalachian Caledonian system. Burk, G.A., and Drake, C.L., eds., The Geology of Continental Margins, p. 933-950.
- Dewey, J.F., 1969, Evolution of the Appalachian/Caledonian orogen: Nature, v. 222, p. 124-129.
- Dewey, J.F., and Bird, J.M., 1971, Origin and emplacement of the ophiolite suite: Appalachian ophiolites in Newfoundland: Jour. Geophysical Res., v. 76, p. 3179-3206.
- Dewey, J.F., and Kidd, W.S.F., 1977, Geometry of plate accretion: Geol. Soc. America Bull.,
- Dewey, J.F., Fox, P.J., and Kidd, W.S.F., 1973, Structure and generation of oceanic crust and mantle: Geol. Soc. America Abstracts with Program, v. 5, #7, p. 597-598.
- Edwards, A.B., 1960, Textures of the Ore Minerals, 2nd ed., Aust. Inst. Min. Met. Engrs., Melbourne, 1960.
- Gass, I.G., 1968, Is the Troodos massif of Cyprus a fragment of mesozoic ocean floor?: Nature, v. 220, p. 39-42.
- Graciansky, P.C. de, 1973, Le problem des "coloured melanges" a propos de formations chastiques associeis cux ophiolites de lycie occidentale (Turquie): Revue de Geogr. Phys. et de Geol. Dynam., v. 15, p. 555-566.

- Greenbaum, D., 1972, Magmatic processes at ocean ridges, evidence from the Troodos massif, Cyprus: *Nature*, v. 238, p. 18-21.
- Griggs, D.T., Turner, F.J., and Heard, H.C., 1960, Deformation of rocks at 500°C to 800°C: In Rock Deformation, Griggs and Handin, eds., *Geol. Soc. America Mem.*, v. 79, p. 39-104.
- Hall, E.O., 1954, Twinning and Diffusion less Transformations in Metals, Butterworths, London.
- Harland, W.B., and Gayer, R.A., 1972, The arctic caledonides and earlier oceans: *Geol. Mag.*, v. 109, p. 289-314.
- Harker, A., 1932, Metamorphism--A Study of the Transformations of Rocks Masses, Methuen, London, p. 362.
- Helmstaedt, H., and Allen, J.M., 1977, Metagabbro from DSDP Hole 334: an example of high-temperature deformation and recrystallization near the mid-Atlantic ridge: *Canadian Jour. Earth Sci.*, v. 14, p. 886-898.
- Higgins, M.W., 1971, Cataclastic rocks, U.S.G.S., Prof. Paper, p. 687.
- Hobbs, B., Means, W., and Williams, P., 1976, An Outline of Structural Geology, Wiley, N.Y., p. 571.
- Hodges, F.N., and Papike, J.J., 1976, DSDP Site 334: magmatic cumulates from oceanic layering: *Jour. Geophysical Res.*, no. 23, p. 4135-4151.
- Howley, J.P., Geologic map of Newfoundland: Geol. Survey of Newfoundland.
- Hu, H., 1963, Annealing of silicon-iron single crystals. In Recovery and Recrystallization of Metals, (L. Himmel, ed.), N.Y.: Interscience, p. 311-362.
- Ingerson, Earl, 1935, Layered peridotite laccoliths of the Trout River area, Newfoundland: *Am. J. Sci.*, v. 29, p. 422-440.
- Ingerson, E., 1937, Layered peridotite laccoliths in the Trout River area, Newfoundland - a reply: *Am. J. Sci.*, v. 33, pp. 389-392.
- Karson, J., and Dewey, J.F., 1978, The costal complex western Newfoundland, an early Ordovician fracture zone: *Geol. Soc. America Bull.*
- Kennedy, M.J., 1975, Repetitive orogeny in the northeastern Appalachians - new plate models based upon Appalachians examples: *Tectonophysics*, v. 28, p. 39-87.

- Kidd, W.S.F., 1977, The Verte Lineament, Newfoundland: ophiolite complex floor and mafic volcanic fill of a small Ordovician marginal basin: The Ewining Series, v. I, Island Arcs, Deep Sea Trenches and Back Arc Basins, American Geophysical Union, p. 407-418.
- Kidd, W.S.F., 1974, Evolution of the Baie Verte Lineament, Burlington Peninsular, Newfoundland: Unpublished Ph. D. Thesis, University of Cambridge.
- Kirby, S.H., and Kronenberg, A.K., 1978, Ductile strength of clinopyroxenite: evidence for a transition in flow mechanics: Am. Geophys. Union Trans., v. 59, no. 4, p. 376.
- Laves, F., 1952, Mechanische zwillingsbildung in feldspaten in abhangigkeit von ordnung - unordnung der s/al verteilung innerhalb des $(Si, Al)_4 O_8$: Gerustes, Naturwissenschaften.
- Laves, F., 1965, Mechanical twinning in acid plagioclases: Am. Miner., v. 50, p. 511.
- Lawrence, R.D., 1970, Stress analysis based on albite twinning of plagioclase feldspars: Geol. Soc. America Bull., v. 81, p. 2507-2512.
- Li, J.C.M., 1962, Possibility of subgrain rotation during recrystallization: J. Appl. Phys., v. 33, p. 2958-2965.
- Logan, Sir William, Geol. Survey of Canada: Report of Progress from its Commencement to 1863.
- Lorimer, G.W., Champness, P.E., and Spooner, E.T.C., 1972, Dislocation distributions in naturally deformed omphacite and albite: Nature Phys. Sci., v. 239, p. 108.
- Malcolm, F.L., 1978, Mineral chemistry of plutonic rocks from the Cayman Trough, Caribbean Sea: Am. Geophys. Union Trans., v. 59, no. 4, p. 405.
- Malpas, J., 1976, The geology and petrochemistry of the Bay of Islands complex, west Newfoundland: Ph. D. Thesis, Memorial University.
- Malpas, J., Stevens, R.K., and Strong, D.F., 1973, Amphibolites associated with Newfoundland ophiolites: their classification and tectonic significance: Geology, v. 1, p. 45-47.
- Marshall, D.B., and Wilson, C.J.L., 1976, Recrystallization and peristerite formation in albite: Contrib. Mineral. Petrol., v. 57, p. 55-69.

- Marshall, D.B., Vernon, R.H., and Hobbs, B.E., 1976, Experimental deformation and recrystallization of a peristerite: *Contrib. Mineral. Petrol.*, v. 57, p. 49-54.
- Mattinson, J.M., 1975, Early paleozoic ophiolite complexes of Newfoundland: isotopic ages of zircons: *Geology*, v. 3, p. 181, 183, and reply p. 479.
- Melson, W.G., and Thompson, G., 1970, Layered basic complex in oceanic crust, Romanche Fracture: equatorial Atlantic Ocean: *Science*, v. 168, p. 817-820.
- Mercier, J.C.C., 1978, Application of the olivine geopiezometers to mantle dynamics: *Am. Geophys. Union Trans.*, v. 59, p. 375.
- Miyashiro, ., Shido, F., and Ewing, M., 1970, Crystallization and differentiation in abyssal tholeiites and gabbros from mid-oceanic ridges: *Earth and Planetary Sci. Letters*, v. 7, p. 361-365.
- Miyashiro, A., Shido, F., and Ewing, M., 1971, Metamorphism in the mid-Atlantic ridge near 24° and 30°N: *Royal Soc. London Philos. Trans., Ser. A.*, v. 268, p. 589-603.
- Moore, T.G., Fleming, H.S., and Phillips, T.D., 1974, Preliminary model for extrusion and rifting at the axis of the mid-Atlantic ridge, 36° 48' North: *Geology*, v. 2, p. 437-440.
- Moore, E.M., and Vine, J.F., 1971, The Troodos Massif, Cyprus and other ophiolites as oceanic crust: evaluation and implications: *Royal Soc. London Philos. Trans., Ser. A.*, v. 268, p. 443-466.
- Mugge, O., and Heide, F., 1931, Einfache scheidungen am anorthit: *Neues Jahrbach fur Min.*, 1/64, p. 163-170.
- Muir, J.D., and Tilley, C.E., 1966, Basalts from the northern part of the mid-Atlantic ridge, pt. II, the Atlantis collection near 30°N: *Jour. Petrology*, v. 7, p. 193-201.
- Neale, E.R.W., 1972, A cross section through the Appalachian orogen in Newfoundland: 24th Int. Geol. Cong., Excursion A62-C62 Guidebook.
- Nelson, K.D., and Casey, J.F., 1978, (in review).
- Nicolas, A., and Poirier, J.P., 1976, Crystalline Plasticity and Solid State Flow in Metamorphic Rocks, Wiley, N.Y., p. 444.

- Pratt, P.L., 1953, Similar glide processes in metallic and ionic crystals: *Acta Metall.*, v. 1, p. 103-104.
- Quon, S.H., and Ehlers, E.G., 1963, Rocks of northern part of mid-Atlantic ridge: *Geol. Soc. America Bull.*, v. 74, p. 1-8.
- Raleigh, C.B., 1968, Mechanisms of plastic deformation of olivine: *Jour. Geophysical Res.*, 73/14, p. 5391-5406.
- Ramsay, J.G., 1967, Folding and Fracturing of Rocks, McGraw Hill, New York, p. 568.
- Ramsay, J.G., and Graham, R.H., 1970, Strain variations in shear belts: *Canadian Jour. Earth Sci.*, v. 7, p. 786-813.
- Rast, N., 1965, Nucleation and growth of metamorphic minerals: In Controls of Metamorphism, eds., W.S. Pitcher and G. S. Flinn, Oliver and Boyd, Edinburgh.
- Reinhardt, B.M., 1969, On the genesis and emplacement of ophiolites in the Oman mountains geosyncline: *Schweizer Min. Pet. Mitt.*, v. 49, p. 1-30.
- Rettger, R.E., 1935, Experiments on soft rock deformation: *Am. Assoc. Petrol. Geol. Bull.*, v. 19, p. 271-292.
- Rice, A., (1978, in review), Convective fractionation: a mechanism to provide zoning (macrosegregation), layering, crescumulates, banded tuffs, and explosive volcanism in igneous processes.
- Rodgers, J., and Neale, E.R.W., 1963, Possible "taconic" klippen in western Newfoundland: *Am. J. Sci.*, v. 261, p. 713-730.
- Robertson, P.B., Dence, M.R., and Vos, M.A., 1968, Deformation in rock-forming minerals from Canadian craters, p. 433-452 in French, B and Short, N., eds, Shock Metamorphism of Natural Minerals, Baltimore, Mono Press.
- Rosencrantz, E., 1978, Gabbro-dolerite-basalt structure, Worth Arm Massif, Bay of Islands ophiolite Complex, Newfoundland: *N.E. Sec. Geol. Soc. America Bull. Abst.*, v. 10, no. 2, p. 83.
- Salisbury, M.H., and Christensen, N.I., 1978, The seismic velocity structure of a traverse through the Bay of Islands ophiolite complex, Newfoundland, an exposure of oceanic crust and upper mantle: *Jour. Geophysical Res.*, v. 83, p. 805-817.
- Sander, B., 1930, Gefugekunde der Gesteine, Springer, Wien, p. 352.

- Schuchert, C., and Dunbar, C.O., 1934, Stratigraphy of western Newfoundland: Geol. Soc. America Mem. 1.
- Schwerdtner, W.M., 1973, A scale problem in paleo strain analysis: Tectonophysics, v. 16, p. 47-54.
- Seifert, K.E., 1965, Deformation bands in albite: Am. Miner., v. 50, p. 1469-1472.
- Seifert, K.E., 1968, Experimental deformation of anorthosite: (Abs.) Program 1968, Geol. Soc. America Bull., Special Paper 121, p. 272.
- Seifert, K.E., and Ver Ploeg, A.J., 1977, Deformational characteristics of experimentally deformed Adirondack dark anorthosite: Canadian Jour. Earth Sci., v. 14, p. 2706-2717.
- Shand, S.J., 1949, Rocks of the mid-Atlantic ridge: J. Geol., v. 57, p. 89-91.
- Shaw, H.R., Rheology of basalt in the melting range: J. Petrol., v. 10, p. 510-535.
- Sleep, N.H., 1975, Formation of oceanic crust: some thermal constraints: Jour. Geophysical Res., v. 80, p. 4037-4042.
- Smith, C.H., 1958, Bay of Islands igneous complex, western Newfoundland, Canada: Can. Geol. Survey Mem. 290, p. 132.
- Sorby, H.C., 1853, On the origin of slaty cleavage: Edinburgh New Philos. Jour., v. 55, p. 137-148.
- Starkey, J., 1964, Glide twinning in the plagioclase feldspars, In Deformation Twinning, R.E. Reed Hill, J.P. Hirth, H.C. Rogers, eds., Gordon and Breach, New York, p. 177-191.
- Stevens, R.K., 1970, Cambro-Ordovician flysch sedimentation and tectonics in west Newfoundland and their possible bearing on a proto-Atlantic Ocean: In Lajoie, J., ed., Flysch Sedimentology in North America, Geol. Assoc. Canada, Special Paper no. 7, p. 165-177.
- Stevens, R.K., 1976, Lower paleozoic evolution of west Newfoundland: unpublished Ph. D. thesis, University of Western Ontario.
- Strong, D.F., 1974, An "off-axis" alkali volcanic suite associated with the Bay of Islands ophiolites, Newfoundland, Earth Planet. Sci. Lett., v. 21, p. 301-309.

- Strong, D.F., and Williams, H., 1972, Early paleozoic flood basalts of northwestern Newfoundland: their petrology and tectonic significance: *Geol. Assoc. Canada. Proc.*, v. 24, p. 43-54.
- Stroup, J.B., Malcolm, F.L., and Spydell, R., 1978, Petrology of the submersible collected plutonic rocks from the Cayman Trough, Carribbean: *Am. Geophysical Union Trans.*, v. 59, no. 4, p. 405.
- Stukes, V., and Reynolds, P.H., 1974, $^{40}\text{Ar}/^{39}\text{Ar}$ dating of the Brighton gabbro complex, Lush's Bight Terrane, Newfoundland, *Canadian Jour. Earth Sci.*, v. II, p. 1485-1488.
- Talbot, C.J., 1970, The minimum strain ellipsoid using deformed quartz veins: *Tectonophysics*, v. 9, p. 47-76.
- Troelson, J., 1947, Stratigraphy and structure of the Bonne Bay-Trout River area: Unpublished Ph.D. Dissertation, Yale University.
- Tullis, J., 1978, Mylonites--natural and experimental: *Geol. Soc. America Bull.*, Short Course, March,
- Turner, F.J., and Weiss, L.E., 1963, Structural Analysis of Metamorphic Tectonites, McGraw Hill, New York, p. 545.
- Turner, F.J., Griggs, D.T., and Heard, H., 1954, Experimental deformation of calcite crystals: *Geol. Soc. America Bull.*, v. 65, p. 883-934.
- Vance, J.A., 1961, Polysynthetic twinning in plagioclase: *Amer. Min.*, v. 46, p. 1097-1119.
- Vernon, R.H., 1965, Plagioclase twins in some mafic gneisses from Broken Hill, Australia: *Mineralogical Mag.*, v. 35, p. 488-507.
- Vernon, R.H., 1976, Metamorphic Processes, Wiley, N.Y., p. 247.
- Wager, L.R., and Brown, G.M., 1967, Layered Igneous Rocks, San Francisco, W.H. Freeman and Co.
- Wager, L.R., Brown, G.M., and Wadsworth, W.J., 1960, Types of igneous cumulates: *J. Petrol.*, v. I, p. 73, 85.
- Weitz, J.L., 1947, Summary report of the Bay of Islands area: *Geol. Survey Newfoundland*, Unpublished, p. 4.
- Weitz, J.L., 1953, Geology of the Bay of Islands area, western Newfoundland: Unpublished Ph. D. Dissertation, Yale University.

- White, S., 1975, Tectonic deformation and recrystallization of oligoclase: *Contrib. Mineral. Petrol.*, v. 50, p. 287-309.
- Whittington, H.B., and Kindle, C.H., 1963, Middle Ordovician Table Head formation, western Newfoundland: *Geol. Soc. America Bull.*, v. 74, p. 745-758.
- Williams, Harold, 1971, Mafic-ultramafic complexes in western Newfoundland Appalachians and the evidence for their transportation: a review and interim report: *Geol. Assn. Can. Proc.*, v. 24, p. 9-25.
- Williams, Harold, 1973, Bay of Islands, map-area, Newfoundland: *Canadian Geol. Survey Paper*, p. 34-72.
- Williams, Harold, 1975, Structural succession, nomenclature and interpretation of transported rocks in western Newfoundland: *Canadian Jour. Earth Sci.*, v. 12, p. 1874-1894.
- Williams, Harold, and Malpas, J., 1972, Sheeted dikes and brecciated dike rocks within transported igneous complexes, Bay of Islands, Newfoundland: *Canadian Jour. Earth Sci.*, v. 9, p. 1216-1229.
- Williams, Harold, and Smyth, W.R., 1973, Metamorphic aureoles beneath ophiolite suites and alpine peridotites: tectonic implications with western Newfoundland examples: *Am. J. Sci.*, v. 273, p. 594-621.
- Williams, H., and Stevens, R.K., 1969, Geology of Belle Isle-northern extremity of the deformed Appalachian miogeosynclinal belt: *Canadian Jour. Earth Sci.*, v. 6, p. 1145-1157.
- Wilson, J.T., 1963, Hypothesis of earth's behavior: *Nature*, v. 198, p. 925-929.
- Wilson, J.T., 1966, Did the Atlantic close and then re-open?: *Nature*, v. 211, p. 676-681.
- Zen, E-an, 1961, Stratigraphy and structure at the north end of the Taconic Range in west-central Vermont: *Geol. Soc. America Bull.*, v. 72, p. 293-338.